APPLICATION OF RADIOISOTOPES TO STUDIES OF DEFORMATION OF SOLIDS

Thesis

Submitted by

DAVID A. BLACKBURN,
B.Sc.

for the degree of

Doctor of Philosophy

University of Edinburgh,

January, 1961.

C O N T E N T S

C O N T E N T S (Contd.)

C O N T E N T S (Contd.)

PREFACE

The research described in this thesis was carried out in the Department of Natural Philosophy of the University of Edinburgh under the direction of Professor N. Feather, F.R.S. and Dr. A.F. Brown. A paper based on the results to be presented here, and prepared in collaboration with Dr. Brown, was presented at the International Atomic Energy Agency Conference on the Use of Radioisotopes in the Physical Sciences and Industry, Copenhagen, September 1960, and will be published under the auspices of U.N.E.S.C.O. A note based on the technique developed for the evaporation of radioactive metal (Chapter 3) has been published in the Journal of Scientific Instruments.

CHAPTER I

INTRODUCTION AND HISTORICAL REVIEW

I.1. General

It has been the purpose of the present work to measure diffusion rates in metallic grain boundaries; to find whether these rates are influenced by relative motion in the boundary plane of the contiguous crystals, and to interpret the results of the investigation in terms of recent theories of metal structure. The background to this work is of a dual nature and is concerned with the form of intercrystalline boundaries and with diffusion in strained systems. Accordingly a review will be made of past and present grain boundary theories and of the present position with regard to the effect of straining on measurements of bulk diffusion coefficients.

I.2. Older Work on Grain Boundaries

The study of grain boundaries is a fairly recent subject in physics. This is so because only in the last century has it been accepted that metals are crystalline. While it is surprising that metals should have been worked with such success for many centuries without an understanding of their structure, it must be remembered that our evidence relating to this is mostly concerned with small scale phenomena such as etching and X-ray diffraction. In older times the properties of

crystalline substances - hardness, cleavage faces, and often transparency, were at variance with those of metals - elasticity, ductility, and opacity, and the property which first raised the question of crystallinity in metals was that of brittle fracture. This problem was puzzling since brittle fracture could occur at low temperatures in a metal which at high temperature showed the more normal ductile behaviour. Studies of metals having these dual and apparently contradictory properties led to the view that metals were viscous fluids, but that by cooling or reversed bending they could be made to crystallise. Definite evidence to show that metals were normally crystalline was found in 1900 by Ewing and Rosenhain[1], who studied slip lines and etch pits, and any doubt which might have been left was removed by the X-ray diffraction experiments which began shortly after this.

The picture which emerged from this work was that metals were made up of grains and that each grain was a crystal. It was supposed that the grains grew independently from the melt and that their shapes were determined as the chance surfaces developed when one grain grew into contact with the next.

Having decided on the nature of metallic grains and of their formation it was natural next to consider what forces held the grains together. The first theory

of grain boundary structure was the 'amorphous cement' theory which held that the crystals of the metal were held together by a thin layer of the metal in amorphous form, interposed between the grains. The properties of this layer were supposed to be those of a supercooled liquid. It is characteristic of the time (about 1910) that such a theory should have appeared, for although almost all the metallurgists of the day believed that metals were crystalline, absolute rejection of the idea that metals could be amorphous had not occurred. Evidence to support the amorphous cement theory was found by Rosenhain and Humphrey[2] who stretched steel slowly at high temperature and obtained micrographs showing that the grains slid slowly over each other. At lower temperatures no such sliding was found. It was supposed that sliding took place across the amorphous layer, and the variation with temperature fitted well with the idea that the interface had the properties of a viscous liquid. This experiment provided the best verification of the amorphous cement theory ever found and dominated work on grain boundaries for some years.

Other work to confirm the theory consisted in showing that metal tended to break by intercrystalline fracture at high temperature when the amorphous layer would be only slightly supercooled and hence would be weak, but did not occur at lower temperatures when it was highly supercooled and strong.

Measurements made of the reduction in mass of coarse and fine grained polycrystals, due to evaporation when maintained for a time close to their melting points, seemed to support the view that the vapour pressure of the intercrystalline layer was ~~lower~~ higher than that of the bulk metal. Desch, however, showed that the boundary thickness required to explain the measured values was some thousands of atoms thick and this was regarded as very improbable since atomic forces are significant only over spacings of a few times the lattice parameter.

In 1924 Jeffries and Archer[3] suggested the 'transition lattice' theory of grain boundaries in which it is supposed that a layer of atoms one atom thick lies between the grains and that the atoms in this layer have positions intermediate between those of the adjoining atoms of the two crystals. Slight displacement of the first atomic plane in each crystal was allowed but, sensibly, these atoms were to be positioned as if no boundary existed. With this theory the thickness of the amorphous cement was brought to one lattice spacing, and the cement was not even truly amorphous since the atom positions were not random. This theory does not give a satisfactory explanation of grain boundary sliding.

Perhaps the strongest evidence to support the transition lattice theory at the expense of the amorphous cement one was put forward by Chalmers [4] who suggested that slip in the crystals forming the boundary should not vary with orientation according to the amor-

phous cement theory, whereas it should almost certainly occur on the transition lattice theory. By straining bicrystals he obtained conclusive evidence that the amorphous cement theory was incorrect.

Until 1945 the 'transition lattice' theory, as stated by Jeffries and Archer[3] and by Hargreaves and Hills[5] was the accepted picture of a grain boundary. Since then a number of new theories have been suggested but they are all, in essence, transition lattice theories retaining the old grain boundary width and suggesting different matching criteria in the thin transition layer.

I.3. The Modern Picture

The post-war period was notable for two theories, due to Mott[6] and Kê[7], of how slide might occur in boundaries of the transition lattice type. In both theories it is postulated that the slide does not take place uniformly over the boundary but rather that regions of high stress concentration move about the boundary causing local slide. Slide in a particular region relieves the stress there and it is then experienced by some adjacent region.

I.3.1. The Mott 'Island' Theory

Mott's picture of the situation is that, in the boundary plane there are regions or 'islands' of good fit between the ends of the lattice rows in the two

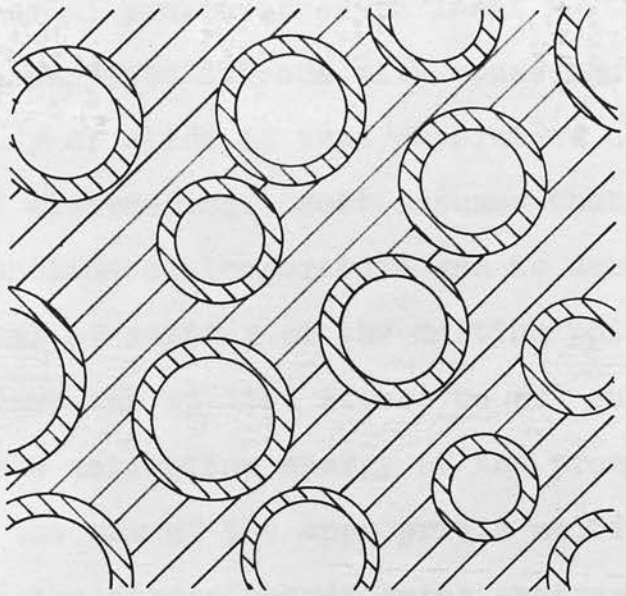

Fig.(1) The Mott 'Island' Theory.

The circles represent areas of fit between the lattice planes of crystals situated above and below the plane of the paper; the widely hatched areas are ones of poor fit, while those closely hatched are of high stress concentration and the deformation will take place by their motion.

crystals, and that these islands are separated by a continuous region of poor fit (Fig. (1)). Slide occurs by slow movement of the islands. It is supposed that random thermal processes cause local melting in the regions around the islands with consequent slide. The probability of slide is thus determined by the free energy of disordering. Mott assumes that this is a linear function of temperature and is equal to the latent heat of melting at the melting point. Since slide allows the applied stress to put energy into the system, the activation energy of the process is determined by the sum of the appropriate melting and stress energies, the stress energy being subtracted from the disordering energy (i.e. making slide more probable) when it puts energy into the system. On the average the ratio of good to bad fitting areas is supposed constant.

Mott's expression for the rate of slide is:

$$\nu = \frac{2\nu a^4 \sigma n}{kT} \exp\frac{nL}{kT_m} \exp\frac{-nL}{kT}$$

- ν atomic vibration frequency
- a elementary slip distance, or approximately the lattice parameter
- σ stress
- k Boltzmann's constant
- L latent heat of melting/atom
- T_m melting temperature
- T temperature
- n number of atoms taking part in an elementary act of sliding $\sim$ 10.

I.3.2. The Kê Theory

As a basis for his theory Kê noted that grain boundary slide could be described by an activation energy and that this energy was equal to that of bulk diffusion in the metal. He presumes from this that sliding is a process dependent on the same detailed phenomena as control diffusion; consequently his theory requires that slide be caused by the thermally activated movement of vacancies and dislocations in and around the boundary.

Kê's equation for the rate of slide is:

$$v = \frac{C\sigma}{RT} \exp \frac{-Q}{RT}$$

σ stress

k Boltzmann's constant

Q an activation energy equal to that of bulk diffusion

T temperature

C constant

Experimental confirmation of the above equations was found by Kê[7] with his torsional oscillation experiments. He found an activation energy term giving acceptable fit with either equation, but the predicted slide rates were both too high. Mott[6] showed that Kê's equation led to slide rates a factor of about 10^4 too high. His own equation gives a better fit but is still well out.

On balance the Mott equation is probably to be preferred, since it has now been found that in not all substances are the activation energies of diffusion and grain boundary slide equal.

I.3.3. The Smoluchowski Boundary

The Smoluchowski picture[8] of grain boundaries arises naturally out of Mott's theory. In their measurements of grain boundary diffusion rates Achter and Smoluchowski[9] noted that, in pairs of crystals having a common cubic direction and misoriented by rotation about this direction, the rate of diffusion in the boundary along the common cube direction increased with increasing misorientation. (Fig. (2))

At small angles of misorientation the boundary is assumed to be composed of parallel lines of dislocations which act as pipes of rapid diffusion so that when the misfit angle is sufficient (about 8^{o}) diffusion significantly beyond that of bulk diffusion in the surrounding crystals can be detected. For higher angles of misfit the dislocations are considered to form groups so that rod-like regions of concentrated dislocations appear, separated by a continuous area of good fit. As the misfit angle is increased more area is covered by the dislocations until this misfitting region becomes continuous with islands of good fit, At very large misfit angles the boundary is covered effectively by a continuous misfitting region. Although the model is suggested

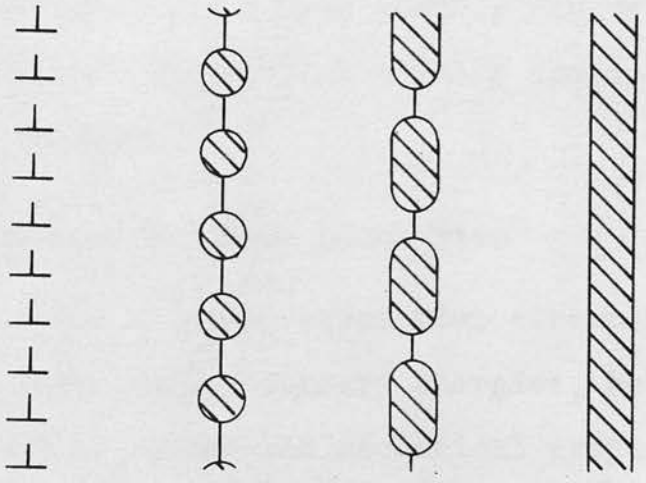

Fig.(2) The Smoluchowski Boundary.

A section of the boundary plane is shown, the crystals being misoriented by rotation about an axis normal to the plane of the paper.
a) Small angle boundary as described by Read.
b) Angle $\sim 20°$: grouped dislocations form regions of disorder separated by a continuum of matching lattice.
c) Angle $\sim 35°$: the disordering is continuous with islands of matching.
d) Maximum misorientation; complete disorder is found.
In b) and c) the islands are extended parallel to the axis of misorientation.

specifically for a simple edge type dislocation boundary, it is obviously possible to extend it to more complex forms of boundary.

If this grain boundary model be regarded as complementary to the Mott model, a theory results giving a reasonably satisfactory explanation of both grain boundary slide and diffusion.

1.3.4. Other Theories of Grain Boundaries

In other theories of grain boundaries attempts have been made to calculate grain boundary energies, but there has been a tendency to ignore the mechanical properties. For example we have the dislocation model of Burgers[10] and its elaboration by Read and Shockley[11], and by van der Merwe[12], attempting to compute grain boundary energies as a function of orientation, and a model by Friedel, Cullity, and Crussard[13] evaluating the same function from a law of interatomic force.

1.3.5. Summary

At present, grain boundary theory can give a reasonable, but rarely quantitative, explanation of most phenomena but there is no comprehensive theory to relate all the commonly measured variables.

1.4. Strain Enhanced Diffusion

Diffusion in sliding grain boundaries may be considered from another aspect.

Recently a number of investigations have been made into the effect on bulk diffusion of a plastic strain applied during the period of diffusion. The results of these studies are not conclusive, the reported ratios of strained to unstrained diffusion coefficients being in the range 1 - 100 for applied strain rates of 10^{-8} - 25.10^{-5} sec^{-1}. Within given sets of results there appears to be a correlation between enhanced diffusion and the applied strain rate, but the effects are not consistent between sets of results, and some investigations consistently show no effect. We find thus that Lee and Maddin[14], using torsional strains, report factors of up to 100, and Forestieri and Girifalco[15] report somewhat smaller factors under compressive strain, while Darby, Tomizuka, and Baluffi[16] using tension and compression, and Barr[17] and Inman[18] using tension, report no effect.

From these results the only general statement possible seems to be that enhanced diffusion is associated with complex slip systems. In such systems we should expect to find the greatest numbers both of line and point lattice defects for a given strain, and it remains to decide which defect will dominate the diffusion effects. Baluffi[19] has reported, from his work on the Kirkendall effect, that vacancy supersaturations of less than 1% lead to porosities. In most systems diffusion is by a vacancy mechanism, where the diffusion coefficient

is proportional to the vacancy concentration; it therefore seems impossible that measurable diffusion enhancement can result from strain produced vacancies. This leads us to assume that diffusion effects must be due to high dislocation concentrations in the lattice. From the work of Turnbull and Hoffman[20] on grain boundary diffusion, we know that, at low diffusing temperatures, the diffusion coefficient along the length of a dislocation is about 10^6 times that of bulk diffusion. Assuming that a dislocation has a cross section of (one lattice parameter)^2, we may calculate the dislocation concentration which will produce a factor of 100 in the bulk diffusion coefficient.

Consider diffusion through unit area composed of an area A subject to bulk diffusion with coefficient D, and an area A' subject to dislocation diffusion of coefficient D'. The measured diffusion coefficient 100D is given by:

$100\ D\ 1 = DA + D'A'$ where $A' = 1 - A$

or $100\ D \sim D'A'$ but $A' = C\ a^2$

$\therefore\ 100\ D \sim D'Ca^2$ where C = dislocation concentration

$\sim 10^6 DC\ 10.10^{-16}$ a = lattice parameter

$\sim \sqrt{10}.10^{-8}$ cm.

and $D' \sim 10^6 D$

$\therefore\ C \sim 10^{11}/cm^2$

This dislocation concentration is high but not impossible (see e.g. Koehler[21] and Brown[22]).

I.5. Outline of the Present Work

We must consider the present work against the dual background detailed above.

Referring to the bulk diffusion measurements first, we see the present work as an extension of this series; it may even be regarded as a limiting case of high shear strain, the slide being seen as shear across a plane of one atom thickness. Such a view is however, not realistic, the plane concerned being quite atypical of the lattice. It is better to consider the boundary plane as a sheet composed of an aggregation of line defects so that we are concerned with the effect of relative motion amongst the defects on their diffusing properties.

In terms of grain boundary theory the present work seeks to find the effect of motion in the order/disorder pattern on diffusion, and so to see if any boundary widening is caused by the motion, or if the applied stress modifies the number of atoms taking part in an elementary act of slide so that the temperature variation of the diffusion may not be expressed by a simple, stress independent, exponential variation with temperature.

CHAPTER 2

METHODS OF ANALYSIS AND THE CHOICE OF EXPERIMENTAL CONDITIONS

2.1. General

Before commencing a study of diffusion in metallic grain boundaries it is first necessary to consider the nature of the diffusion process, to deduce the equations describing it, and to apply them to choose appropriate experimental conditions for further analysis.

2.2. Diffusion and the Diffusion Equations

2.2.1. Bulk Diffusion

In his work on diffusion Fick[23] showed that the rate of flow of a diffusing material across a surface should be proportional to the concentration gradient of the material across the surface, and the diffusion coefficient was defined as the constant of proportionality appropriate to a cross section of unit area normal to the direction of the concentration gradient. Such a law of diffusion might be supposed to arise in one of two ways: either the concentration gradient causes a force on the diffusing particles causing a directed flow, or the individual particles experience no force and the flow is a statistical consequence of random motion within the concentration gradient.

For an understanding of diffusion in metals it is

essential to realise that it is the second process which is operative. Because of the short range of atomic forces an atom can be influenced only by the small number of others surrounding it closely, so that a force due to the concentration gradient is not probable as an insufficient number of operative neighbour atoms are available to produce the required continuous variation of concentration effect; also there could be no explanation of self-diffusion. Since diffusion is found to vary with temperature in an exponential manner to fit the Arrhenius form of equation:

$$D = D_o \exp - \frac{Q}{RT}$$

an energy barrier mechanism might be expected. This fits well with the statistical approach since each atom may be considered as able to jump from its mean position to an adjacent lattice site if given a suitable amount of energy. It is supposed that random thermal fluctuations may occasionally concentrate sufficient energy to cause such jumps.

It is a simple matter to show that Fick's Law follows if there is random motion of the diffusing atoms. Consider two adjacent sheets of atoms separated by a distance a, each containing N atoms, and in which the fractional concentrations of the diffusing atoms are C and C'. (Fig. (3)). If the atoms are supposed each to jump with a frequency f a number $\frac{1}{2}$CNf will cross from C

to C' in unit time and a number $\frac{1}{2}C'Nf$ will travel from C' to C, the factor $\frac{1}{2}$ accounting for the equal probability that the atoms in either sheet may jump away from the region considered. The rate of flow from one plane to the other is thus $\frac{1}{2}Nf(C' - C)$. In this region the concentration gradient is $\frac{-(C' - C)}{a}$ so that the rate of flow is:

$$\frac{1}{2}Nf(C'-C) = -\frac{1}{2}Nf\,a\,\frac{\partial C}{\partial x}$$

and this is Fick's Law.

Since analysis of concentration gradients will always be averaged over distances $\gg a$ the atomic spacing, deviations from the law due to the discontinuous gradient will not be measured.

To analyse diffusion data it is necessary to transform Fick's equation. Consider the rate of accretion of the diffusing substance in a rectangular box of sides 2dx, 2dy, 2dz (Fig. (4)). If the rates of flow of material along the various axes be F_x, F_y, F_z, at the point A(x,y,z) (in the centre of the box) the rate of increase of material inside the box will be:

$$4\,dy\,dz\left(F_x - \frac{\partial F_x}{\partial x}dx\right) - 4\,dy\,dz\left(F_x + \frac{\partial F_x}{\partial x}dx\right)$$

$$+\ 4\,dz\,dx\left(F_y - \frac{\partial F_y}{\partial y}dy\right) - 4\,dz\,dx\left(F_y + \frac{\partial F_y}{\partial y}dy\right)$$

$$+\ 4\,dx\,dy\left(F_z - \frac{\partial F_z}{\partial z}dz\right) - 4\,dx\,dy\left(F_z + \frac{\partial F_z}{\partial z}dz\right)$$

$$= -8\,dx\,dy\,dz\left[\frac{\partial F_x}{\partial x} + \frac{\partial F_y}{\partial y} + \frac{\partial F_z}{\partial z}\right]$$

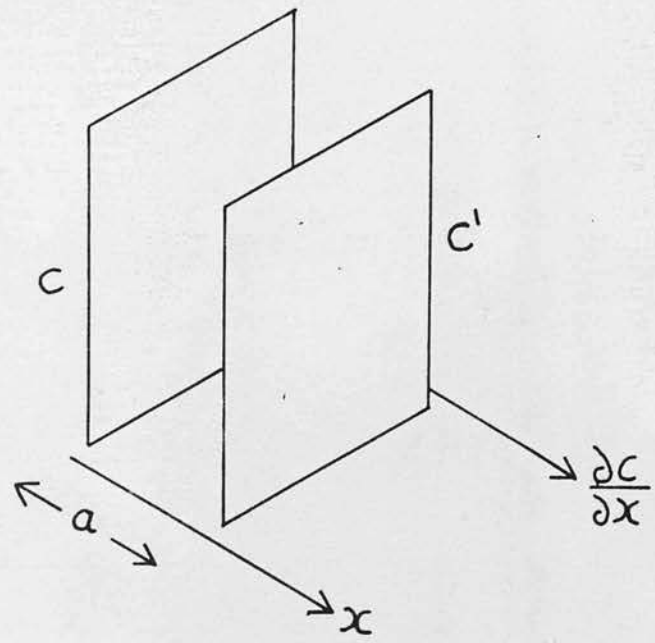

Fig.(3). The Derivation of Fick's First Law.

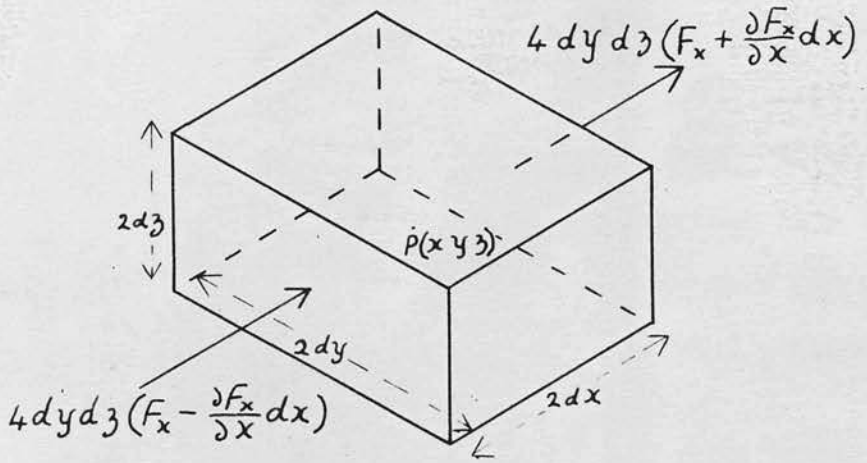

Fig.(4). The Derivation of Fick's Second Law.

This rate is also $V \frac{dC}{dt}$

$$\therefore \frac{\partial C}{\partial t} = -\left[\frac{\partial F_x}{\partial x} + \frac{\partial F_y}{\partial y} + \frac{\partial F_3}{\partial 3}\right]$$

But Fick's Law shows

$$F_x = D_x \frac{\partial C}{\partial x} \qquad F_y = D_y \frac{\partial C}{\partial y} \qquad F_3 = D_3 \frac{\partial C}{\partial 3}$$

and if the diffusion coefficient D is independent of direction

$$\frac{\partial C}{\partial t} + D\left[\frac{\partial^2 C}{\partial x^2} + \frac{\partial^2 C}{\partial y^2} + \frac{\partial^2 C}{\partial 3}\right] = 0$$

For the case of diffusion in one dimension :

$$\frac{\partial C}{\partial t} = D \frac{\partial^2 C}{\partial x^2}$$

This is Fick's second law of diffusion.

In the present investigation the diffusion from a thin layer on the plane, free surface of a metal, into the metal was analysed. Mean depths of diffusion in the range 10^{-3} - 10^{-2} cm. were used and the useful free surface was about 1 cm. x 1 cm. so that diffusion was effectively unidirectional and directed into the metal. For this reason the last equation quoted was an appropriate description of the redistribution of material taking place during diffusion.

Crank[24] has shown that for a mass M per unit area of diffusing material initially situated on the

plane surface of the medium considered, the concentration of the diffusing material as a function of the depth (y) at time t will be

$$C = \frac{M}{(\pi D t)^{1/2}} \exp - \frac{y^2}{4Dt}$$

Chandrasakhar[25] using a statistical method obtained a similar result for self diffusion.

The above equation was that used for the analysis of the bulk diffusion data.

2.2.2. Diffusion in Grain Boundaries

Analysis of grain boundary diffusion data has been made in a number of ways. The earliest work was that of Langmuir[26] who investigated the electron emission properties of tungsten; this was followed by investigations of grain diameter effects on precision measurements of bulk diffusion at low temperatures[27]. Such work is not appropriate to the present experiment since it leads to a mean value of the grain boundary diffusion coefficient averaged over many boundaries having different orientations.

A number of methods used for the evaluation of diffusion rates in single grain boundaries are detailed below.

2.2.3. The Smoluchowski Analysis

Work on diffusion in individual grain boundaries was pioneered by Achter and Smoluchowski[28] whose approach was to assume that the concentration distribution of a tracer element within a grain boundary after diffusion was identical in form with that obtained in bulk diffusion, but was due to a much higher diffusion coefficient. The model for calculation (Fig. (5)) is, therefore, a slab of highly diffusing material separating two pieces of material having the normal bulk diffusion coefficient, and diffusion of the tracing material from the boundary into the adjoining crystals is completely forbidden.

Experimentally, the method was to determine the depths at which tracers could just be detected both in the bulk material, and in the grain boundaries.

With this analysis the fractional concentrations of the tracer will be determined by equations of the form:

$$C_{Bulk} = erfc\left[\frac{y}{2\sqrt{D\,t}}\right]$$

$$C_{Boundary} = erfc\left[\frac{y}{2\sqrt{D'\,t}}\right]$$

C = Fractional tracer concentration referred to the surface maintained at constant concentration

y = Depth

D = Bulk Diffusion Coefficient

D' = Grain Boundary Diffusion Coefficient.

If we assume that the measured end points of the tracers will be at the same fractional concentration:

$$1 = \frac{C_{BULK}}{C_{BOUNDARY}} = \frac{erfc\left[\frac{y'_{BULK}}{2\sqrt{Dt}}\right]}{erfc\left[\frac{y'_{BOUNDARY}}{2\sqrt{D't}}\right]}$$

y' = Depth at Limit of Detection of Tracer.

$$\therefore \sqrt{\frac{D'}{D}} = \frac{y'_{BULK}}{y'_{BOUNDARY}}$$

Since all parts of the specimen will be annealed for the same time.

The Smoluchowski treatment leads to a very simple analysis of the problem for diffusion from a source of the tracer of effectively infinite thickness. For any other situation, such as the diffusion of the tracer from a thin surface layer, a diffusion dependent multiplying term would be required, as well as the exponential one, to describe the concentration contour and a slightly more complicated analysis would be necessary.

It is obvious that the assumption that diffusion does not take place between the grain boundary and the adjoining crystals is untrue; however, provided the ratio $\frac{D'}{D}$ is high enough, an atom in the boundary may be expected to make many jumps before leaving it. The Smoluchowski method is therefore quite justified provided the temperature is low enough to give a large ratio of $\frac{D'}{D}$. Since interdiffusion must always take

place it is worthwhile to note that analysis by the above method will always suggest an excessively low value for D' ; it has been used mainly to investigate orientation effects in grain boundary diffusion in which only relative figures are required. As used by Smoluchowski and his coworkers this method was very powerful since they were able simultaneously to analyse the relative diffusion in a number of grain boundaries of differing orientation; but they did not evaluate boundary diffusion rates as detailed above. If this is done using their figures, ratios D'/D of $\sim$ 10 are found.

2.2.4. The Fisher Analysis

A more precise analysis of the problem of grain boundary diffusion was made by Fisher[29] who made allowance for the transport from the grain boundaries into the grains. His method was to set up the differential equation describing the concentration of tracing material in and around the boundary assuming that the boundary was a sheet of high diffusivity material (Fig. (6)), and to solve this numerically, on a fairly coarse grid, using reasonable values for the diffusion coefficients and boundary width. For this calculation he assumed that the boundary tracer concentration changed so slowly with depth that diffusion into the grains could be considered perpendicular to the boundary. Examination of his numerical solution showed that the

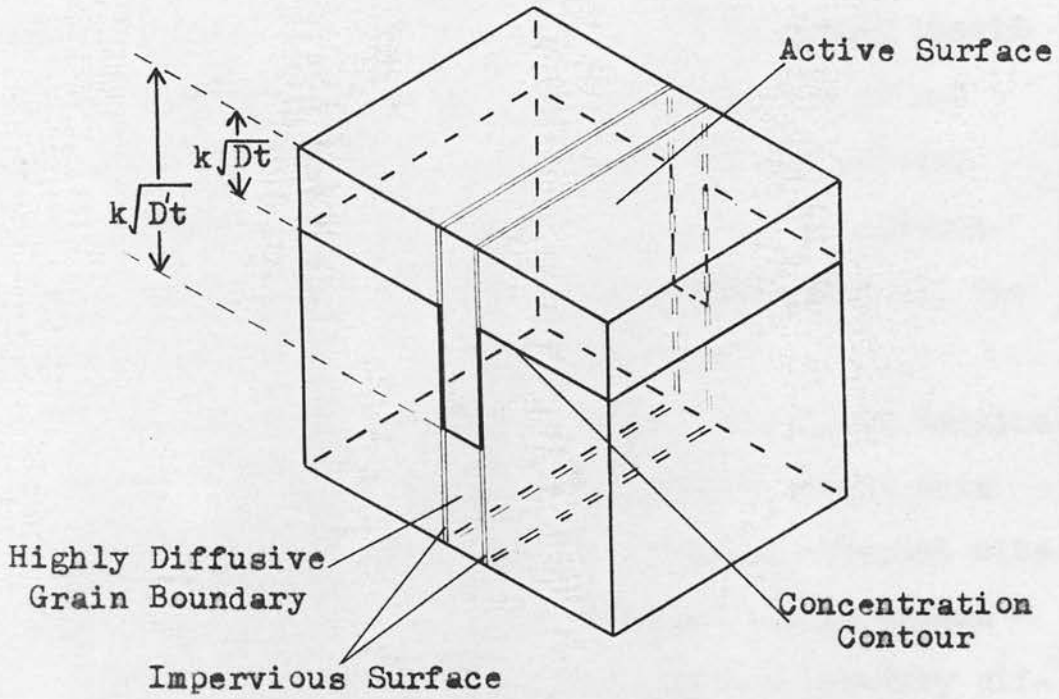

Fig.(5). Smoluchowski's Model for the Calculation of Grain Boundary Diffusion.

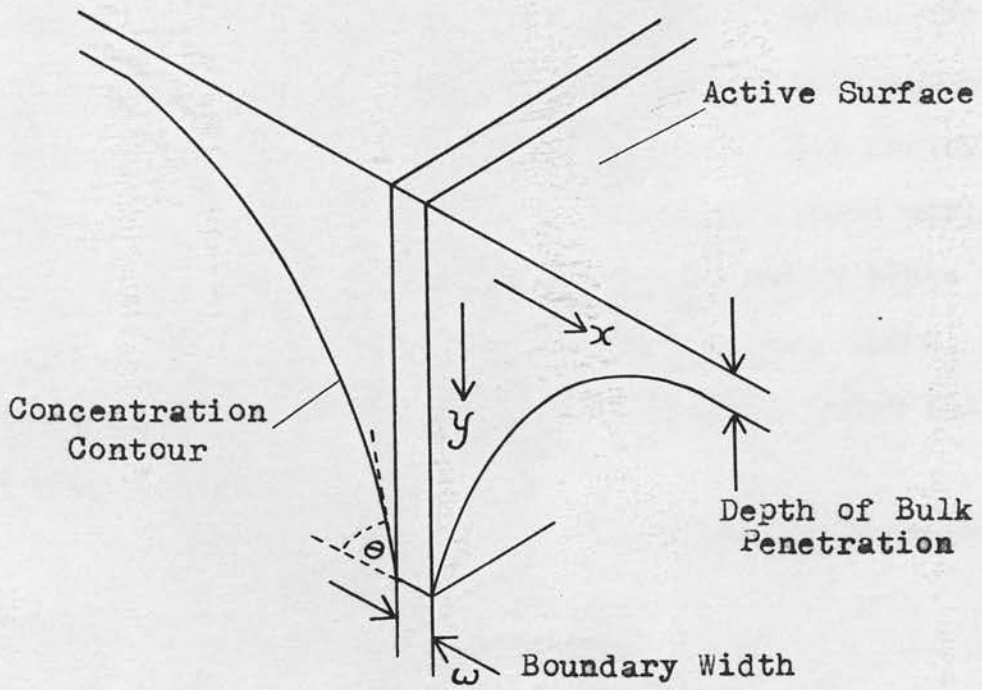

Fig.(6). Fisher's Model for the Calculation of Grain Boundary Diffusion.

concentration of tracer material in the boundary itself rose rapidly to a value close to the final value and suggested that an analytical solution to the problem might be obtained by assuming that the tracer concentration was fixed at its final value throughout all the diffusion.

In terms of atomic motion, this theory will require that an atom in the plane of the boundary should move by a thermally activated jump either to an adjacent site in the boundary or in the bulk lattice. Jumps within the boundary require small energy, that of boundary diffusion, while jumps out of the boundary have an energy of activation intermediate between those of boundary and bulk diffusion. Since the boundary is assumed very narrow, and atoms in it may be regarded as having properties appropriate both to the boundary and to the bulk lattice, it is reasonable to assume this second energy equal to that of bulk diffusion. Any deviation from this simple two activation energy picture would be very difficult to demonstrate experimentally since the other parameter of the system, the boundary width, is unknown and is merely assumed to be about twice the lattice parameter.

Fisher showed that the boundary tracer concentration C' was defined by:

$$\frac{\partial C'}{\partial t} = D' \frac{\partial^2 C'}{\partial y^2} + \frac{2D}{\omega} \left(\frac{\partial C}{\partial x} \right)_{x=0}$$

where C = concentration in bulk material

ω = boundary width $\sim$ 2(lattice parameter)

y = depth from surface

x = perpendicular distance from boundary plane

where the first term represents diffusion down the boundary and the second diffusion from the boundary into the adjoining lattice.

Since the boundary concentration is to be independent of time, at a given depth the concentration at any point will be given by an equation of the form

$$C = M(y)\, erfc\left(\frac{x}{2\sqrt{Dt}}\right)$$

Here, the second term is that for bulk diffusion from a source of constant concentration, and M(y) is the boundary concentration. Using the condition that the grain boundary concentration is constant in time and substituting the above equation into the original differential equation we have:

$$\frac{\partial^2 M}{\partial y^2}\cdot\frac{\omega^2 D'}{D} - \frac{2M\omega}{\sqrt{\pi D t}} = 0$$

$$\frac{\partial^2 M}{\partial y^2}\cdot\frac{\omega D'}{2D}\sqrt{\pi D t} - M = 0$$

And expressing the concentration as a fraction of that at the surface this leads to the condition that:

$$M = exp\left(-y\sqrt{\frac{2D}{\omega D'\sqrt{\pi D t}}}\right)$$

and

$$C = exp\left(-y\sqrt{\frac{2D}{\omega D'\sqrt{\pi D t}}}\right) erfc\left(\frac{x}{2\sqrt{Dt}}\right)$$

Since analysis of diffusion data must normally be done using some form of sectioning technique, it is necessary to integrate this expression to correspond with the experimental slices. The amount of tracer between the depths y and y + dy, and spread over all distances from the boundary is:

$$Q = \int_V C\,dV = \int_y^{y+dy}\int_{-\infty}^{\infty} C\,dx\,dy$$

$$\therefore \quad Q \sim \frac{\sqrt{Dt}}{\omega}\, exp\left(-y\sqrt{\frac{2D}{\omega D'\sqrt{\pi D t}}}\right)\Delta y$$

The mean concentration in a section $\underline{C}$ is thus:

$$\underline{C} = \frac{Q}{\Delta y}$$

$$\therefore \quad \underline{C} \sim \frac{\sqrt{Dt}}{\omega}\, exp\left(-y\sqrt{\frac{2D}{\omega D'\sqrt{\pi D t}}}\right)$$

and $$\frac{d\,Log_e \underline{C}}{dy} = -\left(\frac{2D}{\omega D'\sqrt{\pi D t}}\right)^{1/2}$$

In this treatment of the problem the effect of bulk penetration of tracer elements has been ignored. It is evident that the above equation can be applied only at depths from the surface so great that the tracer concentration due to this will be negligible. If measurable effects due to grain boundary diffusion

are to be examined it will be necessary to arrange that the depth of bulk diffusion is relatively small compared with that of grain boundary diffusion. Experimentally this means that low temperatures and long annealing times must be used.

The application of Fisher's equation to diffusion measurement by analysis of a concentration profile is obvious, but it is of interest to note two other modes of application. Le Claire[30] has noted that by differentiating Fisher's concentration equation to obtain $\frac{dy}{dx}$ at $x = 0$ we find that

$$\frac{D'}{D} = \frac{2}{\omega}(\pi D t)^{\frac{1}{2}} \tan^2\theta$$

where θ is the angle between the surface and the line of constant concentration whose gradient we are measuring. Such a line may be found by etching, or noting the limits of detection in an autoradiograph.

Yukawa and Sinnott[31] have noted that the depth of boundary penetration at some fixed concentration should, according to Fisher, be proportional to t and it would be possible to determine the rate of boundary diffusion from the constant of proportionality by annealing for different times.

2.2.5. The Whipple Method

A mathematically more rigorous method than that of Fisher was suggested by Whipple[32]. In this the effect

of bulk diffusion through the grains is assessed. As before the equation for diffusion in the boundary is:

$$\frac{\partial C'}{\partial t} = D' \frac{\partial^2 C}{\partial y^2} + \frac{2D}{\omega}\left(\frac{\partial C}{\partial x}\right)_{x=0}$$

and for bulk diffusion, Fick's equation is used:

$$\frac{\partial C}{\partial t} = D \nabla^2 C$$

The approach used is to calculate the lines of equal tracer concentration.

In its simplified form the final solution is:

$$C = erfc\,\eta + \frac{\eta}{\sqrt{\pi}}\int_0^{\pi} exp\left(\frac{-\eta^2\gamma^2}{4}\right) erfc\,\frac{1}{2}\left(\frac{1}{\gamma^2\beta} - \frac{1}{\beta} + \xi\right) d\gamma$$

where

$$\xi = \frac{x - \frac{1}{2}\omega}{\sqrt{D t}} \qquad \eta = \frac{y}{\sqrt{D t}} \qquad \beta = \left(\frac{D'}{D} - 1\right)\frac{\omega}{2\sqrt{D t}}$$

This solution is relevant for $\frac{D'}{D} >> \frac{y}{\sqrt{D t}}$

Turnbull and Hoffman[33] have evaluated their results using an integrated form of the above equation and also using Fisher's equation. They found that their answer for D' using Whipple's equation was 3.4 times that for the other method.

For the present work in which the precision is not very high and where only a calculation of an activation energy for the diffusion process will be of value, the difference between the two methods is not significant, although Whipple suggests that the Fisher equation is in error.

2.2.6. The Calculations of Borisov et al.

A detailed analysis of the above equations has been made by Borisov, Golikov, Ljubov, and Shtsherbedinsky[34] who show that the Fisher and Whipple equations are in fact compatible. They suggest that the Fisher equation could be made more precise by modification to the form:

$$\frac{\omega}{2}\left(\frac{D'}{D}-1\right)=0{\cdot}185\left(\frac{d\,Log_{10}\,C}{dy}\right)^{-2}(Dt)^{\frac{1}{2}}$$

which gives results differing from those of Fisher by a factor $\frac{185}{105}$. They have also examined the range of validity of this equation and shown that it is adequately precise provided that, at the penetrations used, :-

$$\frac{2\sqrt{Dt}}{\omega\,\frac{D'}{D}} \ll 0{\cdot}45+0{\cdot}32\,\frac{y}{(Dt)^{\frac{1}{4}}\left(\frac{\omega D'}{2D}\right)^{\frac{1}{2}}}$$

2.3. The Experimental Conditions

2.3.1. The Choice of Diffusing System

The requirements of the material into which diffusion was to be studied were:

1) The slip system should be a simple one.
2) It should be possible to grow precisely oriented bicrystals with flat boundary planes.
3) The temperature range for measurable diffusion should be reasonable (i.e. $< 1{,}000^{\circ}C.$)
4) Comparison data from other experiments should be available.
5) It should be possible to prepare flat unworked surfaces from which to measure the diffusion.

The materials best satisfying these requirements are copper, silver, gold, and zinc. Of these copper is to be preferred, since for it only are there comparison measurements both of sliding phenomena and of grain boundary diffusion phenomena. It also has the advantage over the others that it may readily be etched and polished in non-toxic solutions.

It was decided to measure diffusion using radioactive tracers. Three methods of measurement of the amounts of tracer at given depths were considered; namely lathe sectioning, chemical sectioning, and autoradiography. Facilities were not available for turning radioactive specimens so this method could not be used. Chemical sectioning is unsuited to grain boundary work since perfect uniformity of attack of the polishing solution on and off the grain boundary can not be assumed. The autoradiographic method was therefore chosen despite its known marginal resolution and its unsuitability for mathematical analysis.

In deciding the tracer element to be used the properties to be considered were:

1) Metallurgical suitability.
2) The half life of the radioactive component.
3) The predominant energy of the emitted radiation.
4) The specific activity.
5) The suitability for application to the specimen surface.
6) Health hazard.

The rate of diffusion in grain boundaries is such that suitable measurements of it may be made only after anneals of some 100 hours, and suitable exposure times for autoradiographs are in the range 10 - 100 hours. If excessively strong initial source strengths are to be avoided it is necessary therefore to use radioactive isotopes having half-lives of at least 500 hours, and half lives of about a year are advantageous since they allow repeated autoradiographs to be made. For this reason the radioisotopes of copper and gold, (Cu^{64} and Au^{198}) are not suitable for use. The radioisotopes of nickel, silver, antimony, and zinc all have suitable half-lives but those of nickel and silver (Ni^{63} and Ag^{110}) are best for autoradiography since their emitted radiation is largely of low energy β-particles.

There is little difference in the properties of Ag^{110} and Ni^{63} as far as this experiment is concerned, and Ag^{110} was finally chosen as the tracer element because a somewhat shorter neutron irradiation was required to obtain a suitable specific activity.

A system of self diffusion would have been preferred to one of mixed diffusion, and the silver system was considered, but it was decided that the relative ease of chemical polishing and etching in copper, combined with a knowledge of its sliding characteristics from previously reported work[35] was a weighty argument in favour of the copper system. Also, silver self

diffusion may be an abnormal system (see Gertsriken[36] and Arkharov[37]).

The system finally investigated was the diffusion of small quantities of silver containing Ag^{110} into bi-crystals of copper.

2.3.2. The Choice of Diffusing Conditions

The framework of information already known about diffusion and slide in grain boundaries into which an investigation of these combined effects must be fitted is as follows:

1) Grain boundary diffusion coefficients vary with temperature as do bulk diffusion coefficients, i.e. :

$$D' = D_o' \exp - \frac{Q}{RT}$$

The multiplier D_o' is effectively unity and the activation energy Q is $\frac{1}{2}$ to $\frac{2}{3}$ that for bulk diffusion.

Thus these diffusion coefficients diminish with diminishing temperature but their rate of reduction is less than that for bulk diffusion. At low temperatures therefore, we have low grain boundary diffusion coefficients, but their ratios with respect to those of bulk diffusion are high.

2) Measurements of grain boundary diffusion coefficients can be performed within a limited range of temperature. At high temperatures grain boundary tracer penetration is masked by bulk diffusion in the adjacent

lattice and in most investigations a ratio of diffusion coefficients $\frac{D'}{D}$ of about 10^6 has been required for reasonable measurement. At low temperatures the absolute value of the grain boundary diffusion coefficient is too low for a significant mean penetration depth to be reached in a reasonable time, and the total effect is beyond the limits of the detection technique.

3) Grain boundary diffusion coefficients vary with the misorientation of the grains used. At low misfit angles enhanced tracer penetration down grain boundaries cannot be detected against the bulk penetration. At higher angles some additional penetration is found and a maximum is reached at the maximum angle of misfit. The form of the angular variation is not peaked, a broad maximum being found[9].

4) When grain boundaries are caused to slide it is found[38] that voids are formed in them. The fractional length of any grain boundary section occupied by voids is proportional to the frequency of voids in it, and this frequency depends on the sliding which has taken place. Voids are not found for slide distances of less than about 20μ, but beyond this they appear with a frequency varying approximately linearly with slide. Separation occurs at about 150μ of slide.

From these observations it is possible to deduce reasonable conditions from which to start an experiment on diffusion in sliding grain boundaries. In the silver/

copper system, using the data of Achter and Smoluchowski[9], it is found that with a temperature of 725°C. and an annealing time of 5.10^5 sec. the extremities of measurable penetration are 550μ in the boundary and 200μ in the bulk penetration. Similarly, in silver self-diffusion[20] at a temperature of $(725 + 273)\frac{T_{m\,Ag.}}{T_{m\,Cu.}} = 637°K.$ we find that $\sqrt{Dt} = 25\mu$ and $\sqrt{\frac{\omega D'}{2D}}\sqrt{\pi D t} = 50\mu$. If we assume that the diffusion coefficients may approximately be evaluated from the melting points in this way, these figures confirm that analysis using autoradiographs should be possible, and the initial work was centred on this annealing time and temperature.

All bicrystals were oriented so that the crystals had a common [100] direction, and the misorientation was by rotation about this direction. The misorientations used were approximately the minimum value of 0° and the maximum of 45°, the second value being chosen since, being on a maximum, it is the setting least critical of errors in orientation. Using these values any enhancement of diffusion might be detected, either by finding tracer penetration where it would not normally be found, or by measuring differences in penetration. Of the two types of boundary the low angle one might be expected to show an effect more obviously, but the high angle one was considered the more essential since, in

the event of a nil result, only it provides a check (the measured value of the diffusion coefficient) that the system of detection is adequate.

Since annealing times of $\sim 10^6$ sec. were required and the boundaries were expected to rupture at about 150μ of slide, the rates of strain applied were of up to 0.5μ/hour. Constant slide rates were to be preferred, so a straining device using constant load would probably not have been satisfactory and a mechanically driven straining machine was used.

CHAPTER 3

APPARATUS AND EXPERIMENTAL TECHNIQUE

3.A. Metallurgical Aspects of the Work

3.A.1. The Crystal Furnace and Crucibles

The crystals used in the experiments were grown by the Bridgman method from specpure copper strip, supplied by Johnson Matthey, in the vacuum (10^{-4} mm. Hg.) furnace shown in Fig. (7) and Plate (1).

In this machine the heating element was of molybdenum wire wound on a recrystallised alumina tube surrounded by four radiation shields, the outer one of which was water cooled. A power dissipation of 3K.V.A. was used to produce a peak temperature of 1,400°C. and a temperature gradient of about 100°C./cm. ; and a suitable dropping rate for the crystals was found to be about 10 cm./hour. Under these conditions it was possible to grow single or bi-crystals with almost complete reliability.

Since a large number of crystals was to be made, a motor driven Variac transformer was used to raise the furnace temperature to the required value, at which point the motor was switched off by an Ether controller regulated by a Pt./Pt.13% Rh. thermocouple touching the furnace windings. The heating time was arranged to be

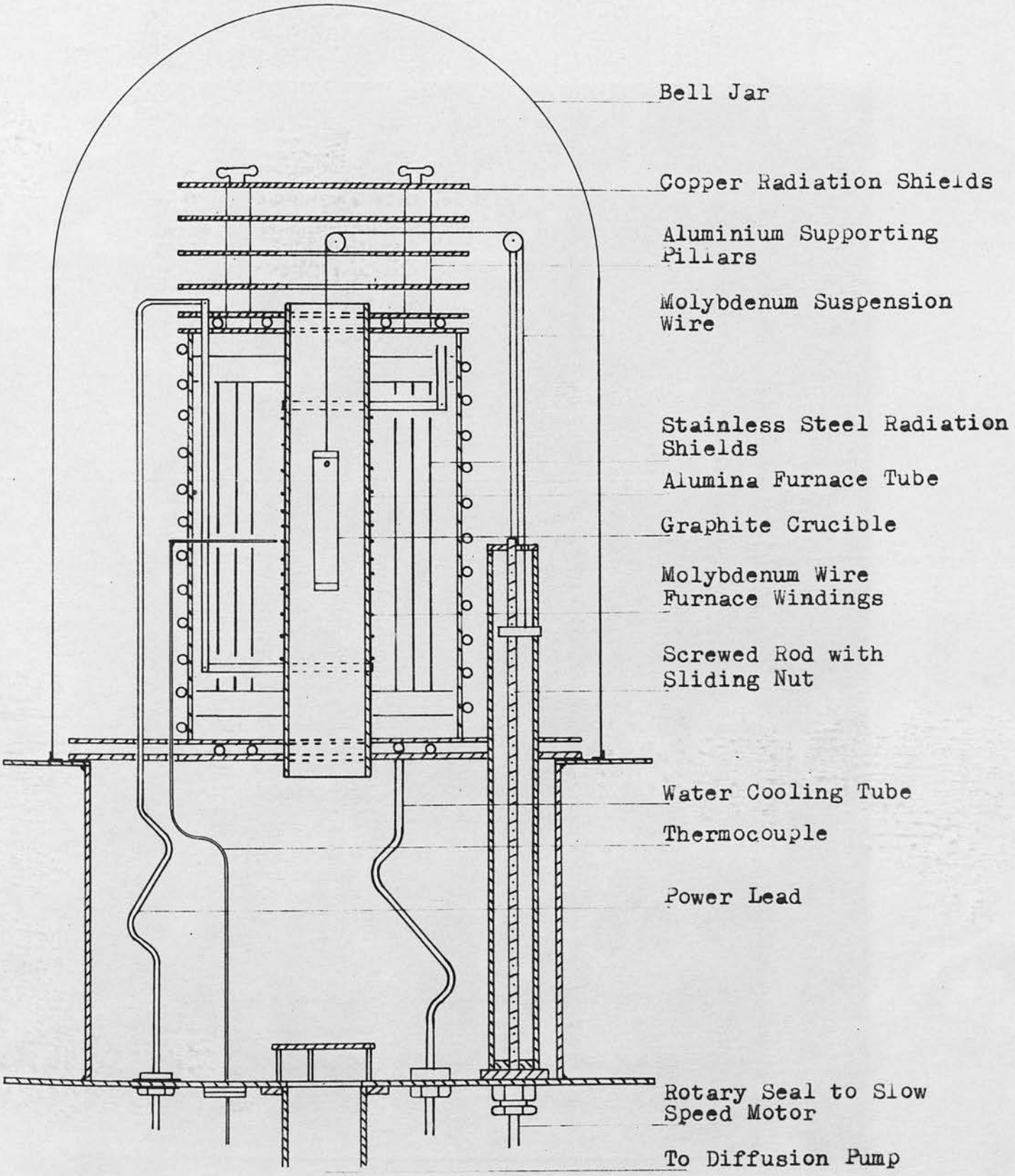

Fig.(7). Single Crystal Vacuum Furnace.

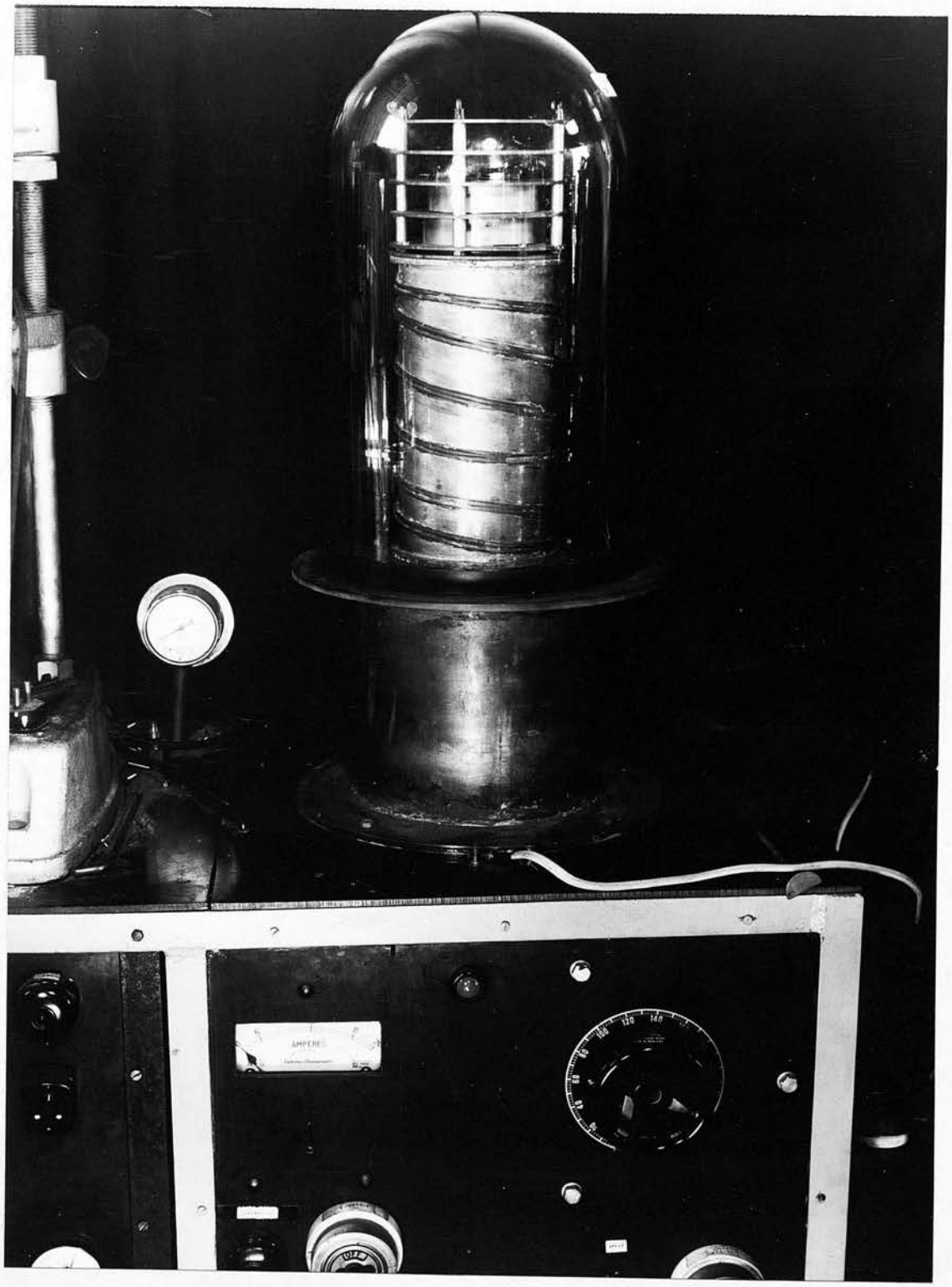

Plate (1). Single Crystal Vacuum Furnace

5 hours so that the rate of outgassing was never excessive. Time switches were used to control the dropping motor and to switch off the furnace.

By the common standards of crystal growth[39] the peak temperature is somewhat high and the dropping rate low, but it was found that these values produced single crystals of good quality, and bi-crystals in which the boundary was very straight. In trials using more conventional conditions some waviness was always found in the line of the boundary. It was noted that in such irregular bi-crystals variations in orientation of some 2° were often present in the individual crystals. The crystals used in the experiments showed no such variations in orientation throughout their lengths, and it is considered that short range irregularities of 1° would have been detected in the orientation tests.

Difficulty was expected in producing grain boundaries whose plane contained the normal to the crystal faces, and systems to force the boundary into this plane using moulds in which the required boundary plane had a reduced cross-section were considered. They were found to be unnecessary in practice, provided the edge of the graphite mould at which the seed crystals met was kept sharp and in the required boundary plane. No special effort was made to measure this form of grain boundary offset, as it is regarded as one of the less important misorientation effects, but an offset of 5° would certainly have been detected.

All crystals were grown in graphite crucibles of the split type (Plate (2)). These proved reliable in use and only once did one of them start to initiate spurious crystals of the wrong orientation. A necessary precaution, when using these crucibles for crystals of large cross-section, is to ensure that the edges are tightly closed. If this is not done, metal evaporates through the join and crystals of varying orientation result; in bad cases marks due to the dropping of metal to compensate for that evaporated are found. A number of crystals of variable orientation were made before evaporation was suspected as a possible cause of the effect. After this very tight end pieces were used on the crucibles and crystals of constant orientation were obtained without further trouble. Perfection in crystals grown in such moulds is quite critical of this effect as only a slight amount of evaporation seems sufficient to spoil them.

3.A.2. Crystal Growth.

Four separate crystal growing operations were necessary to produce the crystals of copper used in the experiments. Randomly oriented single crystals 10 cm. long and 2 mm. diameter were grown in threes in graphite crucibles packed with alumina powder. The orientations of these crystals were determined, and a length of about 6 cm. was bent onto a [100] direction of the remainder of the crystal. Pairs of such crystals were packed with

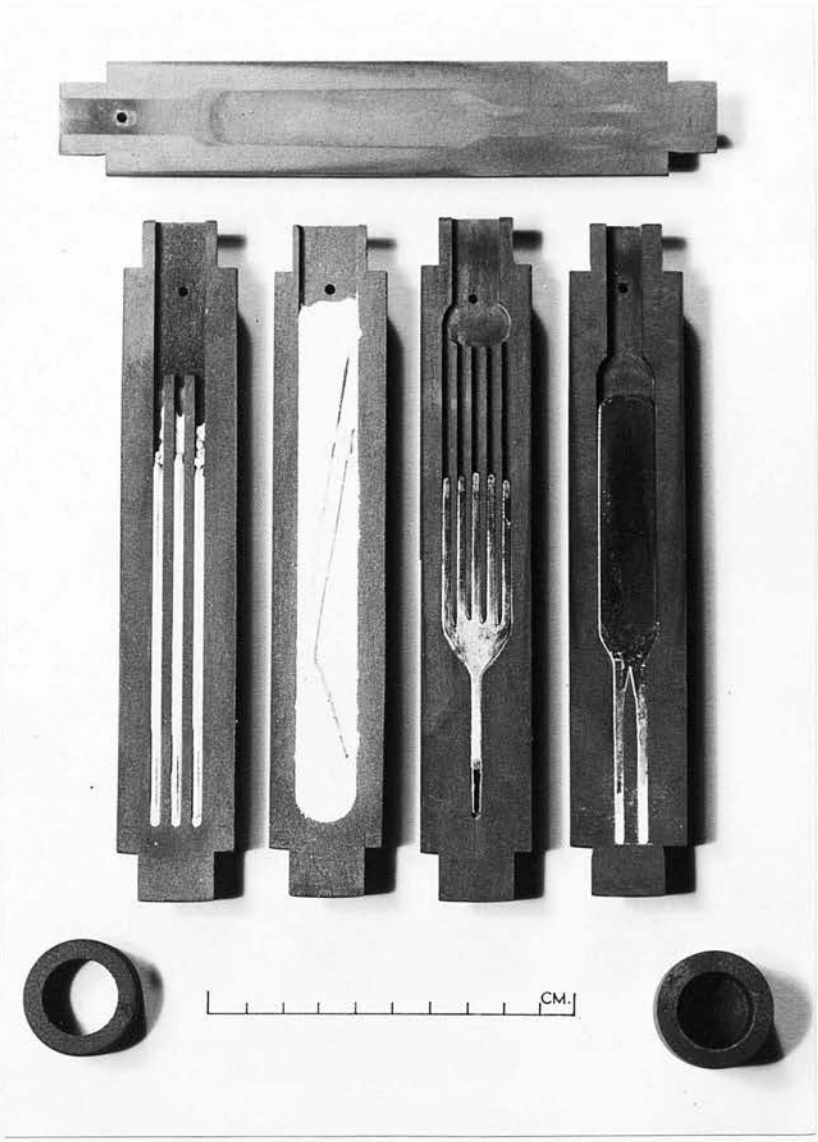

Plate (2). Crucibles.

alumina into crucibles and the main lengths regrown to form [100] axis crystals, using the shorter parts as seeds. These crystals were of circular cross section and proved difficult to mount in the graphite crucibles for use as bicrystal seeds, so they were used as seeds for crystals of square section, the former seed part of the crystal being bent into the upper part of the crucible and used as a support to prevent rotation of the seeds after setting. By suitable twisting of the upper part of the seed the [100] direction could be set at the required angle from the normal to the crucible face, and the square section crystals were grown in fives from the lower part of the seed.

Two such square section crystals were used as seeds for the bicrystals, one being inverted with respect to the other to produce the required misorientation in an accurately symmetrical way. Using square seeds of this sort, bicrystals of precisely determined orientation could consistently be grown.

3.A.3. The Determination of Crystal Orientation

All the orientation work necessary to make bicrystals was done using an etching technique. It was found that by etching copper in the mixture recommended by Barrett[40],

Etching Solution

One part concentrated hydrochloric acid

One part water

Mixture saturated with hydrated ferrous chloride.

15 minute etch

very strong reflections were obtained from the (100) faces, and weaker ones appeared from the (110) faces. These reflections were sharp and could be determined with a precision of about 1°. When a slight excess of HCl was added to the mixture it was found that the etching effect was more consistent, but it was necessary to keep the excess small or the reflection directions became rather diffuse and orientation could be determined only to about $3 - 5^{\circ}$.

An ex-R.A.F. astro-compass was used as a three circle goniometer. It was converted by removing the 'Latitude' scale and tapping a 2B.A. hole into the centre of the scale to which it had been fixed. The crystal to be examined was mounted in this hole and illuminated by a beam of parallel light. By sighting along two pointers at the image of the goniometer in a mirror it was possible to determine the positions of the [100] directions, and sometimes the [110] directions, relative to the geometrical form of the crystal. The use of a mirror made it possible to have a long light

path, and hence to obtain good angular resolution, while still being close enough to adjust the goniometer.

To form a crystal having a [100] direction axis, a randomly oriented crystal was fixed into a hollow 2 B.A. screw with Araldite and a pointer fixed to the screw perpendicular to its axis. A small mirror (2 m.m. dia.) was then fixed to the tip of the crystal with plasticene and the normal to the mirror face set along the axis of the vertical goniometer circle. The orientation of the axis was then determined from the reflection positions and the crystal set onto the [100] reflection closest to the crystal axis. By bending the outer part of the crystal with small pliers until the mirror reflected light parallel to the [100] direction in the part of the crystal closer to the goniometer, it was possible to align the main length of the crystal along a [100] direction of the other part.

The accuracy of the bending was confirmed by finding the [100] direction reflection positions for both parts of the crystal, and checking that the axis of the outer part was indeed along a [100] direction of the inner.

Square section seed crystals were grown in fives from the circular [100] direction axis crystals and were seeded so that the [100] directions, other than the axis, were misoriented from the face normals by half of the required bicrystal misorientation (Fig. (8)). This

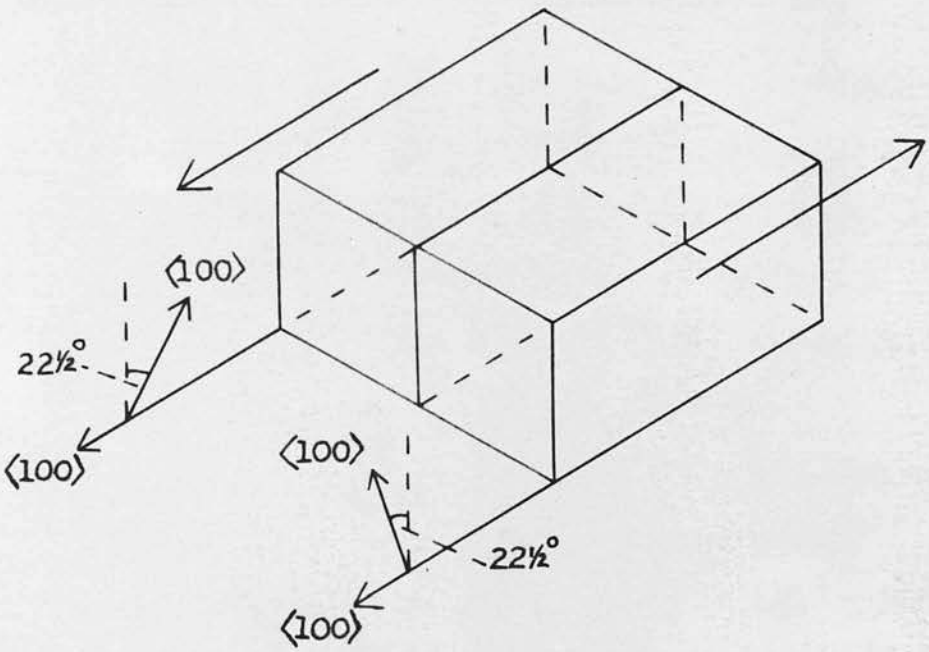

Fig.(8). Bicrystal Orientation.

setting was obtained by bending the excess length of the circular seed so that it lay in the upper part of the crucible and prevented the lower part of the seed from turning. The actual misorientation was set by mounting the crucible on the goniometer and adjusting the reflection to the correct position relative to the crucible face with the seed crystal in the crucible.

The square section seeds were used to make the bicrystals. No adjustment was possible with these seeds as they fitted the slots milled into the bicrystal crucible, but a final orientation check was made on them when they had been set in the crucible.

A check on the orientations of the bicrystals was made and all of those used were precise in axial orientation to about 3°, and in misorientation about the axis to about 2° from the required value (normally 45°).

A detailed examination of the orientation was made in a few cases and the standard deviation of the orientation determinations was found to be in the range $1 - 2^{\circ}$, so any significant variations in orientation throughout the length of a crystal should have been detected. Such variations were not found.

3.A.4. Preparation of Specimens

The bicrystals grown were 15 x 3 mm. in cross section and 7 cm. long. They were cut to the required size (15 x 12.5 x 3 mm.) by mounting them in brass tubes with paraffin wax and then cutting them off in the

sectioning device shown in Plate (3). In this machine the cutting was done by a 4"-diameter carborundum disc 0.015" thick rotating at 5000 r.p.m. Jets of water were directed onto the wheel during the cutting operation, so the whole unit was enclosed in a perspex box. As the machine was designed for use with radioactive materials also, a filter was fitted in the drainage pipe. The edges of the specimens cut with this machine were square and had a good surface showing no evidence of tearing.

After removal from the wax the specimens were cleaned in benzene and polished by dipping in a chemical polish for two minutes. The chemical polish used (due to Teggart[41]) was made up as follows:

Chemical Polish

1 part concentrated nitric acid

1 part concentrated phosphoric acid

1 part glacial acetic acid

The mixture was maintained at a temperature of 65°C.

After polishing, the specimens were inscribed with the lines used to measure the slide. As the total amount of slide was small, and as it was desired that the scratches should not initiate recrystallisation, fine light scratches were required. They were produced by a method of controlled pressure. A razor blade, free to pivot about a horizontal axis, was supported by the chuck

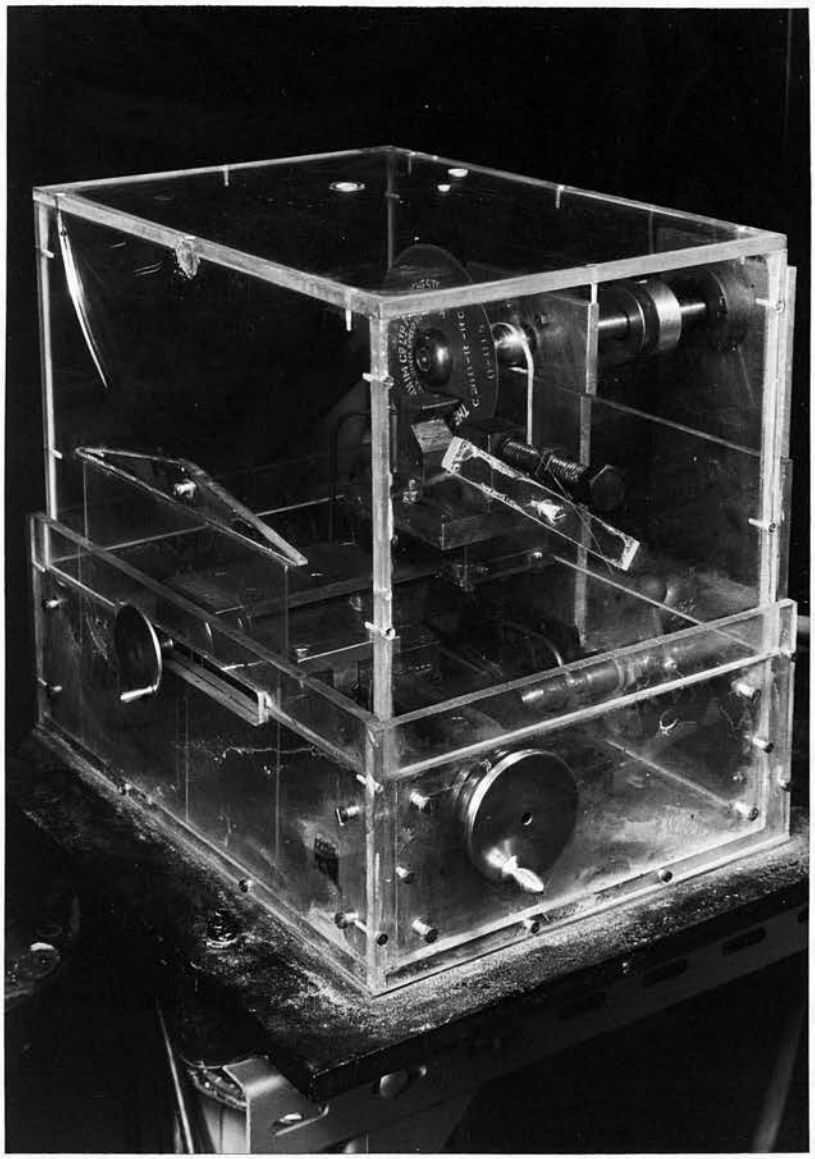

Plate(3). Slitting Wheel.

of a drilling machine and the specimen held lightly, protected with tissue paper, in a toolmaker's vice laid on the drilling table. By raising the drilling table until the specimen came into contact with the blade and then operating the traverse fitted to it, fine straight scratches suitable for measurement were obtained. It was found that a piece of plasticene weighing about 0.5 gm. fitted to the razor blade above the contact point gave the most suitable pressure. A number of scratches were made on each side of the specimens.

3.A.5. Activation of the Specimens

After polishing and marking, the specimens were coated by evaporation with a layer, some 100A thick, of silver containing Ag^{110} on the two main faces perpendicular to the boundary. This was done in the device shown in Fig. (9) which was placed in the conventional evaporator shown in Plate (4). In this system of evaporation, developed for use with most common radioactive materials[42], a ceramic crucible containing the evaporant was placed inside a glass tube. Specimens, supported by brass rails, were held just above the end of the tube and covered with a sheet of glass. The filament, in the form of a flat spiral, lay close to the bottom of the crucible. Radiant heat from the filament produced the required evaporation and caused a somewhat larger fraction of the evaporant to be deposited on the specimens than would have been obtained using evaporant

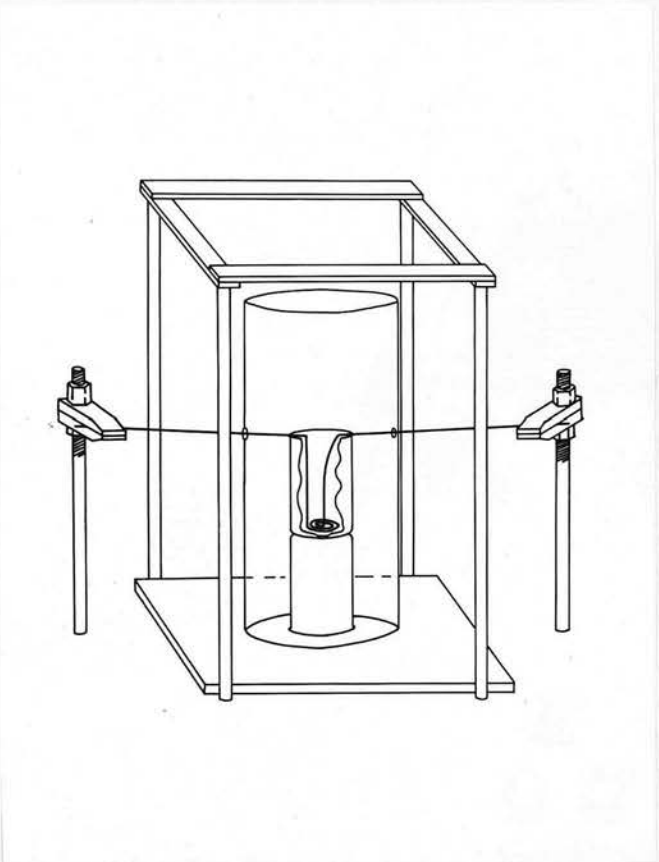

Fig. (9). Arrangement for Evaporation of Radioactive Materials.

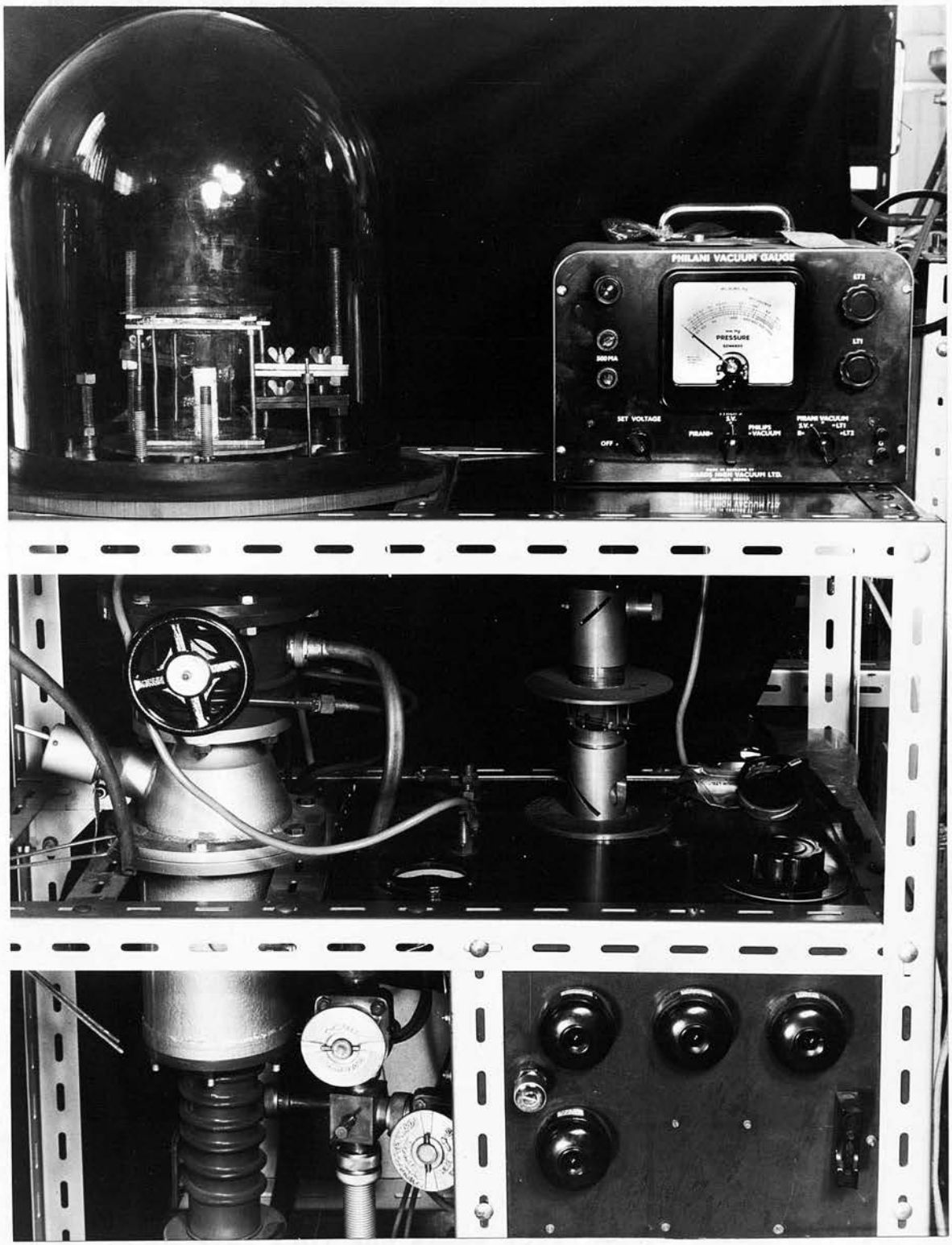

Plate (4). Conventional Evaporator Containing Device for Use with Radioactive Materials.

hung from the filament as there was no loss of downgoing material. With silver it was found that the reflectivity was too high for radiant heating so the evaporant, in the form of a wire, was hung over the filament in the normal way.

The advantages of such a system are that no decontamination is needed, since all the activated parts are cheap and can be scrapped after use, and that (with the exception of silver) evaporants can be dropped into the crucible without delicate manipulation, so that the time spend handling the radioactive materials is kept to a minimum.

To minimise the evaporation of silver from the specimens during annealing, a layer of copper some 100 Å thick was deposited over the silver layer.

The total amount of radioactivity on an activated specimen was $\sim 5\mu c$, which gave reasonable exposure times for the autoradiographs and was safe to handle during the polishing process. Experimentally this meant $\sim$ 100 counts/sec./sq. cm. of activated specimen surface on a Geiger tube held close to the specimen.

3.A.6. Construction of the Straining Machine

The apparatus used to strain the bicrystals is shown in Fig. (10) and Plate (5). An electric motor, geared to a speed of 1 rev. per hour, drove a 60 : 1 reduction worm gear through a variable speed gearbox. Attached to the wheel of the worm gear was a nut, and

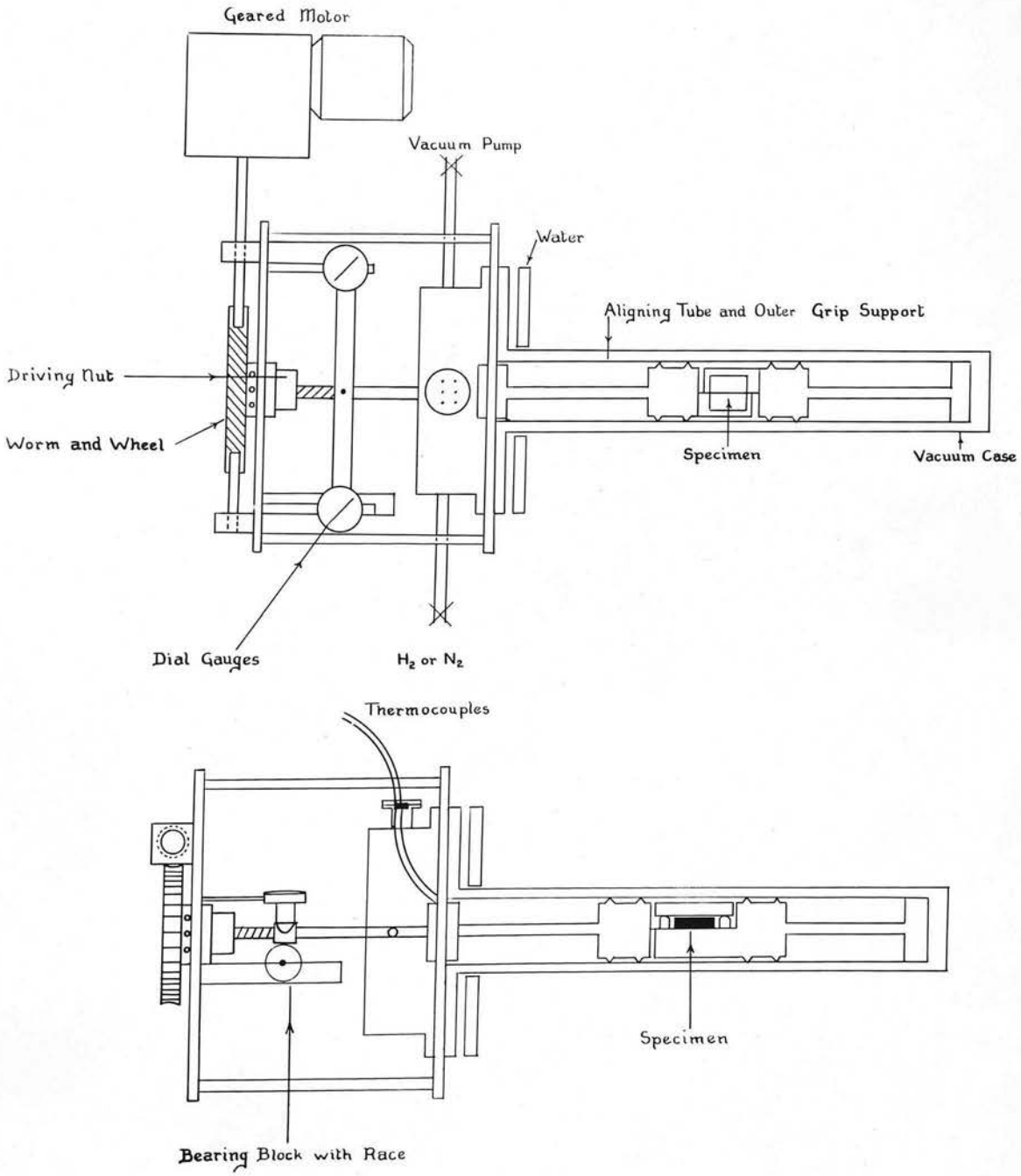

Fig. (10). The Straining Machine.

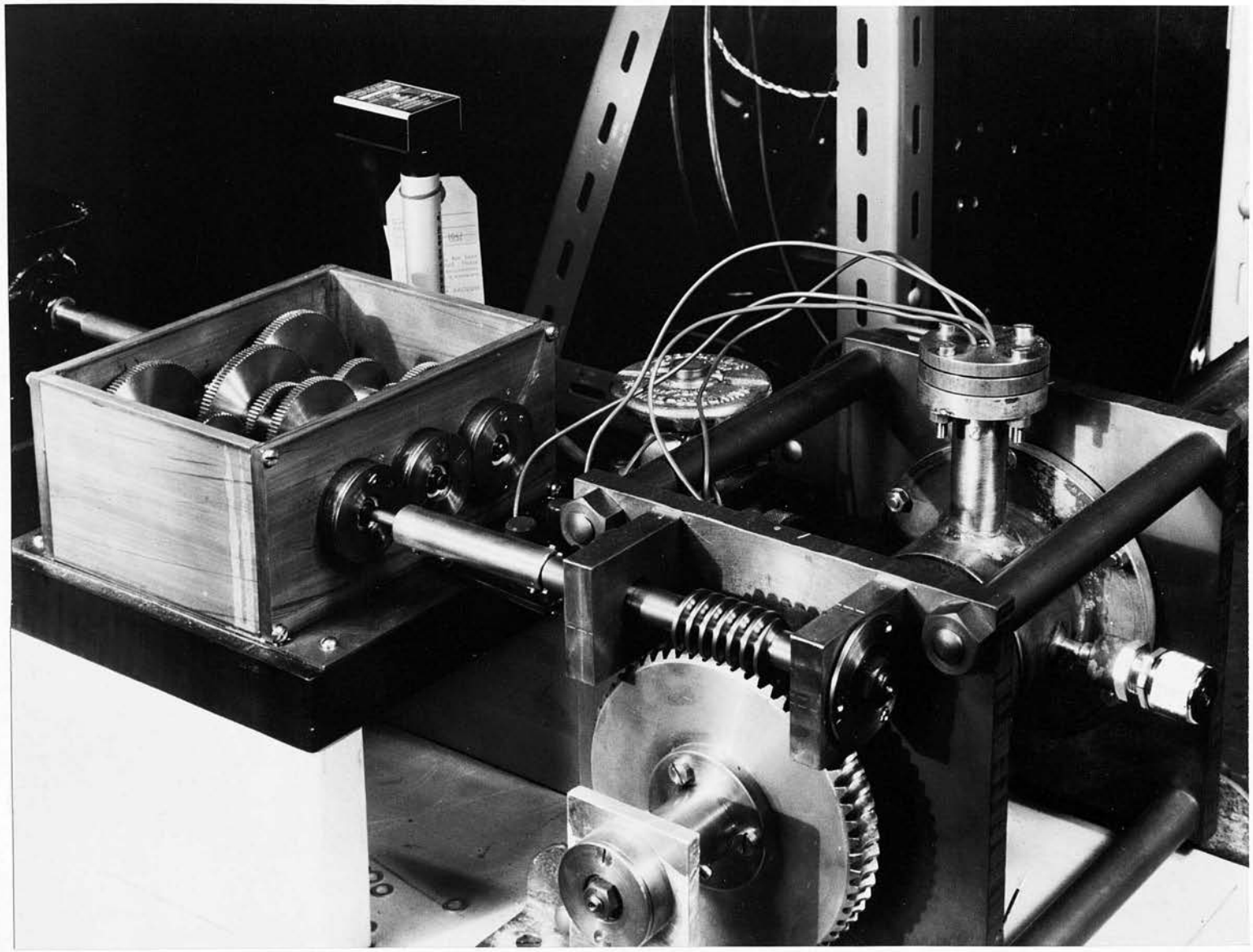

Plate (5). The Straining Machine.

the wheel and nut were secured to a $\frac{1}{2}$" thick steel plate through ball races. A second plate was rigidly bolted to the first at a spacing of 6", and through a bearing in it passed a $\frac{1}{2}$" diameter heat resistant stainless steel shaft, whose end was threaded to fit the driving nut on the other plate. This shaft was constrained so that it could not rotate, but was free to slide. Rotation of the motor thus pushed or pulled the shaft along its axis. A steel tube was fitted over the shaft and bolted to the second steel plate. Grips of heat-resistant steel were fixed to the driving shaft and to the end of the tube.

This system was very rigid due to the heavy pillars connecting the plates, the heavy driving shaft, and the outer tube, which was of $1\frac{1}{4}$" diameter and had $\frac{3}{16}$" walls. Coupling between shafts and grips was made by having the shafts a hammer fit in the grips and then securing them with taper pins. To minimise sideways motion of the grips in the tube, they were made with raised rings which were a sliding fit in the supporting tube. Slots $\frac{3}{4}$" wide and $2\frac{1}{2}$" long were milled through the tube to allow access to the grips when mounting the specimens, and further holes were drilled in the side of the tube for the thermocouples.

A vacuum casing of stainless steel was fitted over the specimen tube and sealed to the second base plate. Another case was fitted to the other side of the plate, and was fitted with the thermocouple inlets, the

pumping tube, and a seal to pass the driving shaft.

The whole assembly was mounted in a horizontal position, and a muffle furnace, using nichrome wire on a mullite tube, was arranged on rails so that it could slide freely over the vacuum casing. A reasonable temperature for the O-ring seals of the vacuum system was obtained by circulating water through a flat tank fitted tightly over the vacuum case between the furnace and the second mounting plate.

Movement in the system was recorded by two dial gauges (reading to 0.0002 cm.) secured to the driving shaft so as to measure its movement relative to the first plate.

The grips used, shown in Fig. (11), were made of heat resistant steel. Their arrangement in the mounting tube was such that they lay with their vertical, flat faces in contact, and with the serrated horizontal faces accurately in the same plane. Specimens were clamped to the grips by 2B.A. steel socket cap screws which passed through the upper plates of the grips and the copper spacers, and then were screwed into the main part of the grips. A firm grip on the bicrystals was ensured by the serrated faces of the grips and it was found that a depth of serration of 0.01" was most suitable.

The horizontal faces of the grips were milled off to below the level of the serrations over a length just greater than that of the specimens so that in a zone 3/16" wide centred on the boundary the crystals were not

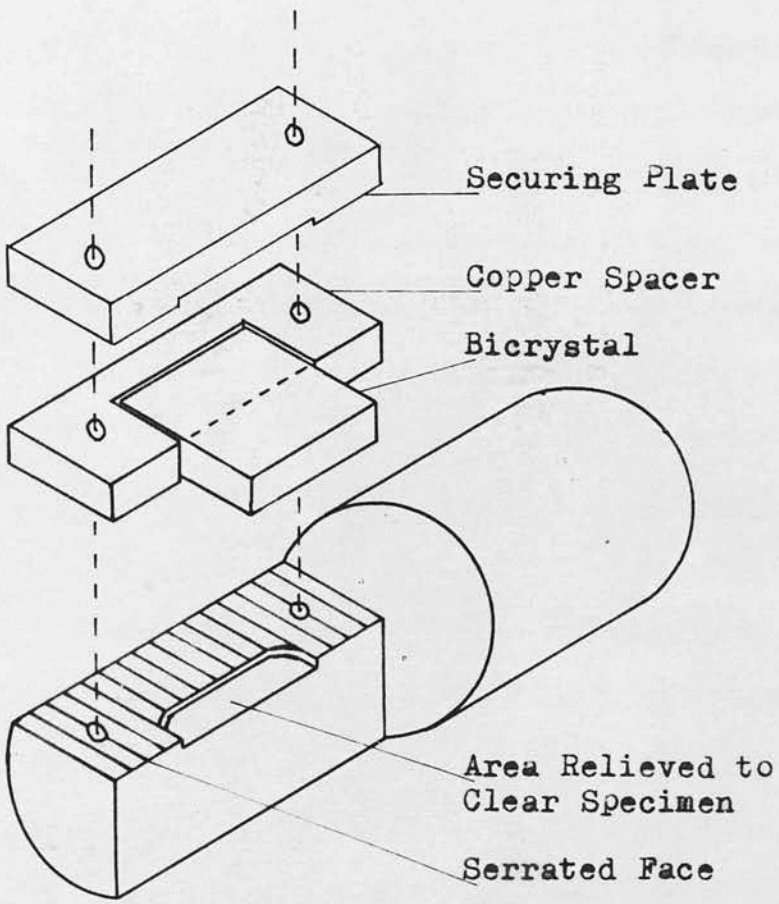

Fig.(11). Method of Gripping
Specimens.

subject to compression.

The purpose of the spacers was to keep the upper part of the grips parallel to the main face, and to determine the amount of compression given to the specimens. Copper was preferred for this purpose as it expanded under temperature in the same way as did the specimens, and could readily be reduced in thickness by chemical polishing to suit the specimen in use. Some trouble was experienced with recrystallisation but it was minimised by using spacers 0.007" thinner than the specimens. The specimens were compressed to the correct degree if the securing screws were tightened until pressure was just felt against the spacers.

Thermocouples were mounted close to the specimen to measure and control the temperature. Two Pt./Pt. 13% Rh thermocouples were led through holes in the sides of the mounting tube and lay against the copper spacers, which in turn were in close contact with the specimen. A Chromel-Alumel thermocouple was held just above the dummy specimen which lay on top of the grips, and another was fixed close to the windings of the furnace. A platinum resistance thermometer was also fitted close to the furnace windings.

3.A.7. Use of the Straining Machine

Although the grain boundaries were not visible on the polished specimen, they could generally be distinguished after the silver had been put on, if the lighting

were suitable; therefore, by suitable adjustment of a reading lamp, it was possible to check that the grain boundary lay accurately along the axis of the straining machine.

To mount a specimen in the machine its thickness was first measured and a pair of spacers manufactured 0.007" thinner. With the spacers in position the specimen was held very lightly in the machine using one grip only and the boundary position adjusted. The grip was then tightened slightly to secure the specimen, the other grip fitted, and the four fixing screws tightened a little at a time until the grips were felt to be compressing the spacers. No great pressure was ever applied. With such compression recrystallisation was reasonably infrequent, although it could not be avoided with certainty. Less pressure on the specimen resulted in slip at the grips and was quite useless.

A dummy specimen was placed on the grips between the heads of the socket-caps securing screws.

Before heating, the vacuum case was fitted and the whole unit evacuated to a pressure of 10^{-4} cm. Hg and then flushed with oxygen free nitrogen. This was done five times, and finally the case was left at a pressure of 25 p.s.i. of nitrogen.

Very great difficulty was experienced at first in bringing the specimens to temperature when anneals under vacuum were attempted. The tube and shaft which supported the specimen had similar expansion coefficients, but

when the temperature was rising the tube was necessarily hotter than the central shaft, with consequent deformation of the specimen. Two methods were used to overcome this difficulty. By using a nitrogen atmosphere for the furnace instead of a vacuum, increased heat transfer was produced between the shaft and the tube, and by cutting the heating rate to about 100°C/hour, the expansion effect was brought to a reasonable level. As it was essential to keep the heating rate fairly constant and thus have the minimum heating time for the chosen maximum heating rate, an automatic method was used to maintain the heating rate. The chromel-alumel thermocouples on the furnace windings and on the specimens were connected in series, but with their polarities reversed, so that the e.m.f. developed was proportional to the difference in temperature. The output was fed into an Ether-Transitrol, thermocouple-operated, temperature controller. The controller thus was able to control the temperature difference between the windings and the centre of the furnace. Since the heating took place by conduction from the windings to the centre of the furnace, the temperature difference thus controlled was proportional to the rate of power supply and to the rate of rise of temperature, provided the range of temperature was not too great. By making the controller short circuit a large resistor in series with the furnace, an effective on/off control was obtained, and it was found that an almost linear temperature/time graph was obtained even for

temperatures up to about 1,000°C.

The resistance thermometer fitted close to the furnace windings was used to control the steady state temperature. A Sunvic RT_2 controller, operating by short circuiting another smaller resistor in series with the furnace windings, was used with this thermometer to maintain the annealing temperature. With this controller the temperature was maintained uniform to $\pm$ 1°C over periods of up to three weeks. This controller came into action as the correct annealing temperature was reached, and left the difference controller at the ON position. When reducing temperature it was necessary only to set the temperature difference controller to a difference value somewhat below that of the steady state to obtain a linear reduction of temperature with time. Typical values for the temperature differences are 80°C for a temperature increase of 100°C/hour, 55°C for the steady state, and 30°C for a decrease of 100°C/hour.

This method of heating and cooling produced much less strain in the specimens than could have been achieved by hand, and in fact, in one test, it was found possible to heat a specimen to 950° C and to cool it again without causing slide on the boundary.

Temperatures during the anneal were measured using a Tinsley potentiometer and two Johnson Matthey Pt./Pt. 13%Rh. thermocouples. A record of the temperature rise and fall was made on a Honeywell-Brown potentiometric recorder so that time to temperature

corrections could be applied, but in fact they were never made, as the long annealing times made them negligible.

When the specimen reached temperature the straining motor was set running. Originally this motor drove the specimen through a variable ratio gearbox, but a certain amount of whip was observed in the gear shafts and it was considered necessary to use another method. Suitable driving rates were therefore obtained by using an electrically driven, interval-timing switch which ran the straining motor for a short while every few minutes. Typical switching times ranged from 5 to 120 seconds ON time, every 5 minutes. This method of varying the driving rate was preferred to the gearbox, because at the very low speeds involved (the shaft of the electric driving motor rotated at 1 revolution/hour) it seemed unlikely that the gearbox could move in any but a jumpy motion, and it was better to cause a motion consisting of a known frequency and amplitude of jump, than to chance the variable effects which might occur in the mechanical system.

The on/off mechanism seems justified when it is considered that a typical driving rate is 0.5 micron/hour and that this would be executed in 12 jumps of 0.04 microns. Although the structure of the straining machine was designed to be rigid, it is improbable that its elastic strain and that of the ungripped part of the

specimen should total to less than a few microns, so that only a relatively small fluctuation in stress on the boundary should be caused by the intermittent nature of the drive.

3.A.8. The Slide Measurements

To determine the amount of slide which had taken place in a specimen the various fiducial scratches were photographed using a Cooke M3000 microscope and the amount of slide measured off the plates. This method was preferred to the use of an eyepiece micrometer, or of the microscope slide vernier, since it gave a permanent record, and the amount of slide could not again be checked after the specimen was mounted in plastic. Such photographs are shown in Plates (6), (7), and (8).

In some test specimens significant differences in the amount of slide were found between the various scratches. Differences of as great as 10μ were found in one test specimen subjected to a total slide of 120μ, the strain being applied at a temperature of 650°C over a period of 100 hours. In the diffusion specimens this effect was not observed, but here the total slide and the slide rate were always smaller. The low angle boundary specimens may have shown this effect, but in them the maximum slide recorded was in the region 5 - 10μ and the variations found can be attributed to the coarseness of the measuring scratches.

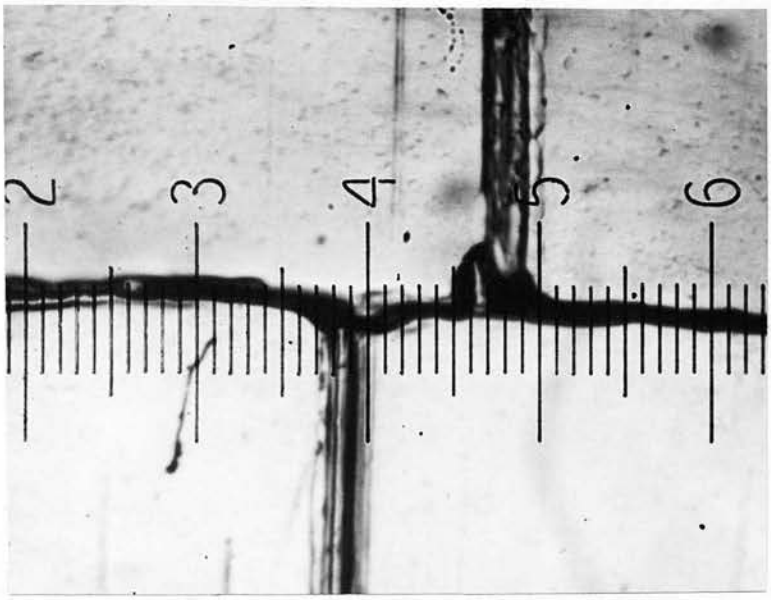

Plate (6). Grain Boundary Sliding.
Displacement 28μ : T = 731°C. : t = 3.43 10^5 sec.

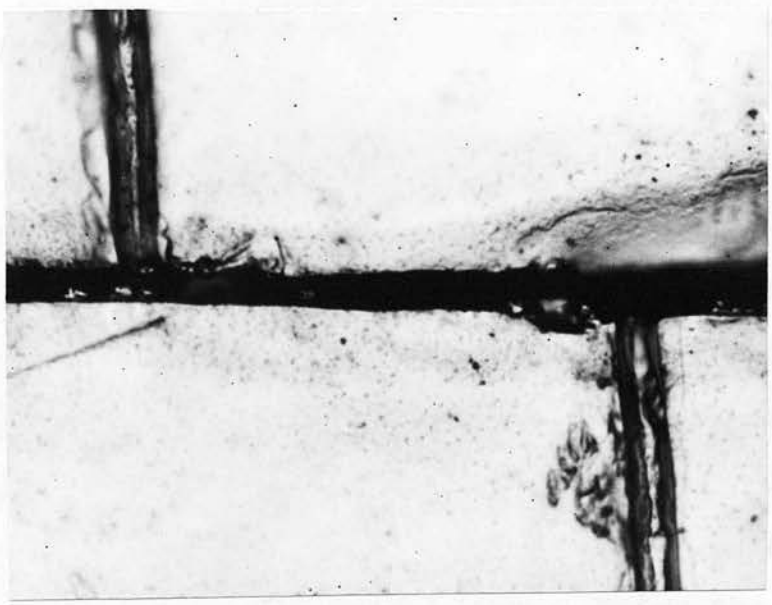

Plate (7). Grain Boundary Sliding.
Displacement 70μ : T = 623°C. : t = 9.97 10^5 sec.

The range of slide caused in the specimens was from about 10^{-3} to 10^{-1} cm. but recrystallisation occurred on all specimens having more than 7.10^{-3} cm. of slide. Plate (9) shows a specimen in which recrystallisation had taken place across the former boundary. Despite the fact that, on etching, no trace of the old boundary can be found, the slide appears to have taken place in its plane.

3.A.9. Cutting and Mounting

Specimens were cut to size for examination on the slitting wheel as described before. All cuts were made perpendicular to the common [100] direction, the specimen with slide being cut into three equal parts of 3 x 4 x 15 mm. and the dummy into two equal parts of 3 x 6 x 15 mm.

Araldite D casting resin was used as the mounting material, the specimens being cast into 1" diameter dies.

Two separate mounts were used for each specimen pair. In one mount were the two parts which had been activated on the end (3 x 15 mm.) faces, one from the dummy and the other from the specimen. These parts were mounted with the common [100] directions lying in the face of the mount and with the active edges parallel to each other and about 5 mm. apart. Using the slitting wheel, these mounts were cut parallel to the face of the die to expose the mid-sections of the specimens which

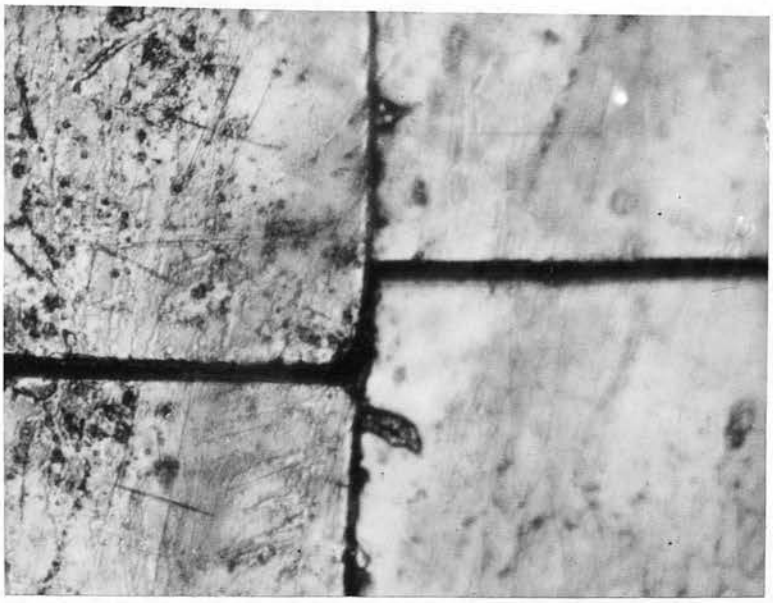

Plate (8). Grain Boundary Sliding.

Displacement 51μ : T = 517°C. : t = $2.04\ 10^{6}$ sec.

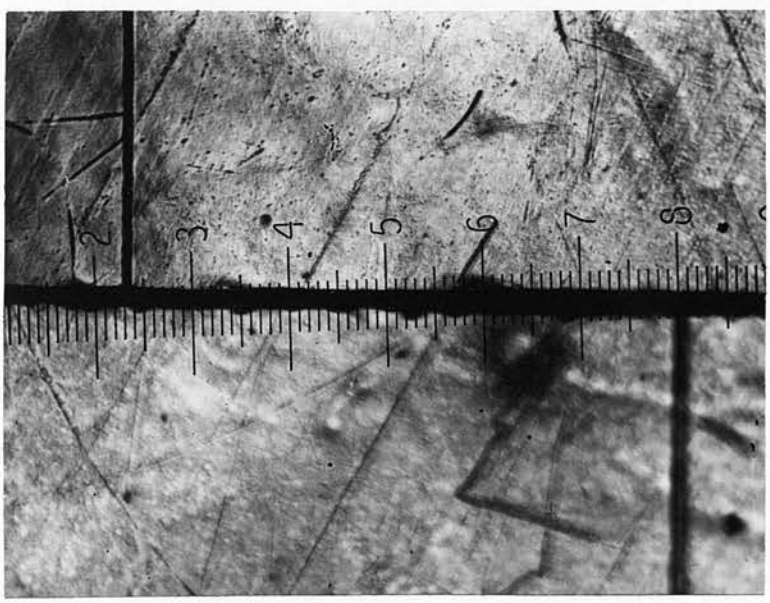

Plate (9). Grain Boundary Sliding.

Displacement 400μ : T = 725°C. : t = $5.28\ 10^{5}$ sec.

were then polished. The remaining three specimens were cast in the other mount. They were all set with the common [100] direction perpendicular to the face of the mount and were arranged with the dummy central and the other two specimens parallel to it and at a distance of about 3 mm. from it. No farther cutting was required for these mounts.

In the first type of mount, void formation was examined along the common [100] direction and parallel to the direction of slide: in the second diffusion and void formation were examined perpendicular to the common [100] direction and to the direction of slide.

3.A.10. Polishing of the Specimens

Examination of the specimens took two forms. Autoradiographs were made, and voids measured or counted. The requirements of the polishing technique were therefore, that there should be no relief between the surface of the specimen and that of the Araldite, to prevent pressure development in the autoradiographs; and that no smearing should occur, so that any voids present would be retained and radioactive material not be spread over the specimen surface.

A number of polishing routines were tried, but the first to achieve reasonably consistent success was to obtain a flat surface using a coarse grade of silicon carbide impregnated polishing paper, and then to polish successively with finer grades until a good surface was

obtained using a 600 grit. All the papers were kept wet during the polishing, partly to prevent the release of radioactive dust, and partly to prevent heating in the specimen and plastic. The specimens were carefully washed between grades to avoid the transfer of coarse grit to a finer stage.

Before starting the final polishing operation the specimens were etched, using the mixture previously described for orienting the specimens, to see if re-crystallisation had occurred. In specimens free of recrystallisation the polishing was continued: in the others an orientation check was made to see if the original crystals had been retained at one of the boundaries so that it might still be used for measurement. The dummy specimens did not recrystallise, so the mounts were still polished even when none of the original boundaries had been retained on the strained specimens.

Polishing was continued using 'Brasso' on a nylon-covered lap on a standard metallurgical polishing machine and this was followed by using 'Silvo' diluted with water to a concentration of about 1 in 10, again on a nylon-covered lap. During these operations the nylon was kept very wet with the polish, since it scratches if allowed to dry.

Because it has no pile, nylon polishing in this way produces a surface showing no relief but it was considered that the 'Brasso' might have a tendency to

cause smear. Although voids were sometimes found on the grain boundaries, results were not compatible with those reported elsewhere[38], so it was decided to resort to diamond polishing which would more certainly retain any voids present.

A method of diamond polishing commonly used for geological specimens was used. Preliminary preparation was done using silicon carbide paper as before. Double weight photographic paper was then impregnated with 5 micron grade diamond polish and sprayed with a commercial polishing lubricant. The specimen was rubbed on this until the marks of the previous process had completely disappeared. After careful washing with alcohol the process was repeated using 1 micron polish. Finally the specimen was polished using $\frac{1}{4}$ micron diamond polish on the polishing machine. The lap was covered with 'Microcloth', a commercial polishing cloth somewhat akin to felt. This final polishing operation was done using the minimum of pressure on the specimen. The final shine was obtained using a lap covered with Alumina-impregnated Selvyt cloth.

It is very difficult to obtain surfaces free from scratches using this technique, but if the process be repeated until a scratch-free run is made, the resulting surface is very good indeed.

When polished this way no relief was detectable on the specimens and the slightly smeared appearance sometimes found with the 'Brasso' was never seen and it is

asserted that any voids present in the specimens would have been detected using this polishing technique.

3.A.11. Voids

A close microscopic examination was made of all specimens to see if voids had formed on the strained boundaries. Photographs were taken of all specimens in which voids were seen, and from them it was possible to measure void frequency and length. Because the results were at variance with previously reported void formation, one specimen was polished a number of times and the voids examined. Reasonable consistency was found between the void distributions for this specimen, and it is concluded that the void distributions found are genuine and not caused by the polishing technique. Typical photographs are shown in Plates (10) to (15).

3.B. Detection and Measurement of the Tracer Material

3.B.1. Autoradiography

The chief advantages of the autoradiographic method for radioactive tracing studies are its extreme sensitivity of detection and its high spatial resolution in two dimensions: its disadvantages are the difficulties of numerical evaluation of source strength, and of providing accurate registry between specimen and autoradiograph. In common with all photographic processes, high sensitivity in autoradiography is obtained

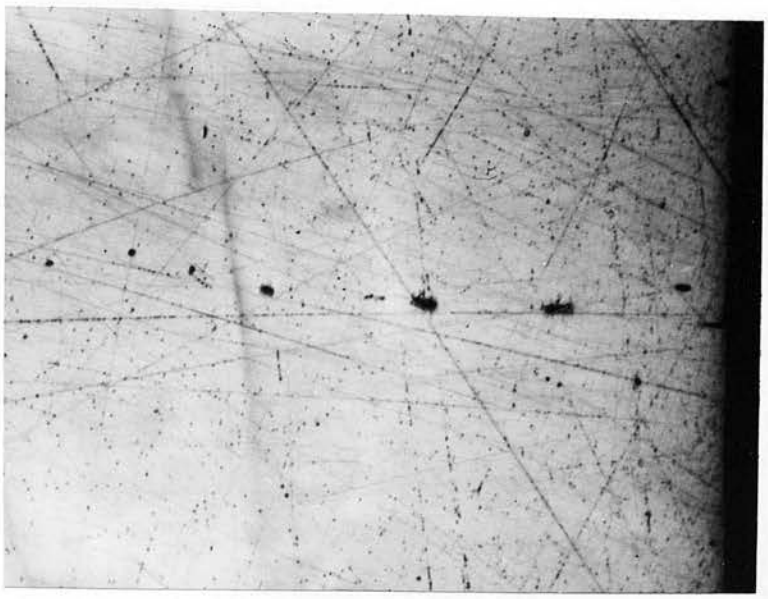

Plate (10). Void Formation.

Plane of section perpendicular to plane of the boundary and to the direction of slide. Surface region X 120: Slide 28μ : T = 731°C. : t = 3.43 10^5 sec. Mean Void Fraction in section .02.

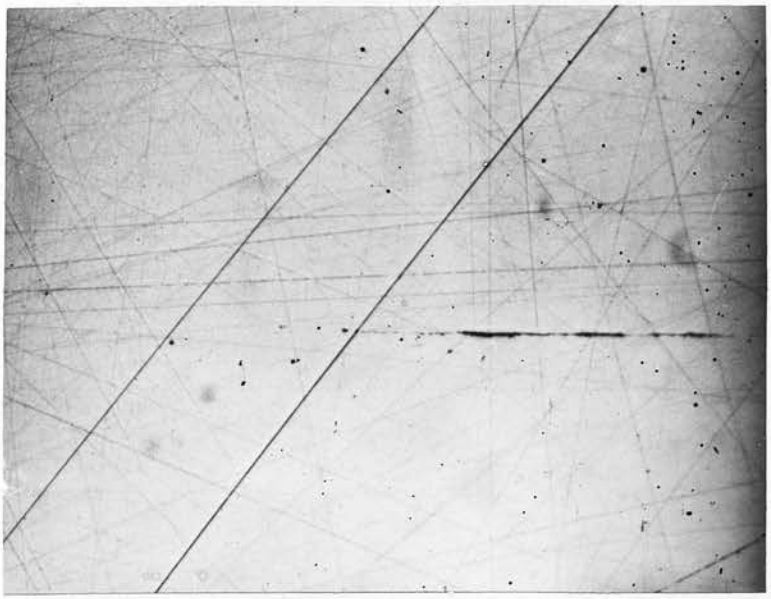

Plate (11). Void Fraction.

Plane of section perpendicular to plane of the boundary and to the direction of slide. Internal region. X 120 : Slide 28μ : T = 731°C : t = 3.43 10^5 sec. Mean void fraction in section .02.

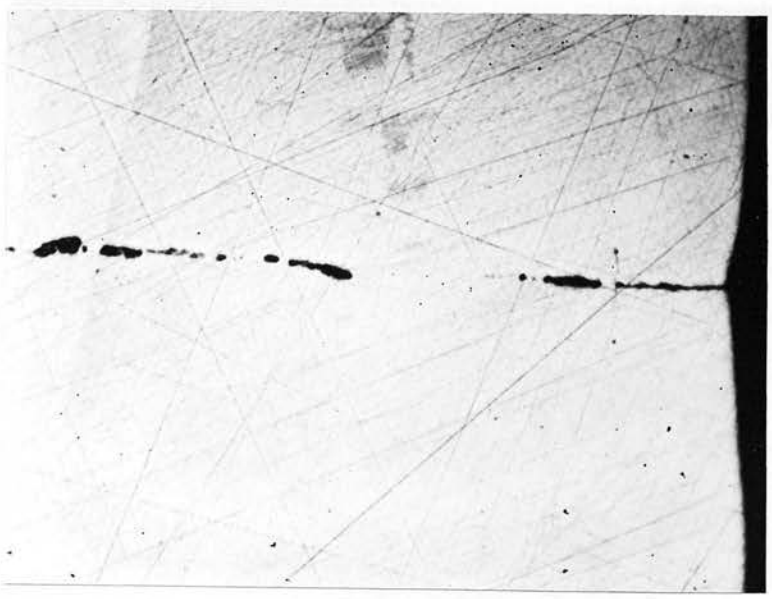

Plate (12). Void Formation.

Plane of section perpendicular to plane of the boundary and to the direction of slide. Surface region X 120: Slide 70μ : T = 623°C. : t = 9.97 10^5 sec. Mean void fraction in section .3.

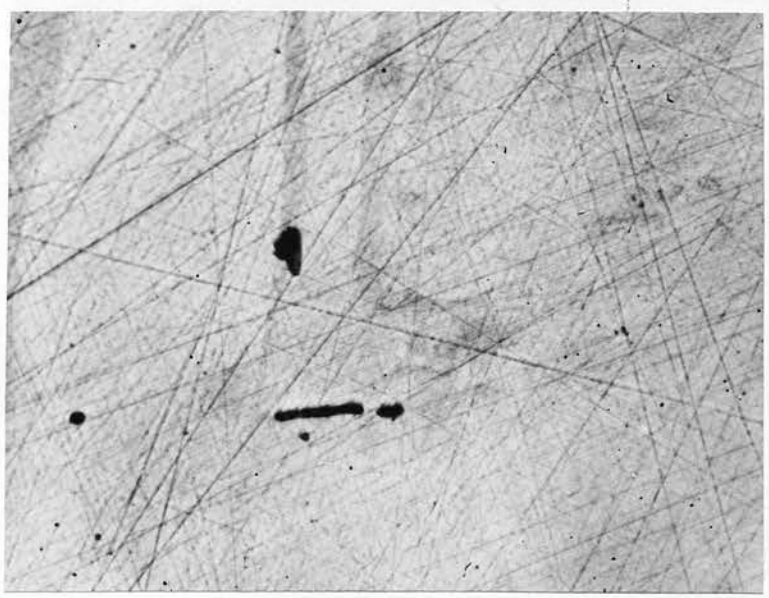

Plate (13). Void Formation.

Plane of section perpendicular to plane of the boundary and to the direction of slide. Internal region. X 120: Slide 70μ : T = 623°C. : t = 9.97 10^5 sec. Mean void fraction in section .3.

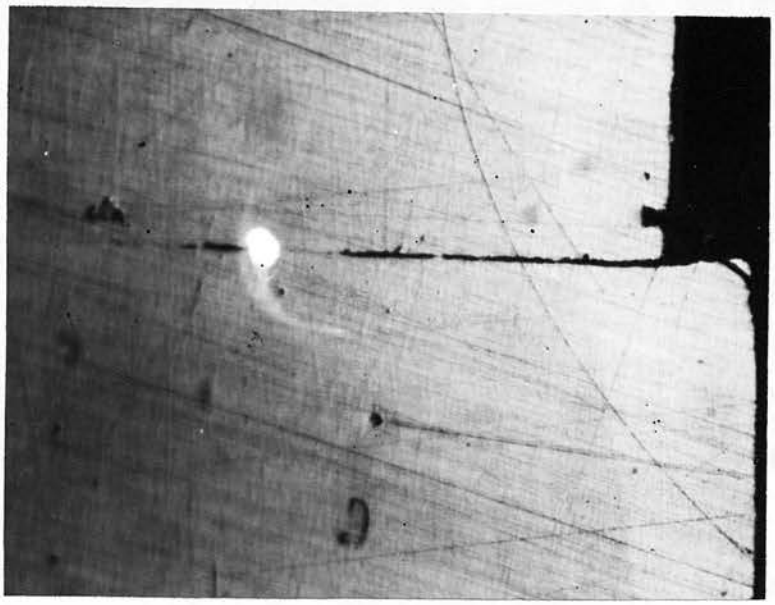

Plate (14). Void Formation.

Plane of section perpendicular to plane of the boundary and parallel to the direction of slide. Surface region. X 120 : Slide 70μ : T 623°C. : t = $9.97\ 10^5$ sec. Mean Void fraction in section ·25.

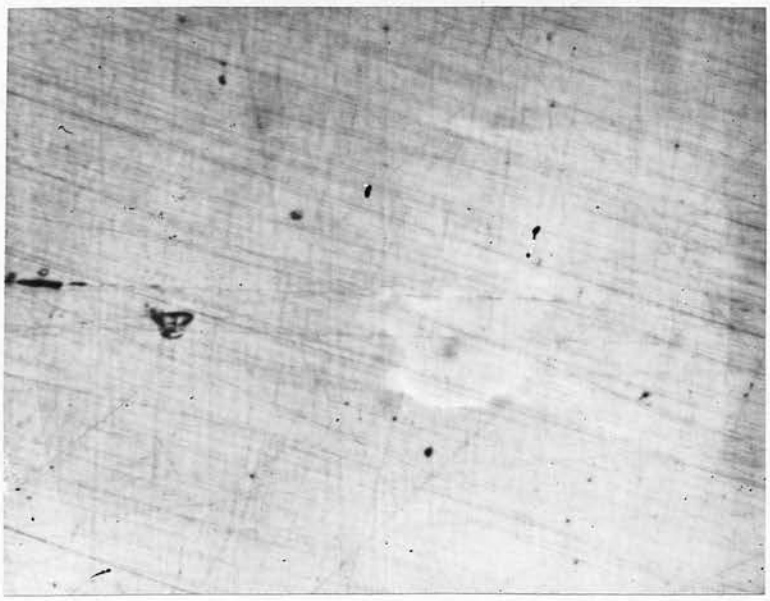

Plate (15). Void Formation.

Plane of section perpendicular to plane of boundary and parallel to the direction of slide. Internal region. X 120 : Slide 70μ : T = 623°C. : t = $9.97\ 10^5$ sec. Mean void fraction in section ·25.

by increasing the size of the grains of the emulsion and is, therefore, associated with a poorer limit in spatial resolution. In the work described here an adequate photographic density was obtainable , even on plates having the highest resolution, without the need for excessive source strength or exposures. The limiting resolution, and experimental convenience were therefore the criteria on which the type of emulsion was chosen.

The autoradiographic film supplied commercially is, with minor variations, of three types. For the coarsest work X-ray film is used and is suitable if the resolution required is about 100 microns. The thicker forms of autoradiographic stripping plates are suitable for intermediate work and have a limiting resolution of 10 to 15 microns. When the highest resolution is required, thin autoradiographic stripping plates are suitable and these will, under ideal conditions, resolve distances of about 5 microns. Since a factor of about 10 in the speed is found between X-ray and thick autoradiographic emulsions, and a similar factor between thick and thin autoradiographic film, it is obviously advisable to evaluate the limit of resolution required and to use the fastest emulsion within this limitation.

Previous work in this laboratory[43] has shown that, using Ag^{110} in thick metallurgical specimens, line widths in fine grain emulsions are about 15 microns at the very best. The discrepancy between this figure and

the reported limiting resolution of the fine grain plates is attributed to the finite range of the β-particles emitted by Ag^{110}, and to the depth of the specimens from which the particles were emitted. Since it was evident from this work that the distribution of ionising particles from thick mounts using Ag^{110} was wider than the limiting resolution of fine grain autoradiographic plates, medium grain plates were used almost exclusively. The plates chosen were Kodak A.R.50 Autoradiographic Stripping Plates.

If autoradiographic plates are to be used at close to their limiting resolution, fairly stringent experimental conditions must be observed. It has been shown theoretically by Doniach and Pelc[44] and experimentally by Stevens[45], that the factors which determine the precision possible in autoradiography are:-

1) The energy and type of radiation.
2) The depth in the specimen from which the particles may come.
3) The thickness of the detecting emulsion.
4) The thickness of any layer which may be present between specimen and emulsion.

The first two criteria are the basis of the argument above, that plates having the maximum resolution are unnecessary. Since they are determined by metallurgical considerations little can be done about them. The radiations from Ag^{110} [46] are of reasonably low energy,

and only Ni^{63} might have been better for the purpose. Since an improvement of resolution due to thinning the specimen would be obtained only with specimen thicknesses comparable with the required limit of resolution, little attention was paid to this aspect of the problem, but it is now known that geological specimens may be ground to thicknesses of about 2 microns, so it may be possible to cut metal in a similar way and obtain an increase in resolution.

While the thickness of the photographic emulsion used determines the limiting resolution of the autoradiographic plate, it is not one of the limiting factors in metallurgical autoradiography since emulsions of about 2 microns thickness are obtainable commercially. The Kodak A.R.50 plates have an emulsion 10 microns thick and a backing of gelatine 25 microns thick.

By far the most important variable influencing the precision in autoradiography is the distance between the emulsion and the surface of the specimen. The calculated and measured values are in reasonable agreement in this matter. The measurements of Stevens show that, in a system which would have a limit of resolution of 5 microns under conditions of perfect contact, only about 10 microns would be achieved with a spacing of 3 microns. Doniach and Pelc estimate a change of from 3 to 17 microns under similar conditions.

A number of autoradiographic techniques were tried before the final one was evolved. The first was the Gomberg[47] wet process of autoradiography. In this method the specimen must remain during the exposure time in a solution of nitric acid and silver nitrate, and must be covered with an inert film. The recommended plastic films were completely unreliable and attempts were made to apply other protective films by vacuum evaporation. Among the films used were gold, silver, aluminium and quartz, but none was found satisfactory. It is possible that the quartz and aluminium films might be improved, since quartz did give temporary protection, and a commercial process is now in use in which evaporated aluminium films may be anodised. Attempts to anodise the aluminium films used in these experiments, were unsuccessful.

Some work was done using the commonly accepted stripping film technique[48] in which the emulsion is floated onto the specimen and the two allowed to dry and expose in the close contact thus caused. This method was found satisfactory, but as the emulsion was in contact with the specimen during processing, a protective layer of plastic (Saran) was necessary, and the use of this was viewed with some suspicion. It was found that occasional artifacts or stains appeared, the process not being wholly reliable.

The original work on autoradiography of Lacassagne

and Lattes[49] involved dry contact between specimen and emulsion, but since Belanger and Leblond[50] painted molten emulsion onto specimens and Evans[51] floated his specimens onto photographic plates, dry contact methods for precision work have tended to fall into disuse.

Recent work of Forestieri and Girifalco[15] has shown that it might be of some advantage to use double autoradiographs with one layer of emulsion on top of another. Such autoradiographs must necessarily be prepared by a dry method. In their work on diffusion Forestieri and Girifalco used relatively large diffusion depths and so used X-ray film, but for the work in hand a finer grained film was required. To use such film a cassette was made by stretching a layer of thin polythene sheet tightly over the top of a Petrie dish and securing it with 'Selotape'. Two layers of stripping film were laid on this with the emulsion side upwards and the plastic mounted specimen placed on top of them. A rubber band, passed over the specimen and Petrie dish, pressed the specimen firmly against the emulsion. It was possible to see the emulsion through the Petrie dish and polythene and to check that no wrinkles were present in it.

Autoradiographs made by this method showed few artifacts, and no trace of pressure development was seen, even around the edge of the specimen mount. A slight increase in speed of the emulsion was noted in this process, as compared with the floating technique,

in agreement with the results of Williams[52], and as no protective film was used, the limit of resolution should have been close to the optimum.

Although the above system was satisfactory, a modification to provide uniform pressure across the specimen face was obviously to be preferred, and so a vacuum cassette (Fig. (12)) based on that of Sherwood[53] was used for the later work. With this system the emulsion layers, followed by two layers of polythene sheet, were placed on top of the specimen and the assembly placed in a brass can, the top of which was then closed with a rubber diaphragm. At atmospheric pressure there was a space of 2 cm. between the rubber and specimen; on reduction of pressure the rubber deformed to press first on the centre of the specimen; the contact area then increased radially, smoothing out possible wrinkles in the emulsion, until uniform pressure was exerted over the whole specimen. Any tendency of the rubber to stretch the emulsion radially was minimised by the polythene layers, which would slide over each other in response to such tendencies.

This system certainly provided close, uniform contact between specimen and emulsion, and again no pressure development was found even on the edge of the mount.

Development of the autoradiographs was done using the perspex holders shown in Plate (16), the two holders being bolted together during the process. Kodak D19B

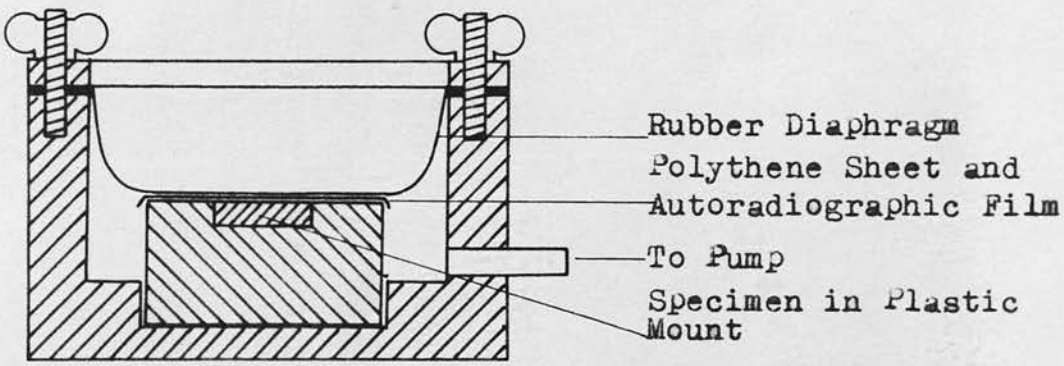

Fig.(12). Vacuum Cassette.

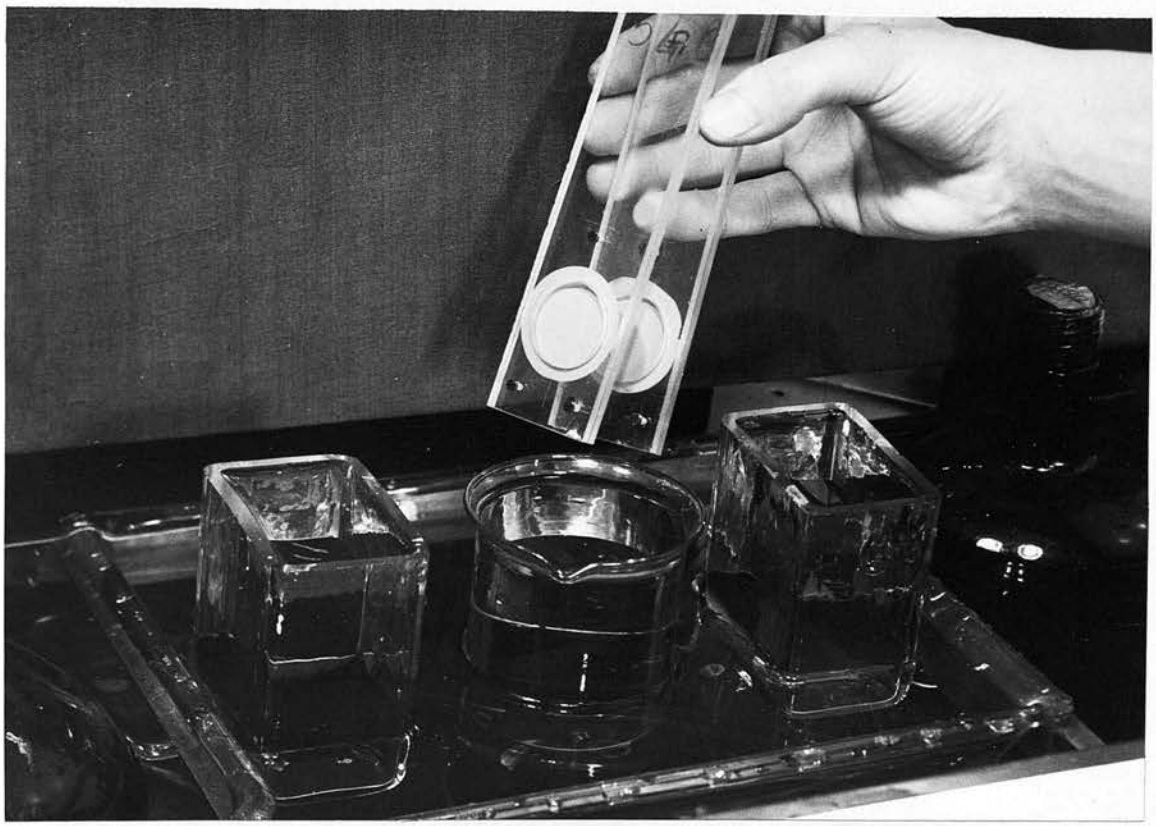

Plate (16). Development of the Autoradiographs.

developer and Kodak acid fixing salt were used, both solutions being made with distilled water and filtered before use. The temperature of developer, wash water, and fixing solution was set at 17.5 ± 0.5°C. throughout the processing, the time of development being 5 minutes and of fixing 2 minutes. Gentle agitation of the autoradiographs, by a motion in their own plane, ensured uniform development without causing anisotropic stretching. After washing for about 30 minutes in running water, the autoradiographs were freed from the holders while being held under water. They were then floated onto cleaned and subbed glass plates and allowed to dry. Great care was taken to ensure that the emulsion was not stretched as it was put onto the glass slides; the glass plate was held vertically touching an edge of the autoradiograph and was slowly lifted out of the water bringing the autoradiograph with it. The plate was then turned through 90° and lowered back vertically into the water, the emulsion separating from it and floating along the surface. When only a small piece of the emulsion remained above the water the plate was again raised bringing the emulsion with it. Since the edge used to pull the emulsion from the water the second time had been formed in a strain free way, the emulsion as a whole was strain free. The process is a delicate one and sometimes wrinkling was noted, or anisotropic expansion suspected; in this event the process was

repeated until the emulsion seemed suitably mounted. Subsequent measurement of the expansion confirmed that any stretching produced was indeed small.

Using this method of autoradiography it was not possible to examine the autoradiograph on the specimen so registry marks had to be made. This was done by putting a drop of a solution of $Ag^{110}NO_3$ in dilute nitric acid into some red ink and marking dots on the specimens with a mapping pen. The dots appeared on the autoradiographs and were used to check the uniformity of the expansion which always occurred on developing.

Despite the present disuse of dry mounting autoradiography, it is considered superior to the floating technique because of the intimate contact which may be obtained between specimen and emulsion, the high degree of reproducibility, and the freedom from artifacts. It is unsuitable for work where the autoradiograph must be examined in registry or where expansion is unacceptable.

For the present work registry was unimportant as the location of the grain boundary trace was always visible by eye, and the stretching was found to be uniform at all points and in all directions to about 2%, so that the correction factor for the length measurements could be determined with certainty. An average value for this factor is 0.9.

3.B.2. Measurements of Photographic Density

Two instruments were used for the photometric analysis of the autoradiographs: all the preliminary tests, in particular the work on double autoradiography, and the measurements of film expansion, were made on a Hilger H451 Non-recording Microphotometer, while the final results presented were measured using a Joyce-Loebl Recording Microdensitometer IIIB. Although in principle measuring the same quantity, the action of the instruments is somewhat different.

a) The Hilger H451 Microphotometer:

In this instrument light from a voltage-stabilised lamp is focused onto the plane of the photographic plate and the fraction of this light transmitted by the plate is focused by a second lens to form an image of the plate, at a magnification of X10, on a combined viewing screen and defining slit. Light entering the defining slit falls on a photocell whose output is fed to a galvanometer through a potentiometer which acts as a sensitivity control.

Referred to the specimen, the slit size on this instrument may range up to 2mm. x 2mm., the lower limit being determined either by the light available or by diffraction. For work in the range of photographic density 0.1 to 1.0 there is adequate light, and as the numerical aperture of the lens is 0.3 giving critical

resolution at $\sim 1\mu$, a slit width, referred to the specimen, of a few times this might well be used. The instrument, therefore, is adequately precise for the autoradiographs in which the densities are in the range 0.1 to 0.5, and the limit of resolution is at best 10μ.

Some limitations of this instrument must be observed. It is dependent for efficient use on constancy of temperature, background illumination, and supply voltage, and also on the linearity of response of the photocell and galvanometer. Of these, the first three conditions were satisfactorily obtained by using the instrument in a thermostatted and darkened room and powering the lamp through a constant voltage transformer; but it must be assumed that the other criteria were ensured in the design of the instrument. To minimise fatigue of the photocell it was exposed to the light only when a reading was being taken. In respect of all these experimental factors the operation of this instrument was very reliable.

Of more importance to this investigation were the variable sensitivity of the instrument and the question of what precise quantity it measures.

We define photographic density as

$$D = \text{Log}_{10} \frac{\text{light intensity transmitted by clear plate}}{\text{light intensity transmitted by region measured}}$$

so for this work

$$D = \text{Log}_{10} \frac{G_o}{G}$$

where G_o is the clear plate galvanometer reading

G is the measured galvanometer reading

$$\therefore \frac{dD}{dG} = - \frac{G_o}{G^2} \cdot \frac{G}{G_o} \cdot .43 = - \cdot \frac{43}{G}$$

$$\text{and } \frac{dG}{dD} = - G.2 \cdot 3$$

so the greatest sensitivity (rate of change of galvanometer reading with density) is at large light transmissions or low density.

At a density of 0.5 (the largest recommended for autoradiographic work) the galvanometer deflection is 35% of full scale, while at 0.1 (the level below which the action of the emulsion becomes erratic) the deflection is 80% of full scale, so 45% of the available range of the instrument may be used for the analysis of the autoradiographs. Since the scale could be read to 0.4% of full scale, density changes of $\frac{\cdot 4}{45} \cdot \cdot 43 = \cdot 004$ should be detected at D = 0.5 and at D = 0.1, a change in D of $\frac{\cdot 4}{80} \times \cdot 43 = \cdot 002$ should be detectable. Random fluctuations in the emulsion were always greater than these variations (particularly at the low density end) so that the instrument sensitivity and variations in it did not limit the precision of the density measurements.

In an instrument such as this the quantity measured is not strictly photographic density above some

arbitrarily assigned level of background, but is rather a quantity differing from this ideal by some multiple whose value is nearly 1. For the relative measurements of photographic density needed in the experiments we need not be critical of the precise quantity measured by the densitometer. However it is known that photographic plates have a linear response only over a limited range, the peak usable density in autoradiography being taken as 0.5[54], so it is necessary to estimate the absolute precision of the densitometer to ensure that the nominal peak density on the instrument of 0.5 is not greatly in excess of this value in absolute terms.

Properly, we must distinguish between SPECULAR and DIFFUSE photographic densities, both being defined as $-\text{Log}_{10}$(transmission coefficient) through the plate, the specular density being a measure of the light transmitted parallel to the input light, and the diffuse density being a measure of the total light transmitted by the plate irrespective of direction. Obviously the specular density is the greater quantity.

In the densitometer the ingoing and outgoing light lie in cones of some 15° angle so that the instrument measures a quantity which is not strictly a density at all. The effect of the convergent input light seems to be small and to a first approximation may be regarded as merely widening the cone of acceptance. This means that

the densitometer acts as if it accepted a cone of $\sim 20^{\circ}$ in the transmitted light and thus records a density intermediate between the specular and diffuse values. It has been shown experimentally[55] that such an instrument should record a density about 1.5 times that of the diffuse density.

Diffuse densities are most commonly used in photography but is not clear from the literature whether the recommended peak value of 0.5 refers to such a density or to a figure determined in a machine similar to that described here. From the above, however, it can be seen that the values derived here either suit this criterion or err on the high side, so that the safe limit has not been exceeded.

A further check on the response of the photographic plates was made by using more than one autoradiograph of the same specimen and noting that no significant variation in the results was caused by the use of different peak densities. This showed that the linearity of the response was adequate for the present work.

b) The Joyce Loebl Recording Microdensitometer:

The optical system of the Joyce Loebl Recording Microdensitometer is similar to that described for the Hilger instrument, an image of the emulsion being presented, at a magnification of X20, on a viewing screen fitted with a defining slit through which light passes

to the detector, but the method of detection and analysis is very different. Light from a common source passes through the emulsion and defining slit and into a photomultiplier, or else through a pair of optical density wedges, and into the same photomultiplier. A rotating sector, driving by a synchronous motor, interrupts the light paths alternately and the a.c. component of the signal from the photomultiplier is amplified to operate the servo circuit so that one wedge which is calibrated moves until the light signals are balanced. By attaching a pen to this wedge and moving a table under it in synchronism with the emulsion as it moves through the analysing beam, a graph of position in the emulsion against optical density is formed. The function of the other uncalibrated wedge is to allow the zero end of the calibrated wedge to be set to suit the background in the emulsion.

The special features of this instrument are that wedges of any density range may be used, that a rigid linkage exists between emulsion and plotting table which provides a choice between their relative rates of motion, and that the driving mechanism operates at a rate varying inversely as the density gradient measured, so that the rate of change recorded is not influenced by the writing speed of the pen. In the experiments described here a wedge having a range of density of up to 0.8 above background, and calibrated to 1% along its length was used. The ratio of distances moved by plotting table and specimen was 50:1.

In this instrument the sensitivity was constant at 1% of maximum density, being determined only by the quality of the wedge, but it was subject to the same uncertainty in absolute density as was the other.

c) Use of the Instruments:

The instruments were used similarly. By rotating the plate holding the autoradiograph until the trace of the specimen surface remained central in the viewing screen when the traverse parallel to the slit length was operated, the direction of diffusion was brought perpendicular to the slit length. A slit width of 15μ was normally used, this being a fair estimate of the limit of resolution in the emulsion, but the slit length had to be set to a value appropriate to the individual specimens. Correctly, the slit length should have been twice the distance of measurable bulk diffusion penetration from the specimen surface to observe all the grain boundary effect, but this length is somewhat excessive experimentally as the width of the grain boundary trace on the emulsion is narrower than this in the region, beyond that of bulk penetration, where boundary effects may be measured. In practice a setting was found by noting that, on both densitometers, the lowest density which could be measured was very close to that which could just be detected by eye in the viewing screen, and so the slit length was adjusted to be just greater

than the visual width of the base of the V marking the boundary diffusion. The slit length used was not critical, provided it was adequate to cover the total boundary diffusion trace, but it was obviously best to keep it to a minimum so that the already small grain boundary effect was not swamped by the background signal from the clear surrounding emulsion.

With the trace of the boundary V central in the defining slit, densitometric traces were recorded from just outside the specimen surface to well past the diffusion zone so that the peak and background densities could be evaluated precisely.

It was found convenient to use the Hilger microphotometer to evaluate the expansions of the emulsions. This was done by measuring the distances between the peak density positions, corresponding to the specimen surfaces, on the autoradiographs and then comparing these with the actual distances on the specimens (which were evaluated with a measuring microscope). This method was more precise than measurement from the marker dots which were used to check the expansions transverse to the diffusion direction; it was particularly valuable for the deeply diffused specimens in which the position of peak density could not readily be estimated by eye in a measuring microscope.

CHAPTER 4

RESULTS

4.1. Preliminary Trials

As a check of the action of the straining machine, some specimens having high angle boundaries, that is ones with little resistance to sliding, were heated to a temperature of 800°C and cooled again, using heating rates of 100°C/hour. These specimens showed no grain boundary slide and were a check that deformation of the specimens was not occurring due to thermal expansion. A further test was to use this heating rate followed by a very slow cooling rate, ~ 20°C/hour, in case reversed sliding had occurred in the previous experiment. Again no effect was observed.

The possible effect on sliding of the silver forming the tracer element was investigated as follows. Bicrystals with, and without, silver surface layers were successively pulled in the straining machine using identical temperatures, times, and straining rates. On examination it was found that specimens with high angle boundaries displayed comparable amounts of sliding (to within about 10%) and that, on sectioning, the fractional lengths of grain boundary occupied by voids were also comparable. Using low angle boundaries the amounts of sliding observed were always very small and were rather

erratic: it was not possible to assign any specific tendency to the presence of silver. On sectioning no voids were found in the low angle boundaries.

This is in general agreement with the work of Wienberg[56], who reports no effect on sliding rates in aluminium from a number of impurities, although iron did inhibit slide.

4.2. Autoradiographs of Low Angle Boundaries

Diffusion in a number of low angle boundaries was investigated. The temperature range used was 530°C to 780°C and the annealing times were of about 10^6 seconds. Despite careful microscopic examination, tracer penetration beyond the bulk diffusion depth was not found in either the strained or dummy specimens.

Since the method of autoradiography used did not provide registry between specimen and emulsion, the position of the grain boundary on the emulsion was estimated with reference to the traces of lines marked on the specimen mounts with radioactive ink. Even setting the microscope to view the known position of the grain boundary did not reveal any sign of the boundary on the emulsion, nor did it show penetration down it. On one specimen, due to mishandling of the specimen grips, a small amount of slide was caused in a direction perpendicular to that caused by the straining machine. An autoradiograph of this specimen showed a slight

displacement of the surface trace at the grain boundary so that its position was evident; again no excess boundary penetration was observed.

It was considered that visual examination alone was not sufficient evidence on which to reject the idea of grain boundary diffusion in low angle boundaries, but traces taken along the estimated line of a boundary could not be distinguished from those obtained elsewhere. In order to estimate whether any measurable effect might have been missed, a microscopic examination was made of a few of the autoradiographs, and it was found that the end point of significant measurements on the densitometer was fairly close to the edge of the autoradiographic traces, as measured visually, so it is certain that no measurable effect could have been missed.

About a dozen specimens were examined before work on low angle boundaries was discontinued.

4.3. Autoradiographs of High Angle Boundaries

Bicrystals with high angle grain boundaries were annealed at temperatures of 500° to 800°C and for times in the range 3 - 20 x 10^5 seconds. During the anneals, slides of up to 70μ were caused in the boundaries.

Autoradiographs of such crystals, exposed so as to have a peak photographic density of 0.5, showed grain boundary penetration easily visible to the naked eye. Typical examples of this effect are shown in Plates (17)

and (18). Densitometric traces of such autoradiographs taken from regions on and off the grain boundary show clearly the excess penetration at the boundaries. A number of such densitometric traces are shown in Graphs (1) to (5). These curves have been drawn from the traces obtained on the Joyce-Loebl Microdensitometer, which were unsuitable for direct reproduction. In use the readings of density were taken directly from the recorder paper, the readings being taken at effective intervals on the specimens of 10 or 20μ.

Double autoradiographs of all specimens were prepared but only a few were analysed; such analyses were performed using the Hilger H451 Non-recording Microphotometer. On the second of the autoradiographs the peak density was not very far below that of the first autoradiograph so, although the image was undoubtedly somewhat more diffuse, the position of the grain boundary could still readily be discerned by the characteristic V of the tracer penetration along it.

4.4. Types of Result

Three types of result were obtained. These were measurements of bulk diffusion, grain boundary diffusion in static boundaries, and grain boundary diffusion in moving boundaries. While only the third of these was the strict purpose of the experiment, it was considered that the other two measurements were essential.

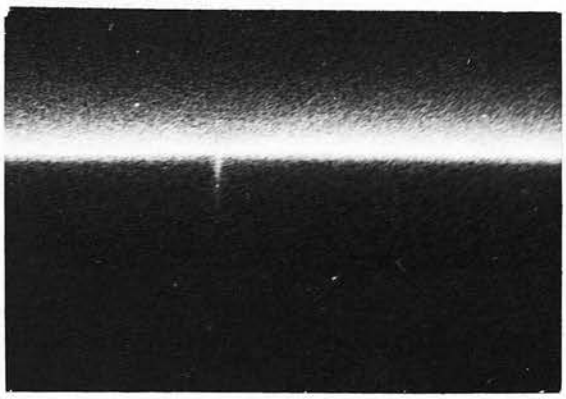

Plate (17). Negative of Autoradiograph.
Strained specimen : X 15 : T = 567.5°C. : t = 9.51 10^5 sec.

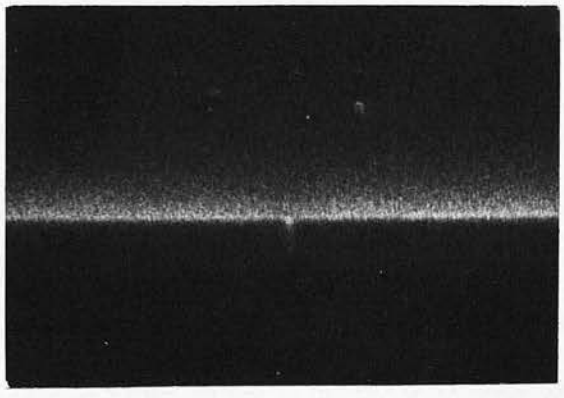

Plate (18). Negative of Autoradiograph.
Unstrained specimen : X 15 : T = 623°C. : t = 9.97 10^5 sec.

The function of the bulk diffusion measurements was twofold: measurements of reasonable precision were evidence that the emulsion was linear in its characteristic up to the density used and that this previously untried system of autoradiography was satisfactory, while the deviation from precision at very short diffusion distances was a direct measure of the limit of resolution of the whole system expressed in its most appropriate form, namely as the maximum concentration gradient which could be expressed by the system. This work was not sufficiently precise for the values deduced to be used in the analysis of boundary diffusion.

Diffusion in static grain boundaries was measured to give a comparison against which the strained figures could be evaluated, and also because of their own interest, since the only previous investigation of the silver/copper system used a method of analysis now known to be in error to some degree, and to be suited mainly to the analysis of comparative results.

4.5. The Densitometric Traces

In all calculations it is assumed that the photographic density observed is proportional to the strength of the radioactive source causing it. All tracer concentrations are referred to the surface concentration which is considered to have the value unity. Thus, relative concentration at a point is the ratio of photo-

graphic density at the point to that at the surface.

In bulk diffusion we find concentration related to position by an equation of the form:

$$C = \exp - \frac{y^2}{4Dt} \qquad (1)$$

or $\log_e C = - \frac{y^2}{4Dt}$

or $\log \log_e C = -2 \log y + const.$

where C is the relative concentration y is a distance coordinate measured from the surface

Similarly for grain boundary diffusion beyond the region of bulk diffusion

$$\underline{C} = \exp - \frac{y}{\sqrt{\frac{\omega D'}{2D}}\sqrt{\pi D t}}$$

$$\text{or } \log_e \underline{C} = -y\left(\frac{\omega D'}{2D}\sqrt{\pi D t}\right)^{-\frac{1}{2}} \qquad (2)$$

$$\text{or } \log \log_e \underline{C} = - \log y + const.$$

where $\underline{C}$ is the <u>mean</u> relative concentration measured over the section.

We see thus that, in suitably annealed specimens, a graph of - Log Log_e(concentration) against Log(penetration) should show two well defined regions having gradients 2 and 1, due to the bulk and grain boundary diffusions respectively. An intermediate zone might also be expected. Such a plot as this is shown in Graph (6), along with a similar plot from a trace taken on a line remote from the boundary. The features to be

noted on this plot are:

1) The bulk diffusion trace has gradient 2 throughout its length until it fades into background.

2) The grain boundary trace starts with gradient 2 and is superposed upon the line of bulk diffusion points.

3) After the region of gradient 2, the grain boundary trace breaks off sharply to form a line of gradient 1.

4) Both traces fade into background at about the same fractional concentration.

Generally these features are to be expected and may be regarded as checks of the analysis, but the sharpness of the break in gradient was an unexpected phenomenon. It was generally pronounced, although naturally less so in the high temperature specimens, and might be worth study in future analysis as a critical parameter of the diffusion system.

It is of some interest to note the content of the various parts of the curve in terms of the variables concerned in diffusion. In work on bulk diffusion, use is commonly made of the parameter $2\sqrt{Dt}$ to express the mean depth of diffusion penetration. This parameter is the half-width of the error function describing the diffusion from a thin sheet, bounded on both sides by an infinite medium into which diffusion takes place. For the present work, it is the distance within which the concentration

falls by a factor $\frac{1}{e}$ (see Equation (1)). To describe grain boundary diffusion we may make use of an analagous parameter, the distance $\sqrt{\frac{\omega D'}{2D}\sqrt{\pi D t}}$ (see Equation (2)) in which the mean grain boundary concentration falls by a similar factor.

Referring again to Graph (6) we see that bulk diffusion effects dominate the concentration distribution to a depth of about $2.2\sqrt{Dt}$. After this grain boundary diffusion predominates to a distance of about $2.\sqrt{\frac{\omega D'}{2D}\sqrt{\pi D t}}$ where background is reached. From the curve we may note also that the autoradiographic technique as used here gives results valid to a relative concentration of about 0.3 ; but usefulness to a figure of $\sim$ 0.1 was more generally found.

In the analysis of results, the double logarithmic plot was used to find the limits of the linear region and then the best straight line for this region on the plot of Log (concentration) versus Depth was computed using the Awbery[57] or 'centre of gravity' method. For dubious cases the extent of the linear range was decided partly on the basis of the double logarithmic plot and partly by comparison with the distances $2.2\sqrt{Dt}$ and $2.\sqrt{\frac{\omega D'}{2D}\sqrt{\pi D t}}$.

A further feature of the double logarithmic plot is the facility with which it may be used to show the effect of errors in the choice of origin, when taking

measurements from the densitometric traces. Graphs (7) and (8) show how Graph (6) is modified when subject to such variations.

In Graph (7) the central line, a repeat of Graph (6), shows the plot obtained using the best estimate of the surface position from examination of the densitometric trace. The other lines show the effect of choosing origins displaced by 10μ. We see that the gradient of the whole curve is modified, the greatest change being at small penetrations, and the curve is also bodily displaced. The changes in gradients represent deviations from the expected laws, while the bodily displacements represent changes in diffusion coefficient. In this instance the change in boundary diffusion is by a factor of 1.1, or an error of 10%.

Many autoradiographs show irregularities in the density traces in the region close to the specimen surface, caused, presumably, by the low absorption of β-particles by the plastic mount and by possible scintillation within it. In such cases a best origin for the analysis was chosen by inspection and the trace plotted. Small variations in origin were then made until a graph with an initial gradient of 2 was obtained. An origin determined in this way was considered more reliable than one chosen solely by inspection. In no case was the change large enough to be unreasonable when related

to the densitometric trace, a typical change being of 5 microns.

Errors in choice of the origin of the concentration coordinate have closer relevance to the measurement of grain boundary diffusion. Two choices of origin may reasonably be suggested. The first is to measure density relative to that of clear film in a region remote from the specimen; the second is to measure relative to the asymptotic level of the density record at increasing distances of penetration into the specimen. Using the first method it is found (see Graph (8)) that on the double logarithmic plot the gradient of the region of grain boundary effect is rather less than 1, and so is not closely linear. Using the second method a gradient of 1 is found and there is no systematic deviation from linearity until background is reached. There is also a bodily displacement of the curves equivalent to an error of about 10% in the diffusion coefficient. In all calculations, therefore, the extrapolated background level was used.

Graph (8) has been chosen with the difference between remote and extrapolated background levels 10% of peak concentration. It thus also illustrates the effect of a large error in the estimation of the level of the extrapolated background. We see that again experimental error in the choice of origin should not

greatly modify the measured diffusion coefficients. The background level used in analysis was chosen by inspection and then small variations tried by comparison on the double logarithmic plot, the level used being that having the longest range of gradient 1.

4.6. Double Autoradiographs

In the analysis of single autoradiographs it has been shown that a local background density level, derived from measurements taken in the region being analysed, is a more appropriate origin for concentration measurement than one measured at a remote position.

Since care was taken to ensure uniform development of the emulsion, the difference in these density levels must have been due to the higher general level of radiation close to the specimens. Double autoradiography may be regarded as an attempt to take the use of local backgrounds to the limit where a continuous function is used. In more detailed terms the method is based on the assumption that the distribution of low energy radiation emitted at the surface is a closer representation of the concentration distribution of the radioactive tracer than is the high energy radiation. As the first emulsion is acted upon by both high and low energy radiation, while the second measures only radiation with an emitted energy greater than some particular value, the difference of densities for any given point should be a measure of the low energy component of the radiation.

In the application of this method to the analysis of diffusion, the major experimental difficulties were the small density difference between the two autoradiographs and the problem of registry between them.

To analyse the autoradiographs the expansion corrections were first applied to the position coordinates, and then the two Density versus Position graphs were plotted on the same paper, with an approximate registry deduced from the positions of peak density. Small adjustments were then made to the registry by correlating any abnormalities common to the two curves, or else by detailed inspection of the region of peak density. The curve of density difference was then computed and analysed as a single autoradiograph.

Graphs (9) and (10) are typical of this sort of investigation and show the difficulties encountered.

From Graph (10) the results derived are:

$T = 731^{\circ}C.$, $t = 3.43\ 10^{5}$ sec.			
	$\frac{d \log_e C}{dy}$ cm^{-1}	Expansion Factor	$D' cm^2/sec.$
Single Autoradiograph	57 ± 3	.855	$(6.65 \pm .50)10^{-5}$
Double Autoradiograph	53 ± 6	.855 common	$(7.65 \pm 1.2)10^{-5}$

Table (1).

Forming the difference $D'_{Double} - D_{Single}$ we find

$$D'_D - D'_S = (1.0 \pm 1.3)10^{-5} \text{ cm.}^2/\text{sec.}$$

If both methods measured the same quantity without systematic variation this difference would be zero. With these results, we find from tables[58] of the normal distribution, that the probability of finding, on continued investigation, a value for $D'_D - D'_S$ as far or farther from $1 \cdot 0.10^{-5}$ than zero is 0.45, so the present figures indicate no definite variation between the techniques. Similar figures were found when investigating other specimens.

From this investigation it seems that the use of the second autoradiograph merely doubles the random error of the concentration measurements without increasing one's confidence that the effect of some systematic error has been randomised. That such confidence would be misplaced is evident from the above results where we see that the gradient measured with the single autoradiograph is higher than that found with the double autoradiograph. In the latter technique we are trying specifically to remove the effect of the high energy component of the radiation, which must necessarily have lowered the concentration gradient recorded by the emulsions, so that the correction to the results should have been towards an increased gradient. Since in fact the reverse was found, and since in diffusion work a

variation towards a higher diffusion coefficient must always be suspect as due to reduced resolution, work on the double autoradiographs was discontinued.

It must be noted that grain boundary diffusion measurements constitute a very severe test of this technique, since they are concerned entirely with measurements at low relative concentrations where the weakness of the method is most evident, so that it may work satisfactorily for bulk diffusion work.

If used with isotopes other than the Ag^{110} mentioned here, the technique would show different responses between the pairs of emulsions, but a better discrimination would not normally be found, as few isotopes have a spectrum more concentrated in the lower energies than that of Ag^{110}.

4.7. Numerical Results

4.7.1. Bulk Diffusion

In Table (2) and Graphs (11) to (13) are presented the data obtained in the analysis of autoradiographs in regions remote from the grain boundaries. These results must be compared with known precision measurements of the diffusion coefficient of low concentration of silver in copper such as those of Tomizuka[59] and of Mercer[60]. The relevant figures are:

Comparative Bulk Diffusion Measurements. ($cm.^2/sec.$)

T^oC	This Investigation	Mercer	Tomizuka
794	$1.76\ 10^{-10}$	$1.58\ 10^{-10}$	$1.76\ 10^{-10}$
731	$8.72\ 10^{-11}$	$3.90\ 10^{-11}$	$4.25\ 10^{-11}$
623	$1.54\ 10^{-11}$	$2.37\ 10^{-12}$	$2.64\ 10^{-12}$

Table (3).

It is readily seen that the results as measured here become increasingly inaccurate at low temperatures, and it must be concluded that, at these temperatures with the annealing times used, the required limit of resolution of the total system is too small. At $731^oC.$ the available resolution is almost adequate, while at $794^oC.$ the precision of the result is as good as might ever be expected from the autoradiographic method used.

These results show that the comparison measurements of bulk diffusion required in an evaluation of grain boundary diffusion, may not be made on the specimens themselves, with the techniques described above, but they do confirm that the technique as a whole may be used for numerical analysis.

4.7.2. Unstrained Grain Boundary Diffusion

Grain boundary diffusion in the unstrained specimens was computed using Fisher's equation, the bulk diffusion measurements of Mercer ($D = 0.846 \exp -\frac{47290}{RT}$ $cm.^2/sec.$) being taken as the standard for comparison and denoted D_E in the tables. Individual diffusion coefficients were evaluated by the Awbery method, while those in combination, where fewer numbers were available, were evaluated using the weighted least squares analysis. The relevant figures are detailed in Tables (4) and (6), and in Graphs (14) to (19).

It will be seen from Graph (19), where the results are shown in combination, that the experimental points vary from the line by distances rather greater than would be expected from their computed standard deviations. This variation indicates the possibility of systematic error, and the analysis was modified to minimise the effect of such error on the computed results Each specimen was assigned a weight (Table (6)) equal to the sum of the weights derived for the strained and unstrained specimens by the squared deviations method. This averaging process reduced the relative weights, the normal way of countering systematic effects, and ensured that, since the sets of results were treated identically, the relative effects between strained and unstrained specimens were not modified by systematic variation.

Using these methods the best line describing the unstrained diffusion coefficients as a function of temperature is:

$$\mathrm{Log}_{10} D'_u = (5.38 \pm .045) - (0.705 \pm .075)\left(\frac{10^4}{T} - 11.15\right)$$

The diffusion coefficients are thus:

$$D'_u = (300\ {}^{+1300}_{-240})\exp\left(-\frac{(32 \pm 3.5)10^3}{RT}\right)\ \mathrm{cm.}^2/\mathrm{sec.}$$

4.7.3. Diffusion in Sliding Grain Boundaries

Diffusion coefficients for sliding boundaries were derived as for the unstrained ones, assuming the validity of Fisher's equation. The relevant data are shown in Tables (5) and (6) and in Graphs (20) to (27).

Since it was not possible to control with precision the amount or the rate of boundary slide in the specimens, the equation for the diffusion coefficient as a function of temperature has no real significance for the strained specimens, however it was computed, using the relative weights detailed above, for purposes of comparison with the unstrained specimens, and may be said to represent diffusion in specimens having a mean slide distance of 35μ or a mean rate of slide of $5\ 10^{-9}$ cm./sec., the deviations in these values being high.

The best line describing this variation of strained diffusion coefficient with temperature is:

$$\text{Log}_{10} D'_S = (5.30 \pm .055) - (.710 \pm .088)\left(\frac{10^4}{T} - 11.15\right)$$

The diffusion coefficients are thus:

$$D'_S = (500\ ^{+3500}_{-\ 450})\ \exp\left(-\frac{32.5 \pm 4)10^3}{RT}\right)\ \text{cm.}^2/\text{sec.}$$

4.8. Precision and Interpretation of the Experimental Results

4.8.1. Random Effects

The sizes of the random errors in the measurements to derive grain boundary diffusion coefficients have been computed conventionally: the results show that an overall precision of 10% has been achieved, about what might be expected with the technique used. It is necessary now to evaluate whether these results are consistent, and whether the variations between strained and unstrained specimens are significant.

1) Consistency of the Unstrained Diffusion Coefficients:

It was possible to compute two, largely independent, diffusion coefficients for each specimen, each with an accompanying standard deviation: the first was by analysis of the appropriate autoradiograph, and the second by calculation from the best line describing the interrelation of the whole group of diffusion coefficients. The compatibility of the two sets of such coefficients is a measure of the consistency of the analysis, since evidently a systematic trend amongst the results away from

the relationship expected must increase the deviations in the grouped analysis to a value incommensurate with the deviations of the individual measurements. In Table (6) are shown the deduced logarithms of the diffusion coefficients for the unstrained specimens both by direct measurement (Log D_u') and by calculation from the best line (Log $\overline{D}_u'$). By forming the differences between the values the probability of occurrence of values more distant from the difference than zero can be evaluated. Thus in the specimen annealed at 731°C. the values are:

$$\text{Log } \overline{D}_u' - \text{Log } D_u' = -(4.54 \pm .10) + (4.72 \pm .04) = .18 \pm .11$$

From tables, and assuming a normal distribution, the probability of a result differing farther from .18 than zero, with this standard deviation, is 0.1. Conventionally a result is declared inconsistent if this probability falls below .01. The collected values are denoted P_u in Table (7). It will be seen that the range is 0.02 to 0.8 and the mean is 0.3. This calculation shows that consistency would be greatly increased by rejection of the result at 517°C. but this is forbidden by the previously stated 1% criterion. The application of Chauvenet's Criterion also confirms that the point may not be rejected.

We conclude that any inconsistencies or systematic trends away from the expected distribution are of a magnitude comparable with or smaller than the random error.

2) Variation Between Strained and Unstrained Specimens:

The problem of whether the results establish a significant difference in diffusion rate between the strained and unstrained specimens may be considered in several ways, but before so doing it is worth while to evaluate the consistency of the measured points to the derived line as was done for the unstrained specimens. The consistency probability P_S is noted in Table (7). It will be seen that, on the 1% criterion one result may certainly be rejected while another is doubtful. This is confirmed by the application of Chauvenet's Criterion.

It will be noted that in Table (5) two results are presented for the diffusion coefficient in the specimen strained at 623°C. One of these, the second, was tacitly deleted when calculating the best straight line to fit the strained diffusion data, because of its high void fraction and its obvious disparity with the other results. The analysis above shows that the other result measured at 623°C. must also be deleted because of its inconsistency with the others of the group. Voids in the boundaries, therefore, seem definitely to inhibit diffusion, although their effect is apparently small at low concentrations as no such effect was observed in deformation at 731°C. where only a very few voids were found.

The best line describing diffusion in the strained specimens as a function of temperature was recalculated with the result at 623°C. deleted. The equation is:

$$\mathrm{Log}_{10} D_S' = (5.28 \pm .07) - (.71 \pm 0.1)\left(\frac{10^4}{T} - 11.15\right)$$

The diffusion coefficients are thus:

$$D_S' = (400\ ^{+5900}_{-370})\ \exp\left(-\frac{(32.5 \pm 4.5)10^3}{RT}\right)\ \mathrm{cm.}^2/\mathrm{sec.}$$

Tests for significant variation between strained and unstrained diffusion coefficients may be made either with the grouped results or with the individual pairs. Considering the grouped effects first, the possibilities are:

1) The gradient of the line relating temperature and diffusion rate - the activation energy of diffusion - may be changed.

2) The level of the line - the frequency factor - may be altered.

3) Adherence to Fisher's equation may be modified, so that in examination of strained and unstrained diffusion over the same range, a variation in the standard deviation of $\frac{d\mathrm{Log}_e C}{dy}$ may be found.

For the first criterion we may compare directly the values (32 ± 3.5)K. cal./mol. and (32.5 ± 4.5)K.cal./mol., and attempt, because of the small numbers involved, to distinguish them in terms of 'Student's' "t^2" distribution. (This was not used previously as the

variables were not independent.)

The t value is as before the difference function:

$$t = \frac{\bar{x}_1 - \bar{x}_2}{S\sqrt{\frac{1}{n_1} + \frac{1}{n_2}}}$$

where the $\bar{x}_i$ are the means and the n_i the number of observations from which they are calculated. S is defined by $S^2(n-1) = \sum_{i=1}^{n} (\Delta_i^2)$ where Δ_i are the differences between the observed points and the means. Since the standard deviations were known this was reduced to:

$$\underline{t} = \frac{\bar{x}_1 - \bar{x}_2}{\sqrt{\sigma_1^2 + \sigma_2^2}} = \frac{32{\cdot}5 - 32}{\sqrt{4{\cdot}5^2 + 3{\cdot}5^2}} = \underline{0{\cdot}88}$$

The number of degrees of freedom

$$\underline{\nu} = n_1 + n_2 - 2 = 5 + 4 - 2 = \underline{7}$$

and from tables (61) the probability of this 't' value with 7 degrees of freedom is $\gg .50$. Since we regard a value of .01 as significant and a value of .05 as marginally significant this investigation establishes no significant effect, as is obvious from the initial values.

In the second test the frequency factors D'_0 could be used but, since this involves extrapolation over three times the range of measurement, precision would be lost unnecessarily. Instead the mean values of Log_{10} D' may be compared as below:

$$\underline{t} = \frac{Log_{10} D'_u - Log_{10} D'_s}{\sqrt{\sigma^2_{D'_u} + \sigma^2_{D'_s}}} = \frac{5{\cdot}38 - 5{\cdot}28}{\sqrt{{\cdot}045^2 + {\cdot}07^2}} = \underline{1{\cdot}2}$$

and again $\nu = 7$.

The probability level is about 0.4 where again .01 would be significant. No effect is thus established.

A misapplication of Fisher's equation to the strained system should show as an increase in the standard deviation of $\frac{d\,Log_e C}{dy}$ in the graphs, assuming a similar range of measurement for strained and unstrained specimens. Table (6) shows the various standard deviations in the gradients combined to form the quotient $\frac{\sigma_{D'_s}}{\sigma_{D'_u}}$, a value which in the absence of the possible distortion should be 1. The mean value of the quantity is 1.01 and the mean variation 0.4 so a variation of this nature is certainly not probable.

The above tests being concerned with mean effects, lose precision by variation between results in each set: by comparing the pairs of results before combination, slightly improved precision may be obtained. In Tables (4) and (5) are noted the values $Log_{10} D'_S$ and $Log_{10} D'_u$: using the t^2 test, and remembering that there are about 15 readings in each diffusion evaluation, we obtain the probabilities of consistency (P) of Table (7). Of the four results one appears to be significant and two marginally significant. No measurable effect appears in the specimen deformed at 567.5°C.

This test does seem to provide evidence of a

significant change in diffusion rate under the action of strain, and since the autoradiographs were made under well controlled conditions the relative measurements between them should be reliable to the limits suggested by the standard deviations of the density measurements, even if the diffusion coefficients are not. The mean factor in the diffusion coefficients suggested by the results is ($1.3 \pm .10$) and the tendency is towards an increasing ratio with temperature.

Simple correlations with slide (S) and mean slide rate ($\bar{S}$) are shown in Table (8), but no strong correlation is evident.

4.8.2. Systematic Effects

Of some interest in this experiment is the assessment of probable sizes for some systematic effects. Two important errors of this nature may occur, these being due to a) poor resolution in the detecting system, and b) invalid use of Fisher's equation in a system to which it might not be appropriate. It is possible to show that neither of these effects causes serious error in the results.

a) Poor Resolution:

The effect of poor resolution in the detector is seen experimentally as the inability of the system to record precisely, rapid changes of photographic density with distance. In the measurement of grain boundary

diffusion coefficients we are concerned with the measurement of the quantity $\frac{d \, Log_e C}{d y}$ and the general range of values found is 40 - 95 $cm.^{-1}$. We wish to decide whether such gradients, when recorded by the autoradiographic method, are likely to be in error.

When measuring bulk diffusion we are concerned with the region in which $\frac{d \, Log_e C}{d y^2}$ is constant, and the experiments show that such constancy is found to some depth y_{max} beyond which the deviation from constancy becomes unacceptable.

Since $$\frac{d \, Log_e C}{d y^2} = m = \text{a constant}$$

$$\frac{d \, Log_e C}{d y} = 2 m y$$

In the bulk diffusion region therefore, the peak useful linear gradient is

$$\left(\frac{d \, Log_e C}{d y} \right)_{max.} = 2 m y_{max.}$$

On the specimen annealed at 794°C. this gradient has the value 100 $cm.^{-1}$, while on that annealed at 731°C. the value is 250 $cm.^{-1}$. Bulk diffusion measurements made on these specimens are in error, when compared with Mercer, by 10%, which is comparable with the random error, on the high temperature specimen, and by 55%, which is not, on the other. We may conclude from these figures that the emulsions are capable of recording values of $\frac{d \, Log_e C}{d y}$

up to a limiting value between 100 and 250 $cm.^{-1}$ with a precision comparable with the random error, so that the grain boundary diffusion coefficients deduced should be insignificantly in error from this cause. Since the measured diffusion coefficient at 794°C. is too low, it is not possible to account for its variation in terms of inadequate resolution which would necessarily produce an error of the opposite sense, and so it is not necessary to associate a 10% error with the gradient 100/cm. as is otherwise required.

b) Invalid Use of Fisher's Equation:

I) Static Grain Boundaries:

In the formulation of his equation for grain boundary diffusion, Fisher assumed that diffusion always took place in a direction perpendicular to the boundary. While this is essentially true at low temperatures and long annealing times when $\sqrt{Dt} \ll \sqrt{\frac{\omega D'}{2D}\sqrt{\pi Dt}}$, it is not so at high temperatures, when bulk diffusion from the surface has an appreciable effect on the form of the concentration distribution. Borisov, Golikov, Ljubov, and Shtsherbedinsky[34] have discussed the range of validity of Fisher's equation, and have shown that it may be applied with precision provided that:

$$\frac{\sqrt{Dt}}{\frac{\omega D'}{2D}} \ll .45 + \frac{.32y}{(Dt)^{1/4}\left(\frac{\omega D'}{2D}\right)^{1/2}}$$

Using the diffusion depth parameters $\sqrt{Dt} = a$ and $\sqrt{\frac{\omega D'}{2D}\sqrt{\pi Dt}} = b$ of 4.5. and Table (4), this condition may be reduced to

$$\frac{y}{b} \gg 4.2 \left(\frac{a}{b}\right)^2 - 1.0$$

The penetrations at which measurements were always made, were from 2a to 2b, so for the point most liable to rejection in each specimen the condition becomes:

$$2\frac{a}{b} + 1 \gg 4.2\left(\frac{a}{b}\right)^2$$

The ratio $\frac{a}{b}$ is smallest for the specimen annealed at 794°C. where the condition is:

$$2\left(\frac{90}{210}\right) + 1 \gg 4.2\left(\frac{90}{210}\right)^2$$

or $$1.86 \gg .77$$

For this point the condition is satisfied only marginally, but at the other end of the experimental range (where y = 2b) acceptance is at the 20% level; and for all other specimens, where $\frac{a}{b}$ ranges from 4 - 50, the condition is easily satisfied.

We see thus, that at the highest temperature a more precise equation might be used but that otherwise the Fisher equation is valid.

The modification to this equation suggested by the above authors, a factor of $\frac{185}{105}$ in the diffusion coefficient, is quite insignificant in this investigation, particularly in view of the arbitrary choice for the width of the grain boundary.

2) Sliding Grain Boundaries:

The questions detailed above, concerning the use of Fisher's equation are applicable also to its use on sliding grain boundaries and, since no significant differences were found between the deduced diffusion coefficients, the same ranges of applicability must be accepted.

The analysis of the sliding boundaries is open to question in other ways, since variation in the gradient of the graph of Log(concentration)versus Depth is only one way in which differences in tracer distribution due to the sliding might be manifested. Other ways in which they might show are by changes in the limits of applicability of the linear law, or by systematic deviation from it. Of these effects the first is the more difficult to establish experimentally, unless gross effects are envisaged, since these limits are variable from emulsion to emulsion, being determined largely by background effects or slit length in the densitometer. No effects of this nature are evident in the graphs. Tests for systematic gradient changes in the graphs of Log(concentration) versus (depth) used in the measurement of grain boundary diffusion coefficients have previously been considered in the analysis of their effect upon the standard deviations of the observed diffusion coefficients.

4.9. Conclusions

4.9.1. Unstrained Grain Boundary Diffusion Coefficients

For the unstrained bicrystals used in this investigation the best value for the grain boundary diffusion coefficient of silver in copper was:

$$D'_u = 300 \exp\left(-\frac{32000}{RT}\right) \text{ cm.}^2/\text{sec.}$$

We may assess this result by direct comparison with the work of Achter and Smoluchowski on the same system, and by its relation to the collected diffusion data for other systems.

The previous result obtained for this system was (9):

$$D' = 1 \exp\left(-\frac{23,800}{RT}\right) \text{ cm.}^2/\text{sec.}$$

and this figure is totally inconsistent with the evaluation made in this work. Such disparity is far beyond the random variations to be expected in either investigation, and so a systematic variation must be sought.

In their work Achter and Smoluchowski used as the comparison figure for bulk diffusion

$$D = 1 \exp\left(-\frac{38,300}{RT}\right) \text{ cm.}^2/\text{sec.}$$

as opposed to that of Mercer[60]

$$D = .846 \exp\left(-\frac{47,290}{RT}\right) \text{ cm.}^2/\text{sec.}$$

used in this investigation, which is unquestionably more precise (see also C.T. Tomizuka[59]). In their analysis the evaluated quantity is $\frac{D'}{D}$, so that we may modify their activation energy by adding (47.29 - 38.3)K.cal./mol. to the previous figure of (23.8)K.cal./mol. This results in an activation energy of 32.8 K.cal./mol., in fair agreement with the present measurement.

In a more general way an activation energy of 32 K.cal./mol. fits with the other known diffusing systems. Expressed as a fraction of the activation energy for bulk diffusion it gives the value 0.68, which is to be compared with the collected values shown in Table (9). Gertsriken[36] has suggested that a value of about $\frac{2}{3}$ should be expected for this fraction, his idea being that, since the activation energy for bulk diffusion is made up of the energy required to create and then to move a vacancy, and since grain boundaries may be supposed always to contain vacancies, the activation energy for grain boundary diffusion should be that for vacancy movement only. This value is commonly about $\frac{2}{3}$ of that for bulk diffusion. Silver self-diffusion in grain boundaries is a notable exception to this rule and Arkharov[37] has suggested that this simple picture is inadequate, since it makes no allowance for stresses in the boundary.

The estimated frequency factor does not fit well with other diffusion data, a value of about 1 being more

normally found. Since, however, the deviation in this value is high the value 1 is not at complete variance with the results.

4.9.2. Diffusion in Sliding Grain Boundaries.

We may conclude from the experiment that sliding in grain boundaries has little effect on grain boundary diffusivity, at least in the range of sliding rates used. It does seem however that a significant change may in fact be caused. The tendency indicated by the results is towards increased diffusivity when slide occurs without the formation of boundary voids, the effect being greater the higher the temperature, and towards reduced diffusivity in the presence of voids.

4.10. Discussion of the Present Experiment

A modern view of grain boundaries accepts that they are extremely narrow, consisting of a central plane one atomic spacing thick, wherein the atoms are sited approximately at positions intermediate between those they would have if the plane were attached only to either of the adjacent crystal lattices. A further atomic plane on either side is supposed to be slightly distorted, but otherwise the crystal lattices are undistrubed by the boundary. We suppose that this results in an atomic arrangement in the central plane such that there is a pattern of good and bad fit between the lattice planes

of the adjacent crystals. The details of this pattern are not known and will depend on the misorientation of the grains, but we should expect that the periodicity of the pattern will increase with misorientation and will be greatest in the direction perpendicular to the axis of relative rotation of the crystals. Certainly the fractional area of misfit will increase with increasing misorientation.

Sliding between the grains is supposed to take place by the thermally activated motion of the distorted zones in such a direction as to relieve the applied stress. The process is somewhat similar to that of slip, in that movement takes place over only a small fraction of the area at a time, but the rate-determining features are quite different.

At very small slide distances this picture is adequate and an appropriate activation energy for the motion is found, but the absolute values of the strain rates, suggested by theory, are in error. For larger slide distances the subject is complicated by the appearance of voids, due apparently, to the motion of grain boundary irregularities.

We may therefore consider grain boundary sliding in two aspects; in the first, the work of Kê[7], and Mott[6], we are concerned with very small distances of slide ($\sim 10^{-5}$cm.) and an idealised boundary picture, wherein the only irregularities are on atomic scale and result

from the mismatching of the adjacent crystal lattices; the second deals with larger slide distances ($\sim 100\mu$), where it is necessary to account for stresses out of the boundary plane due to irregularities in it. In the present work it has been the intention to use slide distances larger than those of the torsional oscillation experiments, yet small enough not to be influenced by the larger type of grain boundary irregularity, the accepted evidence of the transition being the appearance of voids.

In the experiments the quantity measured was $\frac{\omega D'}{\sqrt{D}}$, or assuming the perfection of the bulk diffusion value, $\omega D'$. It is not possible to assess which quantity will be responsible for any change in the diffusion properties, but some general points may be considered.

The effective width ω of the boundary has no precise physical meaning and is merely inserted, using a reasonable value for the width of the highly diffusing plane, so that diffusion in the boundary may be expressed in a manner suitable for comparison with bulk diffusion coefficients. Following McLean[68] the value used was twice the lattice parameter in copper, or 7.6Å. A variation in this quantity should not be caused directly by the introduction of mechanical stresses into crystals, since they cannot compare with the interatomic forces, even for fairly small atomic displacements, but an indirect effect could arise in highly strained specimens.

Intrater and Machlin[35] have investigated void formation in grain boundaries and associated it with slip crossing the boundary plane. In a diffusion specimen in which this condition had been initiated, the lattice adjacent to the boundary would probably be highly dislocated so that there would be a small local increase in the bulk diffusion coefficient which would allow increased transport of the tracing material from the grain boundary into the surrounding crystals. Such an effect would be complicated by the appearance of voids but it would show, if at all, as a diminished total penetration depth for the tracer. In interpretation this can be viewed either as a reduction in the grain boundary diffusion coefficient, or as a reduction in the effective boundary width. A result such as that for the specimen annealed at 623°C. might be explained in this way. The small factors found, if they are indeed of significant size, might be explained by noting that the misorientation of the crystals used was about an axis contained within the boundary plane. Although this misorientation was a minimum and, on the simple picture suggested in Chapter I, should have represented a condition of complete misfit in the boundary, it would be reasonable to suggest that a higher degree of disorder might be obtained by further rotation about other axes, or by plastic deformation in the adjoining lattice. Such effects would reduce the mean area of a region of fit at the lower misorientations and might still have an effect at the high ones. It is possible

therefore that the small effects found might be explained as due to plastic deformation of the crystals forming the boundary and thus are not evidence against the Mott and Kê theories.

In the specimens where no voids were found the Mott 'island' theory or the Kê theory might be supposed to be operative, and from neither of these theories should we expect there to be any effect on diffusion, since they do not depend on processes producing increased numbers of vacancies or dislocations and we assume that diffusion is controlled by the concentrations of these quantities. The negative character of the results of this investigation tends thus to confirm the theories of Mott and Kê.

4.11. Criticism and Suggestions for Improvement

4.11.1. Experimental

It has been found in this investigation that the most troublesome feature of diffusion work in grain boundaries is the very long time required in the treatment of each specimen. In any extention of this work the most important modification must be to use a straining device in which a number of specimens, under slightly different conditions, can be deformed simultaneously. The present system, in which only a single specimen can be produced every second week, forbids an investigation of any scope.

Deformation of the crystals was the most unreliable

aspect of the present work, and it would seem better to attempt further investigation using some form of constant load device, rather than by attempting to produce a constant slide rate as it is not possible to predict what fraction of the total strain applied will cause plastic deformation of the crystals as a whole, and what will go to cause slide.

Specimen grips are an important feature in an investigation such as this, as recrystallised specimens cannot be used at all. A number of types have been used by different investigators, but all appear to have the weaknesses shared by those used here, except possibly the simple wire loops used by Wienberg[56] in his investigation using tricrystals.

Since it has now been established that the autoradiographic technique may be used in the form described here to measure grain boundary diffusion coefficients with reasonable precision, detailed examination of the bulk diffusion zone is no longer required. A significant reduction in the background density level could be obtained by etching off the outer surface of the crystals before mounting, to remove the layer of radioactive tracer introduced into the metal by bulk diffusion. This method might be applied very simply as grain boundary diffusion is described by a linear depth law, and it is not necessary to know the origin of the position coordinate, the gradient only of the concentration being required.

4.11.2. General

From the present investigation it seems that changes in diffusion rates are small, so that, to extend this work, it will be necessary to measure grain boundary diffusion with increased precision. This might be done by chemical or electrolytic sectioning methods, or by counting methods using X-ray absorbtion, but, an effect may also be detectable by suitable modification of the straining methods and of the crystal orientations.

In this investigation an upper limit to the amount of slide which could be produced before parting of the crystals took place, was taken to be about 150μ, but due to the complicating effect of boundary voids this limit was later reduced to 50μ. Any diffusion effect is likely to be increased by increasing the rate of slide, but a time of 10^6 seconds is needed if diffusion is to be measured with any precision so the maximum rate which can be used is $\frac{5.10^{-3}}{10^6} = 5.10^{-9}$ cm./sec. The direction of slide should not influence the diffusion penetration, and so it should be possible to apply reversed slides to the boundary, and, according to Intrater and Machlin[35], at 750°C. and a stress of 2.10^7 dynes/cm.^{2}, a slide of 5μ is reached in $2.1\ 10^3$ sec. and 10μ in $4.8\ 10^3$ sec. For the purpose of the experiment the smallest measurable slide should be applied to keep as close to the Kê work as possible (and in any case the

slide rate reduces with time) so we may take as the possible slide rate 2.10^{-7} cm./sec. Using reversed loadings it might be possible to average this rate over the required 10^6 sec. There is no reason to believe that a diffusion effect would be influenced by the slide direction so that if the effect were rate dependent, this experiment should certainly show it.

In his work on orientation effects in grain boundaries Smoluchowski[28] showed that diffusion rates were highest at high misorientations and fell to a level where they were masked by bulk diffusion at 8° - 20° of misorientation, depending on temperature. In a similar way Wienberg[56] found that slide was readily produced on highly misoriented crystals but was irregular or non-existent at misorientations of less than 5°. Similar effects were found in the present work, there being no tracer penetration and no slide on the bicrystals misoriented by $\sim 0^\circ$. It seems therefore, that boundary diffusion and slide go together and that they may be due either to a common cause or to a pair of consequential causes.

In terms of the Mott 'island' theory, the boundaries investigated here were of the 'all fit' (0°) or 'all misfit' (45°) types. An investigation made at a misorientation of 10° might be suitable for further investigation, since one type of effect which might be caused by the straining would be an increase in the mean

misfit area. This type of increase could not be detected in the present investigation as the boundary was all of a misfit character. Confirmation of such a result would be to find a maximum effect giving a diffusion rate similar to that found in unstrained boundaries of 45° misfit.

REFERENCES

1. Ewing, J.A. & Rosenhain, W., Phil. Trans. Roy. Soc. A., 193, 1900, 353.
2. Rosenhain, W. & Humphrey, J.C.W., J. Iron & Steel Inst., 87, 1913, 219.
3. Jeffries, Z. & Archer, R.S., Science of Metals, McGraw-Hill, 73, 1924.
4. Chalmers, B., Proc. Roy. Soc. A., 162, 1937, 120.
5. Hargreaves, F. & Hills, R.J., J. Inst. Metals, 41, 1924, 257.
6. Mott, N.F., Proc. Phys. Soc., 60, 1948, 391.
7. Kê, T.S., J. Appl. Phys., 20, 1949, 274.
8. Smoluchowski, R., Phys. Rev., 87, 1952, 482.
9. Achter, M.R. & Smoluchowski, R., J. Appl. Phys., 22, 1951, 1260.
10. Burgers, J.M, Proc. Kon. Med. Akad. u. Wet. Amsterdam, 42, 1939, 293.
11. Read, W.T. & Shockley, W., Phys. Rev., 78, 1950, 275.
12. Van der Merwe, J.H., Proc. Phys. Soc., 63A, 1950, 616.
13. Friedel, J., Cullity, B.P. & Crussard, C., Acta. Met., 1, 1953, 79.
14. Lee, C.H. & Maddin, R., Trans. A.I.M.E., 215, 1959, 397.
15. Forestieri, A.F. & Girifalco, L.A., J. Phys. Chem. Solids, 10, 1959, 99.
16. Darby, J.B., Tomizuka, C.T. & Baluffi, R.W., Bull. Am. Phys. Soc., 3, 1958, 124.
17. Barr, L.W., Ph.D. Thesis, Edinburgh University, 1959.
18. Inman, M.C., Vacancies & Other Point Defects in Metals & Alloys, London, The Institute of Metals, 1958, 227.
19. Baluffi, R.W., Acta. Met., 2, 1954, 194.
20. Hoffman, R.E. & Turnbull, D., J. Appl. Phys., 22, 1951.

REFERENCES (CONTD.)

21. Kochler, J.S., Phys. Rev., 60, 1941, 397.

22. Brown, W.F., Phys. Rev., 60, 1941, 139.

23. Fick, A., Ann. Phys. Lpz., 94, 1895, 59.

24. Crank, J., The Mathematics of Diffusion, O.U.P., 1956.

25. Chandrasakhar, S., Rev. Mod. Phys., 15, 1943, 20.

26. Langmuir, I., J. Franklin Inst., 217, 1934, 543.

27. Rhines, F.N. & Wells, C., Trans. Am. Soc. Met., 27, 1939, 625.

28. Achter, M.R. & Smoluchowski, R., Kingston, The Physics of Powder Metalurgy, McGraw-Hill, 77, 1951.

29. Fisher, J.C., J. Appl. Phys., 22, 1951, 74.

30. Le Claire, A.D., Phil. Mag., 42, 1951, 468.

31. Yukama, S. & Sinnott, M.J., Trans. A.I.M.E., 203, 1955, 996.

32. Whipple, R.T.P., Phil. Mag., 45, 1954, 1225.

33. Turnbull, D. & Hoffman, R.E., Acta. Met., 2, 1954, 419.

34. Borisov, V.T., Golikov, V.M., Ljubov, B.Y. & Shtsherbedinsky, G.V., Radioisotopes in Scientific Research, Vol. I., Pergamon Press, 212, 1958.

35. Intrater, J. & Machlin, E.S., Acta. Met., 7, 1959, 140.

36. Gertsriken, S.D., Fizika. Metallov. i. Metallovedenie, 2, 1956, 378.

37. Arkharov, V.I., Fizika Metallov. i Metallovedenie, 2, 1956, 379.

38. Intrater, J. & Machlin, E.S., J. Inst. Met., 88, 1959, 305.

39. Honeycombe, R.W.K., Metallurgical Reviews, 4, 1959, 1.

40. Barrett, C.S., Structure of Metals, McGraw-Hill, 194, 1953.

REFERENCES (CONTD.)

41. Tegart, W.J. McG., The Electrolytic & Chemical Polishing of Metals, Pergamon Press, 94, 1956.

42. Barr, L.W. & Blackburn, D.A., J. Sci. Inst., 36, 1959, 197.

43. MacRobbie, J.M., M.Sc. Thesis, Edinburgh University, 1957.

44. Doniach, I. & Pelc, S.R., Brit. J. Radiology, 23, 1950, 184.

45. Stevens, G.W.W., Brit. J. Radiology, 23, 1950, 723.

46. Siegbahn, K., Phys. Rev., 77, 1950, 233.

47. Gomberg, H.J., Nucleonics, 9, Oct. 1951, 27.

48. Pelc, S.R., Nature, 160, 1947, 749.

49. Lacassagne, A. & Lattes J., Compt. Rend. Soc. Biol., 90, 1924, 352.

50. Belanger, L.F. & Leblond, C.P., Endocrinology, 39, 1946, 8.

51. Evans, T.C., Radiology, 49, 1947, 206.

52. Williams, A.I., Nucleonics, 8, June 1951, 10.

53. Sherwood, H.F., Rev. Sci. Inst., 18, 1947, 80.

54. Herz, R.H., Nucleonics, 9, Sept. 1951, 24.

55. Weaver, K.S., Measurement of Photographic Transmission Density, J. Opt. Soc. Am., 40, 1950, 524 & 1339.
see also:-
Mees, C.E.K., The Theory of the Photographic Process, Macmillan, New York, 820, 1954.

56. Wienberg, F., Trans. A.I.M.E., 212, 1958, 808.

57. Awbery, J.H., Proc. Phys. Soc., 41, 1929, 384.

58. Worthing, A.G. & Geffner, J., Treatment of Experimental Data, John Wiley & Sons, 318, 1948.

59. Tomizuka, C.T., see Lazarus, D. Solid State Physics, 10, McGraw-Hill, 1960.

60. Mercer, L., Ph.D. Thesis, Leeds University, 1955.

61. Weatherburn, C.E., Mathematical Statistics, C.U.P., 1959.

REFERENCES (CONTD.)

62. Wajda, E.S., Shirn, G.A., and Huntingdon, H.B., Acta. Met., 3, 1955, p. 39.

63. Okkerse, B., Acta Met., 2, 1954, 551.

64. Wajda, E.S., Acta Met., 2, 1954, 184.

65. Shirn, G.A. Wajda, E.S., and Huntingdon, H.B., Acta. Met., 1, 1953, 513.

66. Flanagan, R. & Smoluchowski, R., J. Appl. Phys., 23, 1952, 785.

67. Inman, M.C., Johnston, D., Mercer, W.L. and Shuttleworth, R., Radioisotopes Conference 2, Butterworths, London, 1955.

68. McLean, D., Grain Boundaries in Metals, p. 224, Clarendon Press, Oxford, 1957.

Bulk Diffusion Data

$T^{o}C$	t sec.	$\frac{d\text{Log}_e C}{dy^2}$ cm^{-2}	Expansion Factor	D cm^2/sec.
794	$5.20\ 10^5$	$(1.91 \pm .04)10^3$	.835	$(1.76 \pm .04)10^{-10}$
731	$3.43\ 10^5$	$(6.68 \pm .2)10^3$	.895	$(8.72 \pm 0.3)10^{-11}$
623	$9.97\ 10^5$	$(12.7 \pm .6)10^3$	.885	$(1.54 \pm .07)10^{-11}$

TABLE (2).

Unstrained Grain Boundary Diffusion Data

T°C	t sec.10^5	D_E $cm^2/sec.$	$\sqrt{D_E t}$ microns	$\frac{d \log_e C}{dy}$ cm^{-1}	Expansion Factor	$\sqrt{\frac{\omega D'}{2 D_E}\sqrt{\pi D_E t}}$ microns	D'_u cm^2/sec	$\frac{D'_u}{D_E}$ x 10^5	$-\log_{10} D'_u$
794±0.5	5.20	$1.58\ 10^{-10}$	91	48±7	.835	210	$7.9±2\ 10^{-5}$	5.0±1.3	4.05±.090
731 ±0.7	3.43	$3.90\ 10^{-11}$	37	82±5	.900	120	$1.9±15\ 10^{-5}$	4.9±.40	4.72±.040
623±1	9.97	$2.37\ 10^{-12}$	15	67±7	.885	150	$4.0±.55\ 10^{-6}$	17.0±2.3	5.40±.060
567.5±.5	9.51	$3.91\ 10^{-13}$	6.1	98.5±4	.925	100	$8.4±.45\ 10^{-7}$	21.5±1.1	6.07±.025
517±0.5	20.4	$6.5\ 10^{-14}$	3.6	54±2	.835	185	$6.4±.3\ 10^{-7}$	98.0±4.5	6.19±.020

Table (4)

Strained Grain Boundary Diffusion Data

T°C	$\frac{d \log_e C}{d \gamma}$ cm^{-1}	Expansion Factor	$\sqrt{\frac{\omega D'}{2 D_\epsilon}} \sqrt{\pi D_\epsilon t}$ microns	D_s' $cm^2/sec.$	$\frac{D_s'}{D_\epsilon}$	$-\log_{10} D_s'$	Slide Distance microns	Fractional Void Area
794 ± 0.5	36.5 ± 1.5	.835	275	$1.37 \pm 0.7\ 10^{-5}$	$8.6\ 10^5$	3.86 ± .02	48 ± 2	0
731 ± 0.7	70 ± 5	.895	150	$2.8 \pm .2\ 10^{-5}$	$7.25\ 10^5$	4.54 ± .03	28 ± 1	.02
623 ± 1	74.5 ± 4	.885	135	$3.25 \pm .3\ 10^{-6}$	$1.35\ 10^6$	5.49 ± .03	70 ± 2	.3
	106 ± 3		95	$1.60 \pm .07\ 10^{-6}$	$6.75\ 10^5$	5.79 ± .015		.9
567 ± 0.5	94 ± 5.5	.885	105	$8.4 \pm .7\ 10^{-7}$	$2.15\ 10^6$	6.07 ± .035	16.5 ± .5	0
517 ± 0.5	49.5 ± 3	.835	200	$7.6 \pm .6\ 10^{-7}$	$11.7\ 10^6$	6.12 ± .035	51 ± 1	0

Table (5)

Combined Grain Boundary Diffusion Data

T°C	Unstrained Weight ω_u	Strained Weight ω_s	Combined Weight ω_c	$-Log_{10}\overline{D'_u}$	$-Log_{10}\overline{D'_s}$	$\frac{\sigma_{D's}}{\sigma_{D'u}}$
794	1	18	19	$4.14 \pm .14$	$4.05 \pm .16$	.22
731	5	8	13	$4.54 \pm .10$	$4.45 \pm .11$	.75
623	2	8	10	$5.38 \pm .04$	$5.30 \pm .05$	
567.5	15	6	21	$5.91 \pm .07$	$5.83 \pm .08$	1.48
517	16	7	23	$6.45 \pm .12$	$6.38 \pm .14$	1.6

TABLE (6).

Significance Tests

T°C	$Log_{10}\overline{D'_u} - Log_{10}D'_u$	Pu	$Log_{10}\overline{D'_s} - Log_{10}D'_s$	Ps	$Log_{10}D'_s - Log_{10}D'_u$	P
794	$-.09 \pm .17$	.6	$-.19 \pm .16$	.25	$+.18 \pm .09$	.05
731	$+.18 \pm .11$	.1	$+.10 \pm .11$	.4	$+.17 \pm .05$	$<.01$
623	$+.02 \pm .07$	.8	$+.19 \pm .06$	.001	$-.10 \pm .065$	—
567.5	$+.17 \pm .07$	.02	$+.24 \pm .09$	.01	$+.002 \pm .045$	~1
517	$-.25 \pm .12$	.04	$-.26 \pm .14$	.07	$+.076 \pm .04$	.07

TABLE (7)

Possible Correlation between Enhancement of Diffusion and Slide Distance or Mean Slide Rate

$T^{\circ}C$	$\frac{D'_S}{D'_n}$	$S\mu$	$\dot{\bar{S}}$ cm./sec,	$\frac{D'_S}{D'_n} / \dot{\bar{S}}$ sec./cm.	$\frac{D'_S}{D'_n} / S$ cm^{-1}
794	1.74	48	$9.6\ 10^{-9}$	$1.8\ 10^{8}$	$3.6\ 10^{2}$
731	1.48	28	$8.2\ 10^{-9}$	$1.8\ 10^{8}$	$5.3\ 10^{2}$
567.5	1.01	16.5	$1.8\ 10^{-9}$	$5.7\ 10^{8}$	$6.1\ 10^{2}$
517	1.20	51	$2.5\ 10^{9}$	$5.0\ 10^{8}$	$2.4\ 10^{2}$

Table (8).

Activation Energies for Diffusion (K.cal./mol.)

Tracer	Metal	Bulk Diffusion	Boundary Diffusion	Q_{GB}/Q_V	Source
Ag	Cu	47.3	32.1	.68	This Investigation
Cd	Cd	18.6	13.0	.70	Wajda et al. (62)
Pb	Pb	25.7	15.7	.61	Okkerse (63)
Zn	Zn	22.9	14.45	.63	Wajda (64) Shirn et al. (65)
Ag	Ag	45.9	20.2	.44	Hoffman et al. (20)
Th	W	120	90	.75	Langmuir (26)
Ni	Cu	64.8	38.5	.59	Yukawa et al. (31)
Zn	Cu	52.1	24.5 $(33.6)^+$	.47 $(.65)^+$	Flanagan et al. (66) Inman et al. (67)
Ag	Cu	47.3	23.8 $(32.8)^+$	.50 $(.69)^+$	Achter et al. (9) Mercer (60)

$(\ )^+$: Corrected to consistent use of the tabulated values for the Bulk Diffusion Activation Energy.

TABLE (9)

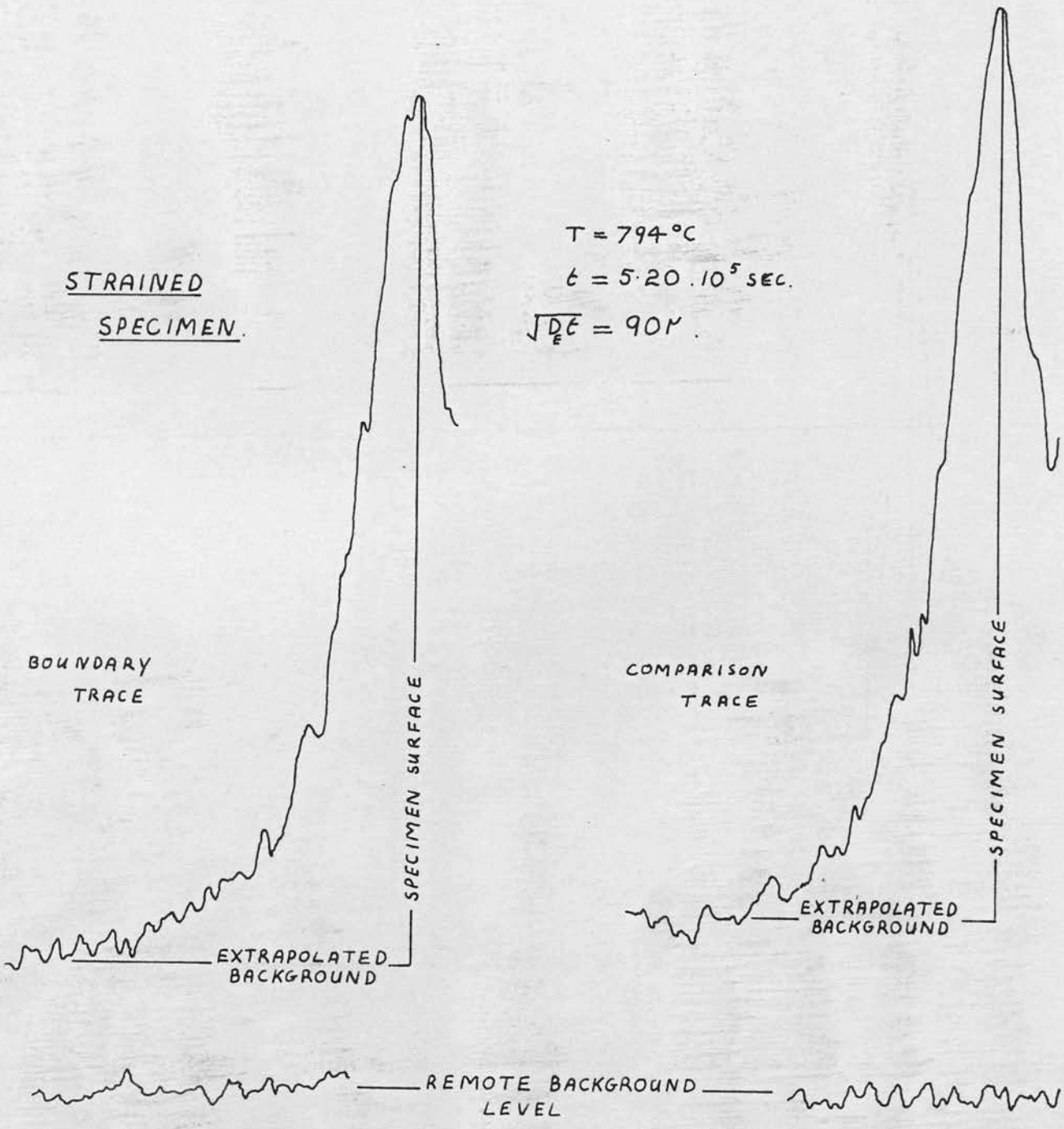
STRAINED
SPECIMEN.
T = 794°C
t = 5·20 . 10⁵ SEC.
√(D_E t) = 90 M.
BOUNDARY
TRACE
SPECIMEN SURFACE
EXTRAPOLATED
BACKGROUND
COMPARISON
TRACE
SPECIMEN SURFACE
EXTRAPOLATED
BACKGROUND
REMOTE BACKGROUND
LEVEL

Graph 1.

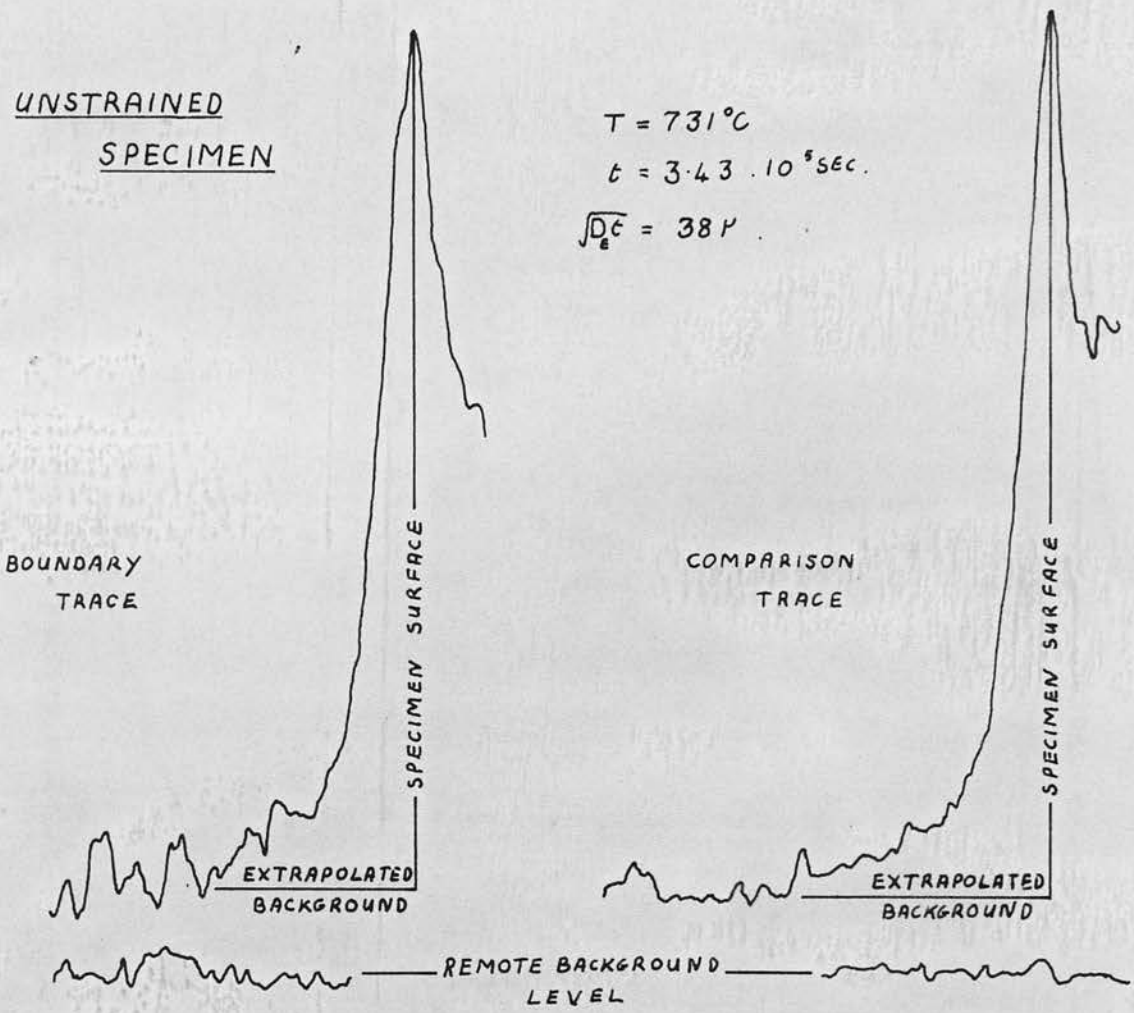
UNSTRAINED
SPECIMEN
T = 731°C
t = 3·43 . 10⁵ SEC.
√(D_ε t) = 38 μ .
BOUNDARY
TRACE
COMPARISON
TRACE
SPECIMEN SURFACE
SPECIMEN SURFACE
EXTRAPOLATED
BACKGROUND
EXTRAPOLATED
BACKGROUND
REMOTE BACKGROUND
LEVEL

Graph 2

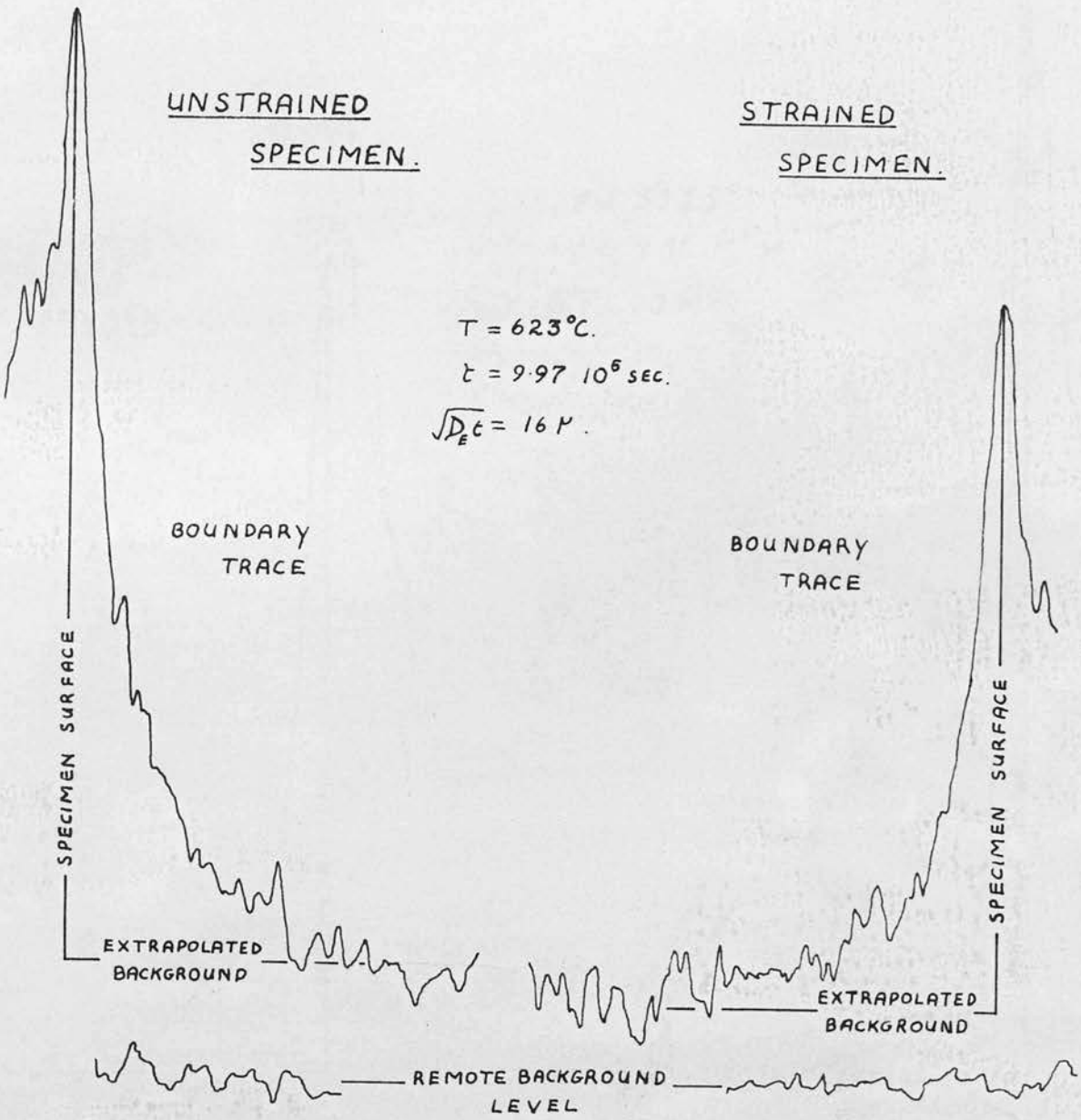
UNSTRAINED
SPECIMEN.
STRAINED
SPECIMEN.
T = 623°C.
t = 9·97 10⁶ sec.
√(D_E t) = 16 μ.
BOUNDARY
TRACE
BOUNDARY
TRACE
SPECIMEN SURFACE
SPECIMEN SURFACE
EXTRAPOLATED
BACKGROUND
EXTRAPOLATED
BACKGROUND
REMOTE BACKGROUND
LEVEL

Graph 3.

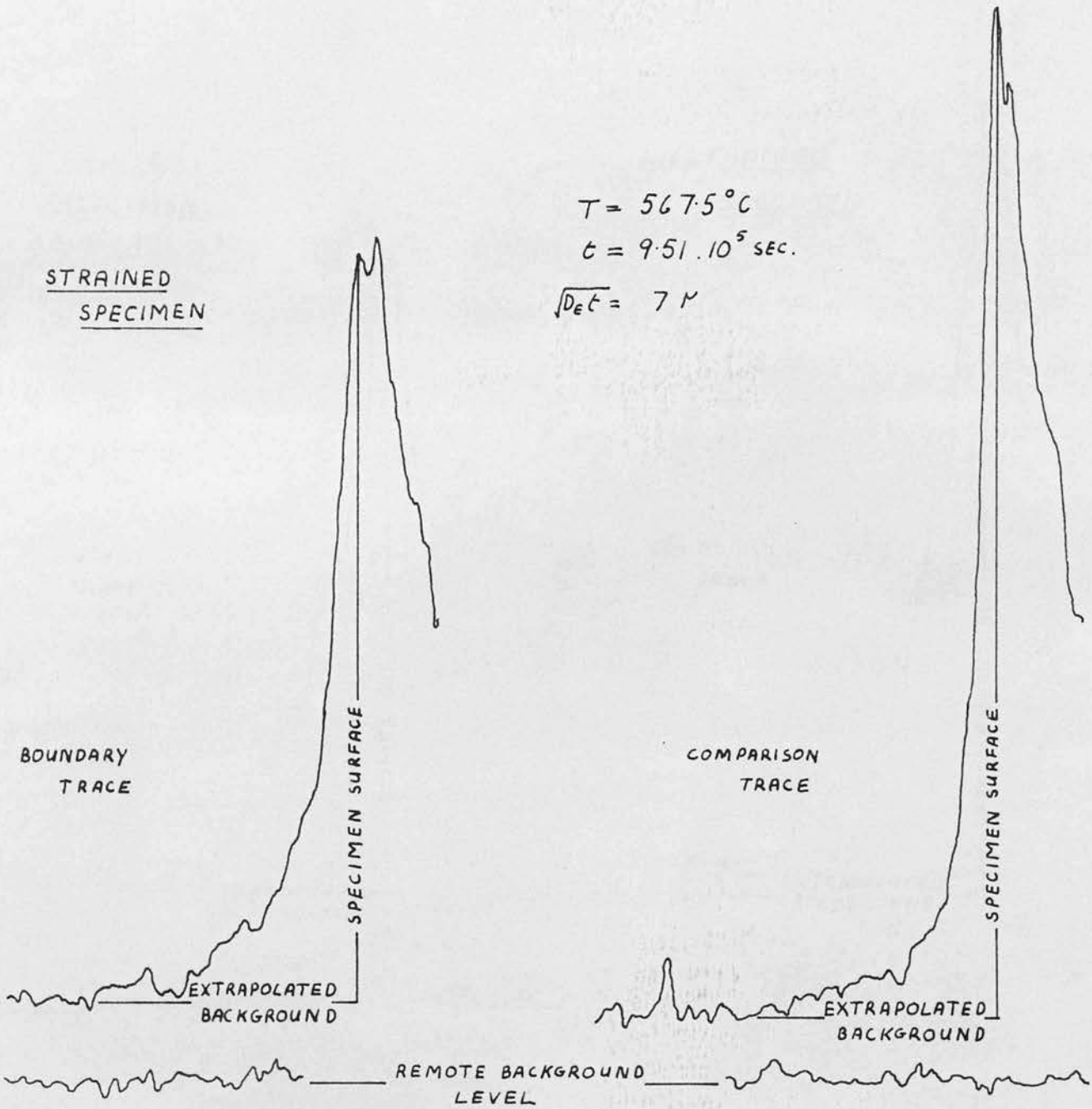
T = 567·5 °C
t = 9·51 . 10^5 SEC.
√(D_ε t) = 7 M
STRAINED SPECIMEN
BOUNDARY TRACE
SPECIMEN SURFACE
EXTRAPOLATED BACKGROUND
COMPARISON TRACE
SPECIMEN SURFACE
EXTRAPOLATED BACKGROUND
REMOTE BACKGROUND LEVEL

Graph 4.

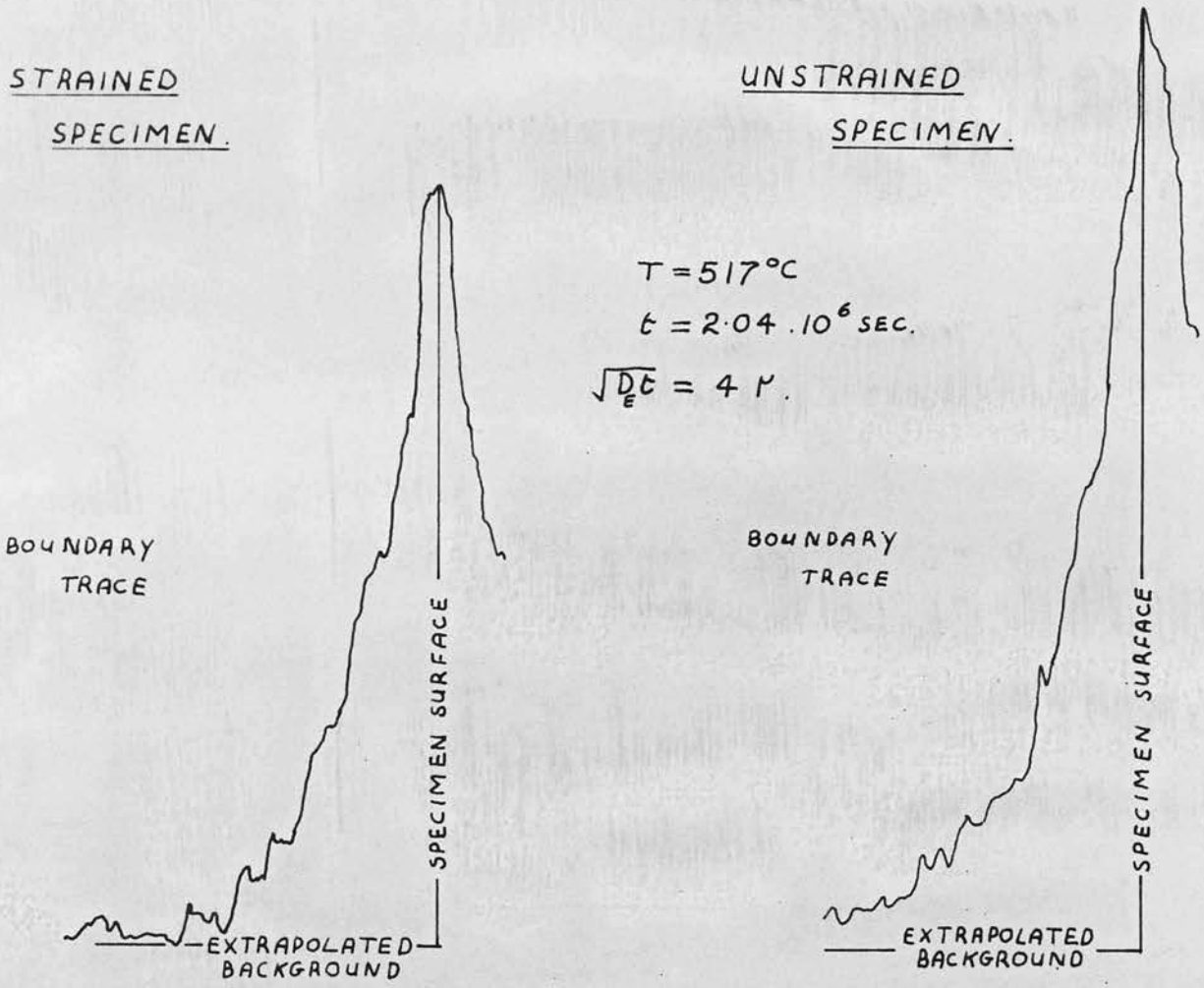
STRAINED
SPECIMEN.
UNSTRAINED
SPECIMEN.
T = 517°C
t = 2·04 . 10⁶ SEC.
√(D_ε t) = 4 μ.
BOUNDARY
TRACE
BOUNDARY
TRACE
SPECIMEN SURFACE
SPECIMEN SURFACE
EXTRAPOLATED
BACKGROUND
EXTRAPOLATED
BACKGROUND

Graph 5.

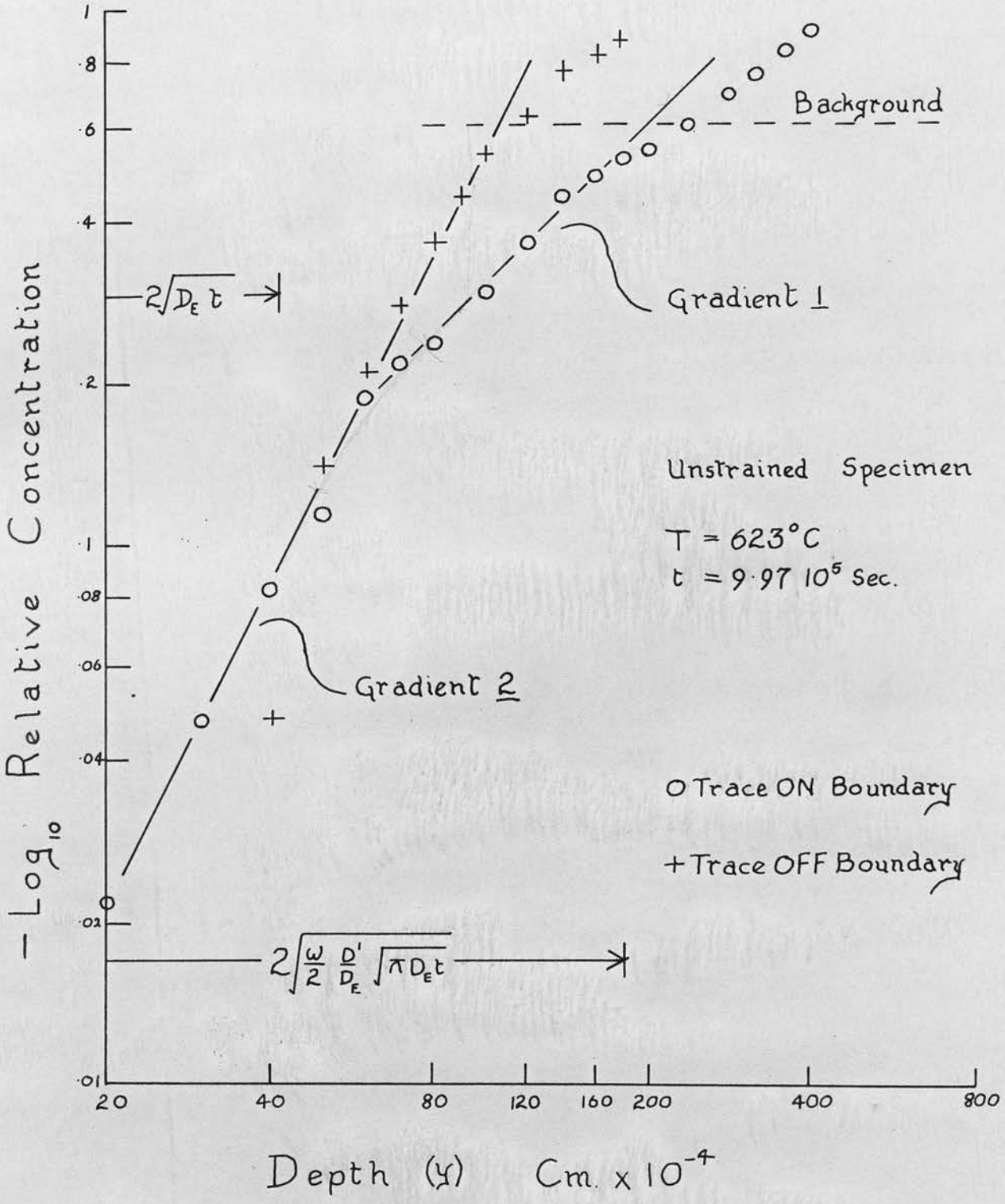
- Log10 Relative Concentration
1
·8
·6
·4
·2
·1
·08
·06
·04
·02
·01
20
40
80
120
160
200
400
800
Depth (y) Cm. x 10-4
Background
2√(DE t)
Gradient 1
Gradient 2
Unstrained Specimen
T = 623°C
t = 9·97 10^5 Sec.
O Trace ON Boundary
+ Trace OFF Boundary
2√((ω/2)(D'/DE)√(π DE t))

Graph 6.

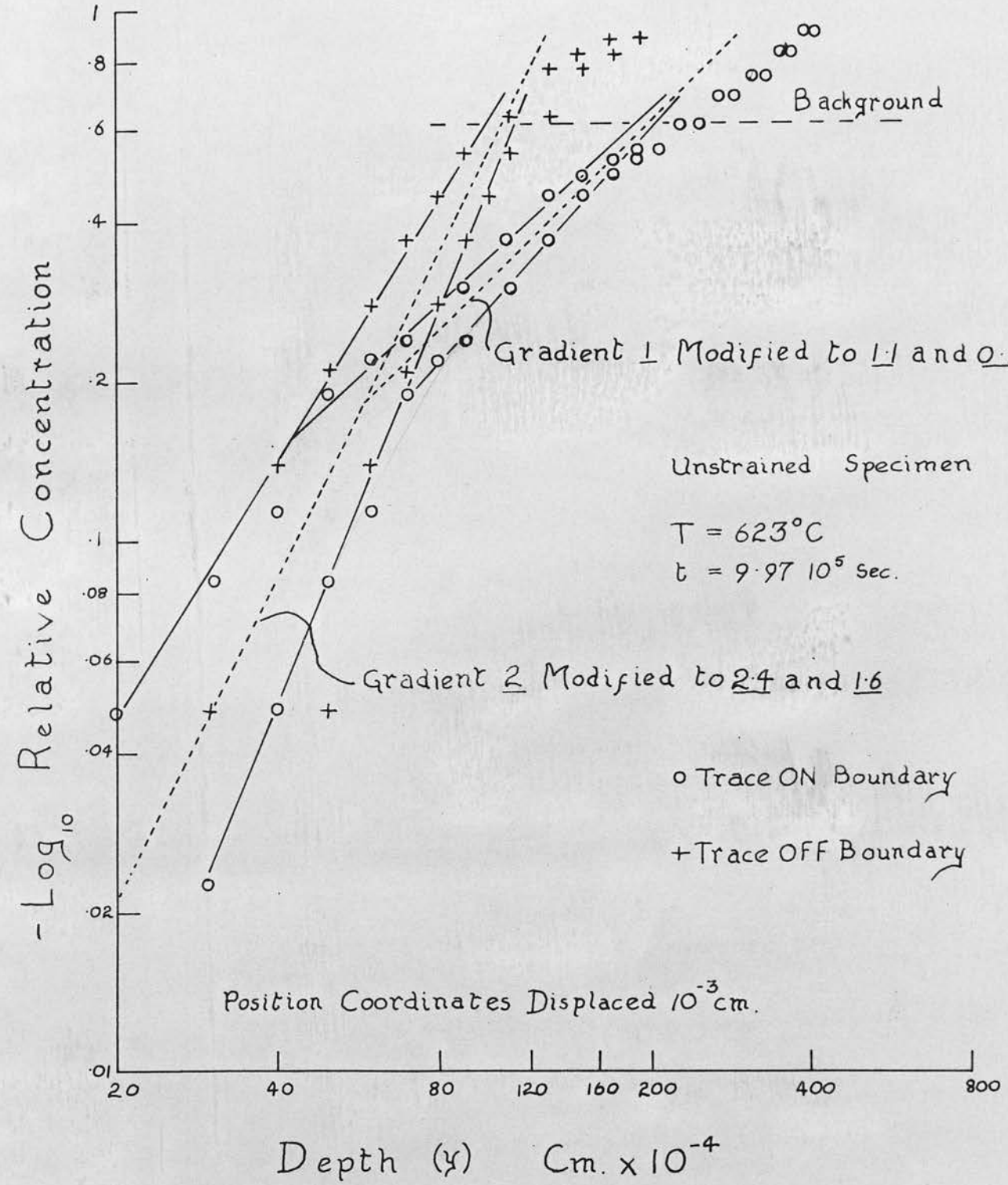
- Log10 Relative Concentration
1
·8
·6
·4
·2
·1
·08
·06
·04
·02
·01
Background
Gradient 1 Modified to 1·1 and 0·9
Unstrained Specimen
T = 623°C
t = 9·97 10^5 Sec.
Gradient 2 Modified to 2·4 and 1·6
o Trace ON Boundary
+ Trace OFF Boundary
Position Coordinates Displaced 10^-3 cm.
20
40
80
120
160
200
400
800
Depth (y) Cm. x 10^-4

Graph 7.

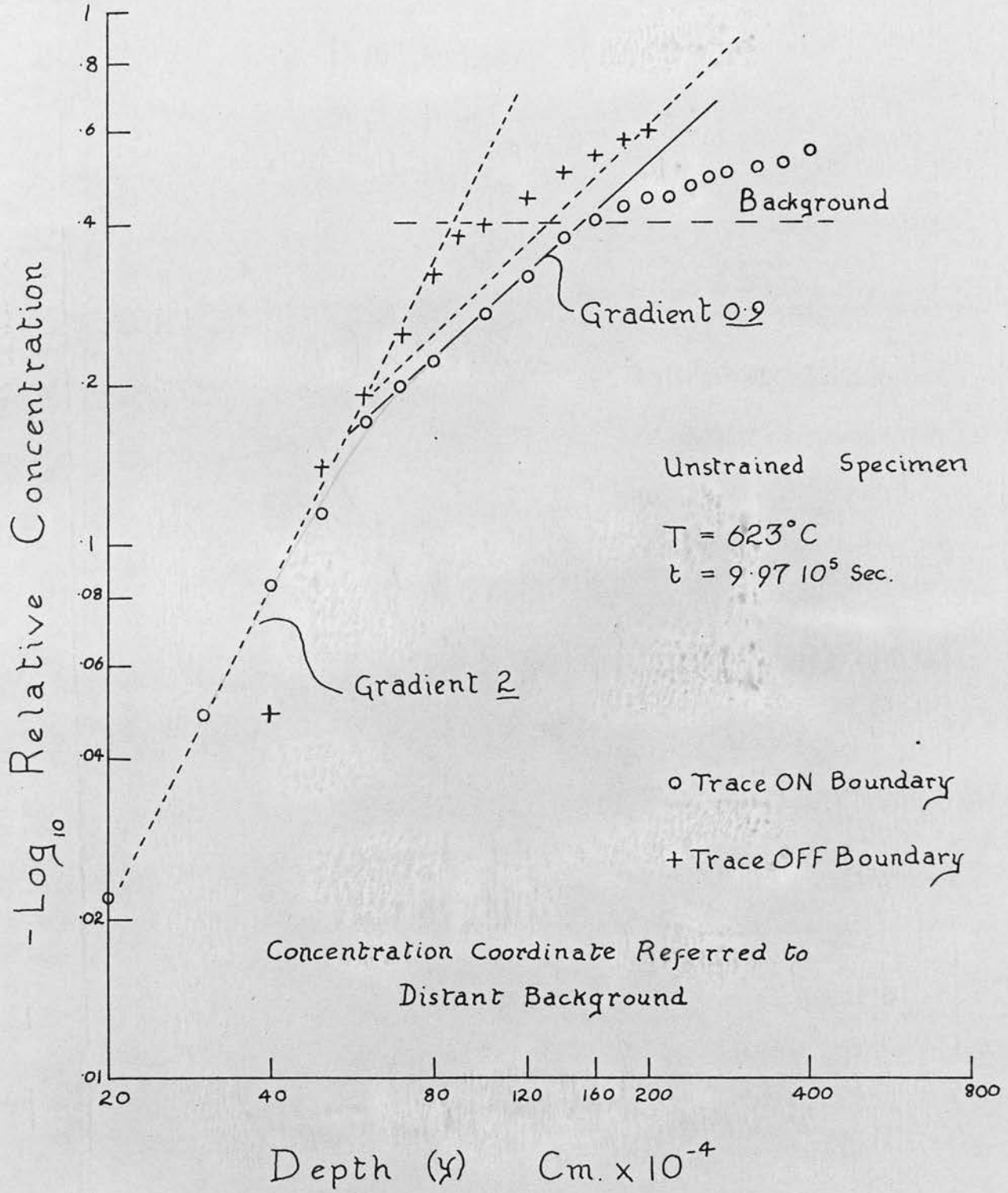
- Log10 Relative Concentration
1
·8
·6
·4
·2
·1
·08
·06
·04
·02
·01
Background
Gradient 0·9
Gradient 2
Unstrained Specimen
T = 623°C
t = 9·97 10^5 Sec.
o Trace ON Boundary
+ Trace OFF Boundary
Concentration Coordinate Referred to
Distant Background
20
40
80
120
160
200
400
800
Depth (y) Cm. x 10^-4

Graph 8.

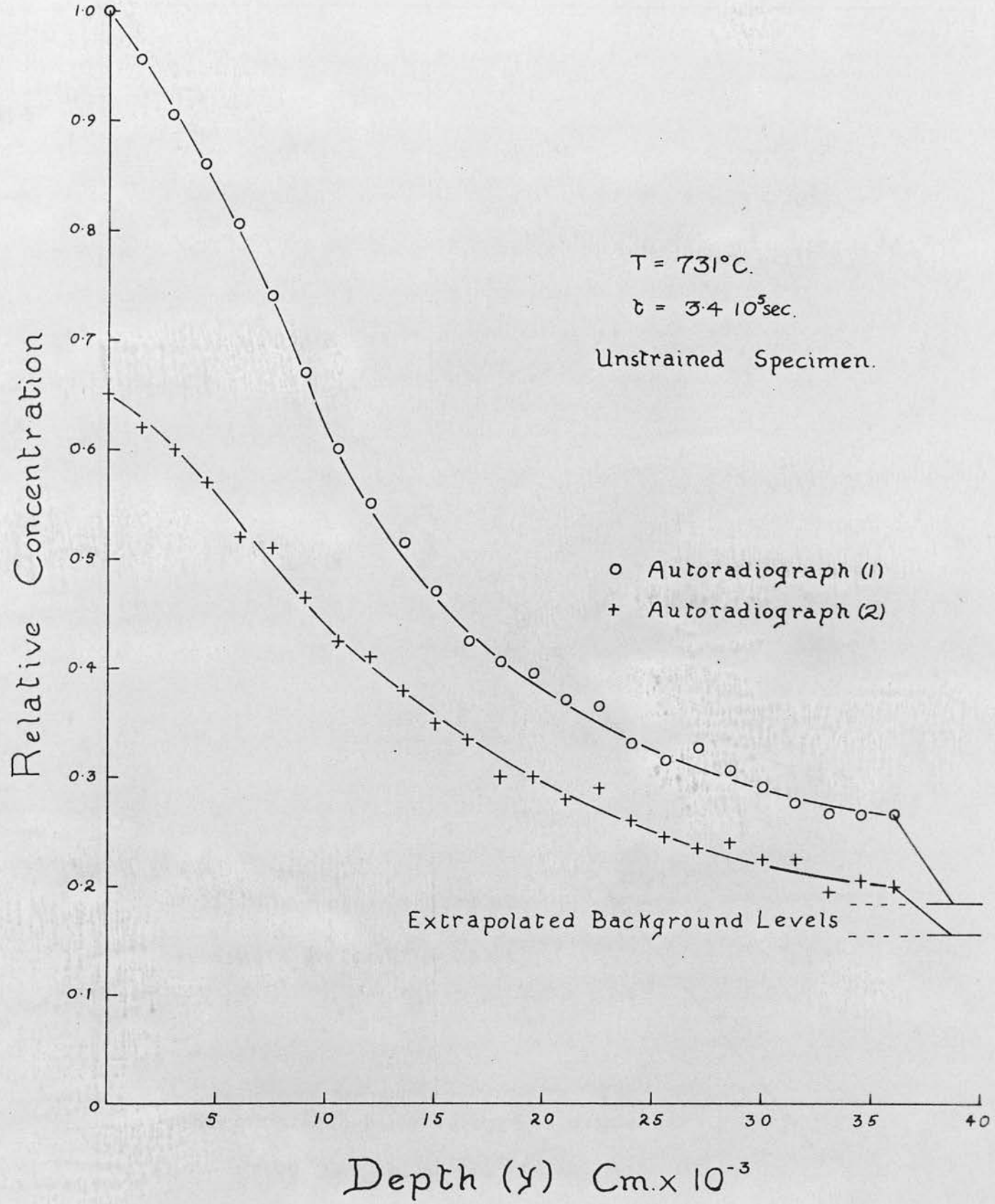
Relative Concentration
1·0
0·9
0·8
0·7
0·6
0·5
0·4
0·3
0·2
0·1
0
5
10
15
20
25
30
35
40
Depth (Y) Cm. x 10⁻³
T = 731°C.
t = 3·4 10⁵sec.
Unstrained Specimen.
o Autoradiograph (1)
+ Autoradiograph (2)
Extrapolated Background Levels

Graph 9.

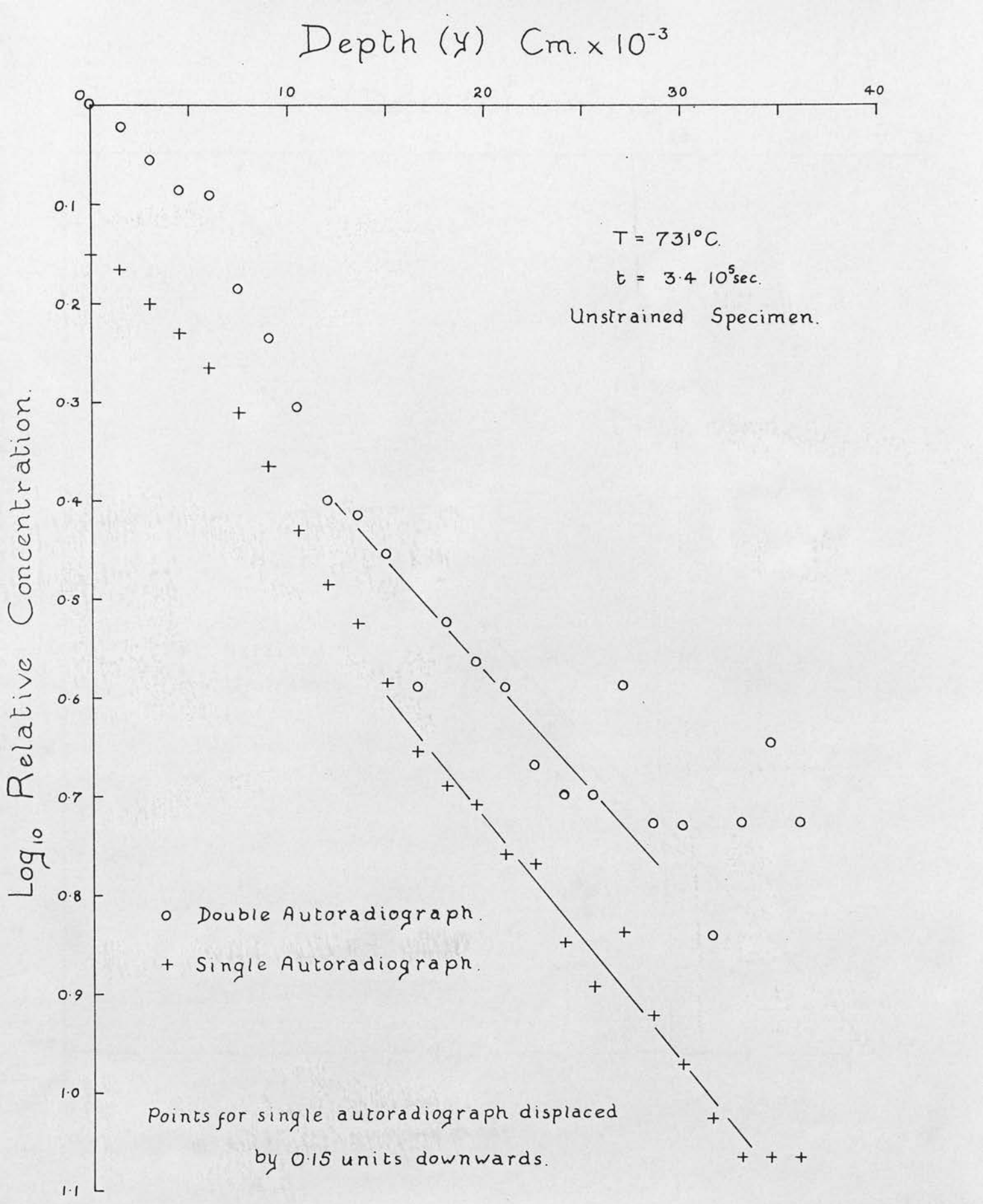
Depth (y) Cm. x 10⁻³
0
10
20
30
40
Log₁₀ Relative Concentration.
0·1
0·2
0·3
0·4
0·5
0·6
0·7
0·8
0·9
1·0
1·1
T = 731°C.
t = 3·4 10⁵sec.
Unstrained Specimen.
o Double Autoradiograph.
+ Single Autoradiograph.
Points for single autoradiograph displaced
by 0·15 units downwards.

Graph 10.

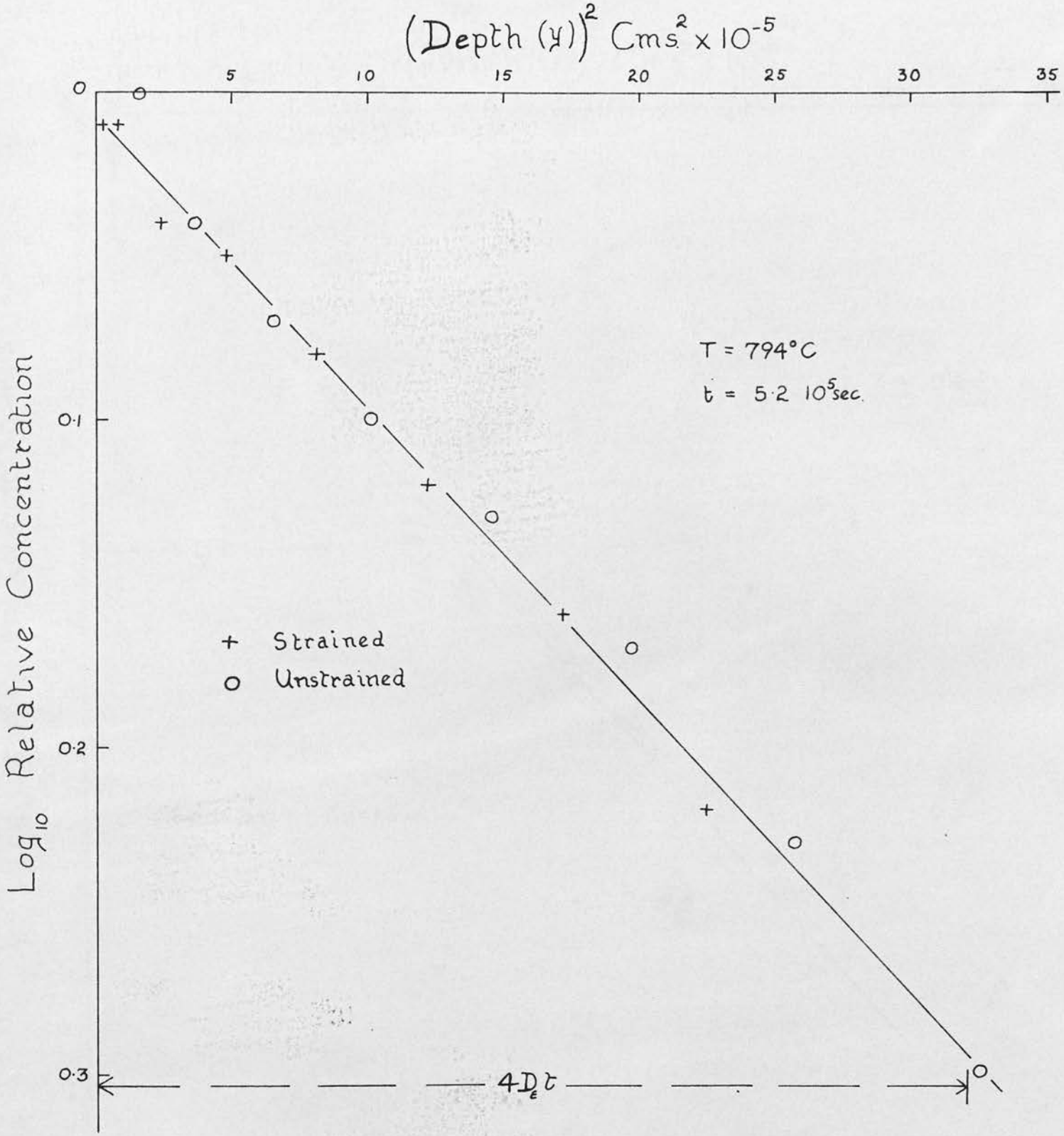
(Depth (y))² Cms² x 10⁻⁵
0
5
10
15
20
25
30
35
Log₁₀ Relative Concentration
0
0·1
0·2
0·3
T = 794°C
t = 5·2 10⁵sec
+ Strained
o Unstrained
4Dₑt

Graph 11.

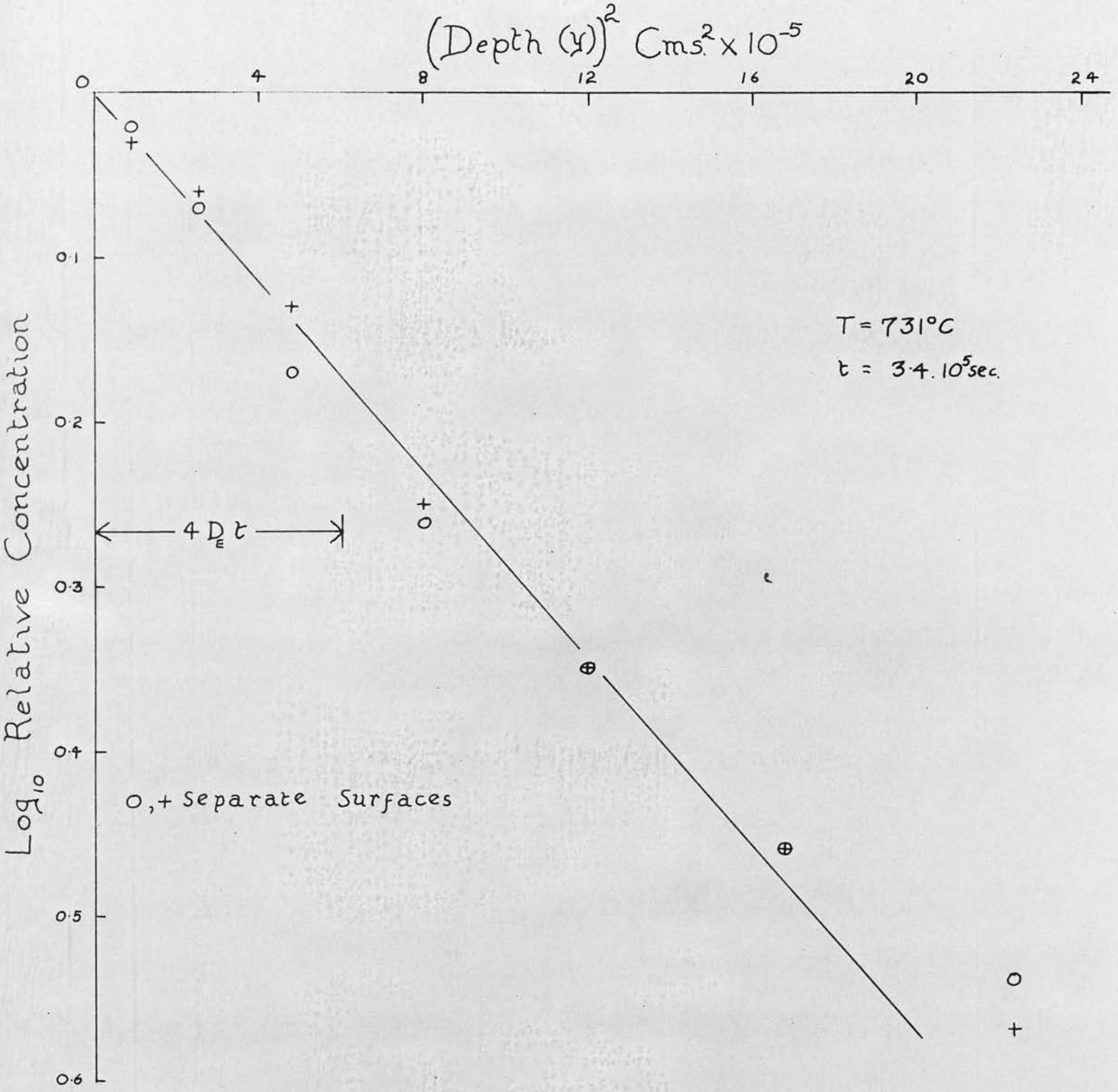
(Depth (y))² Cms.² × 10⁻⁵
0
4
8
12
16
20
24
Log₁₀ Relative Concentration
0·1
0·2
0·3
0·4
0·5
0·6
T = 731°C
t = 3·4.10⁵sec.
4 D_E t
O, + Separate Surfaces
O
+

Graph 12.

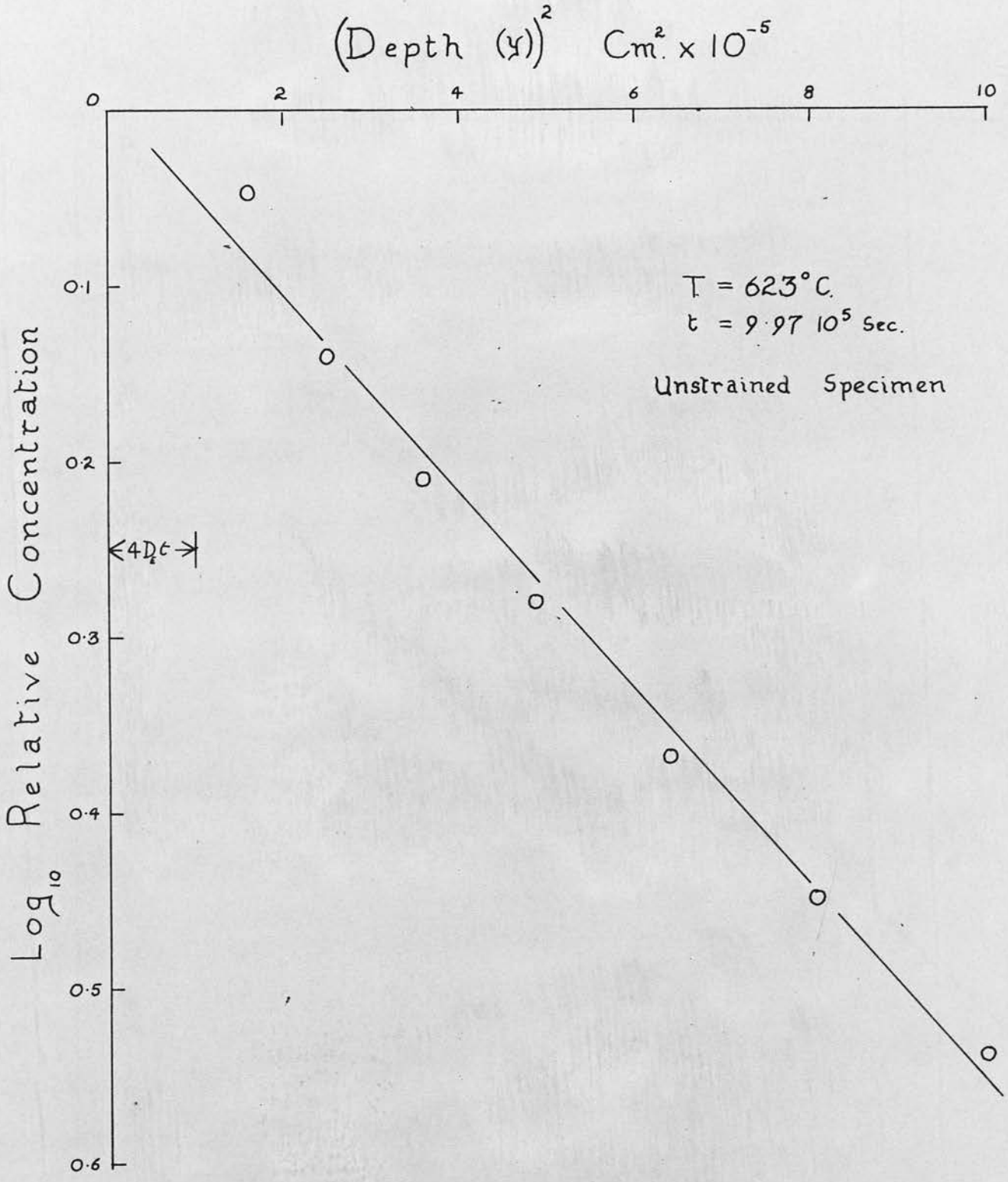
(Depth (y))² Cm². x 10⁻⁵
0
2
4
6
8
10
Log₁₀ Relative Concentration
0·1
0·2
0·3
0·4
0·5
0·6
4Dt
T = 623° C.
t = 9·97 10⁵ Sec.
Unstrained Specimen

Graph 13.

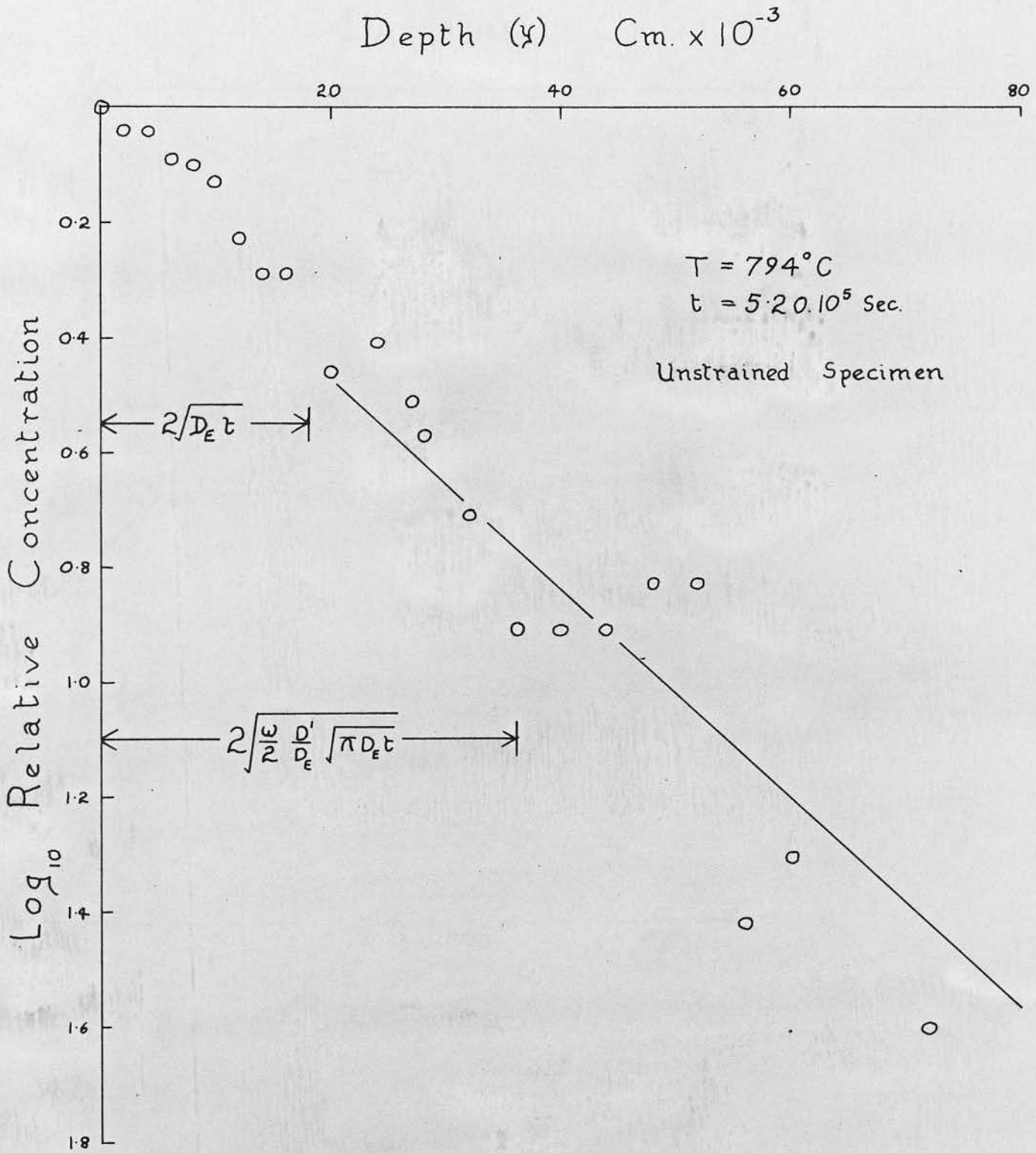
Depth (y) Cm. x 10^-3
20
40
60
80
Log10 Relative Concentration
0·2
0·4
0·6
0·8
1·0
1·2
1·4
1·6
1·8
T = 794°C
t = 5·20.10^5 Sec.
Unstrained Specimen
2√(D_E t)
2√((ω/2)(D'/D_E)√(π D_E t))

Graph 14.

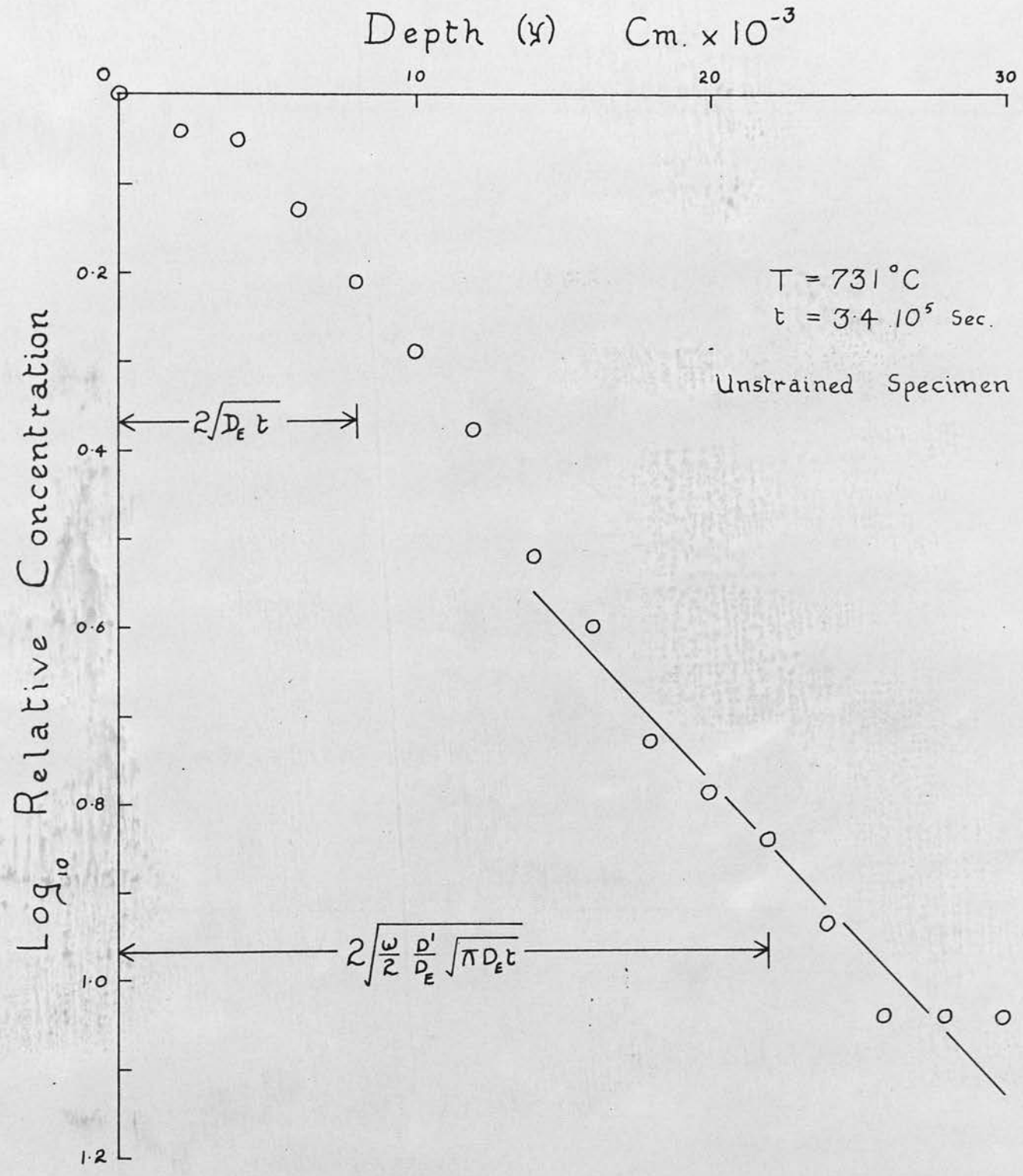
Depth (Y) Cm. x 10^-3
0
10
20
30
Log10 Relative Concentration
0·2
0·4
0·6
0·8
1·0
1·2
T = 731 °C
t = 3·4 10^5 Sec.
Unstrained Specimen
2√(D_E t)
2√((ω/2)(D'/D_E)√(π D_E t))

Graph 15.

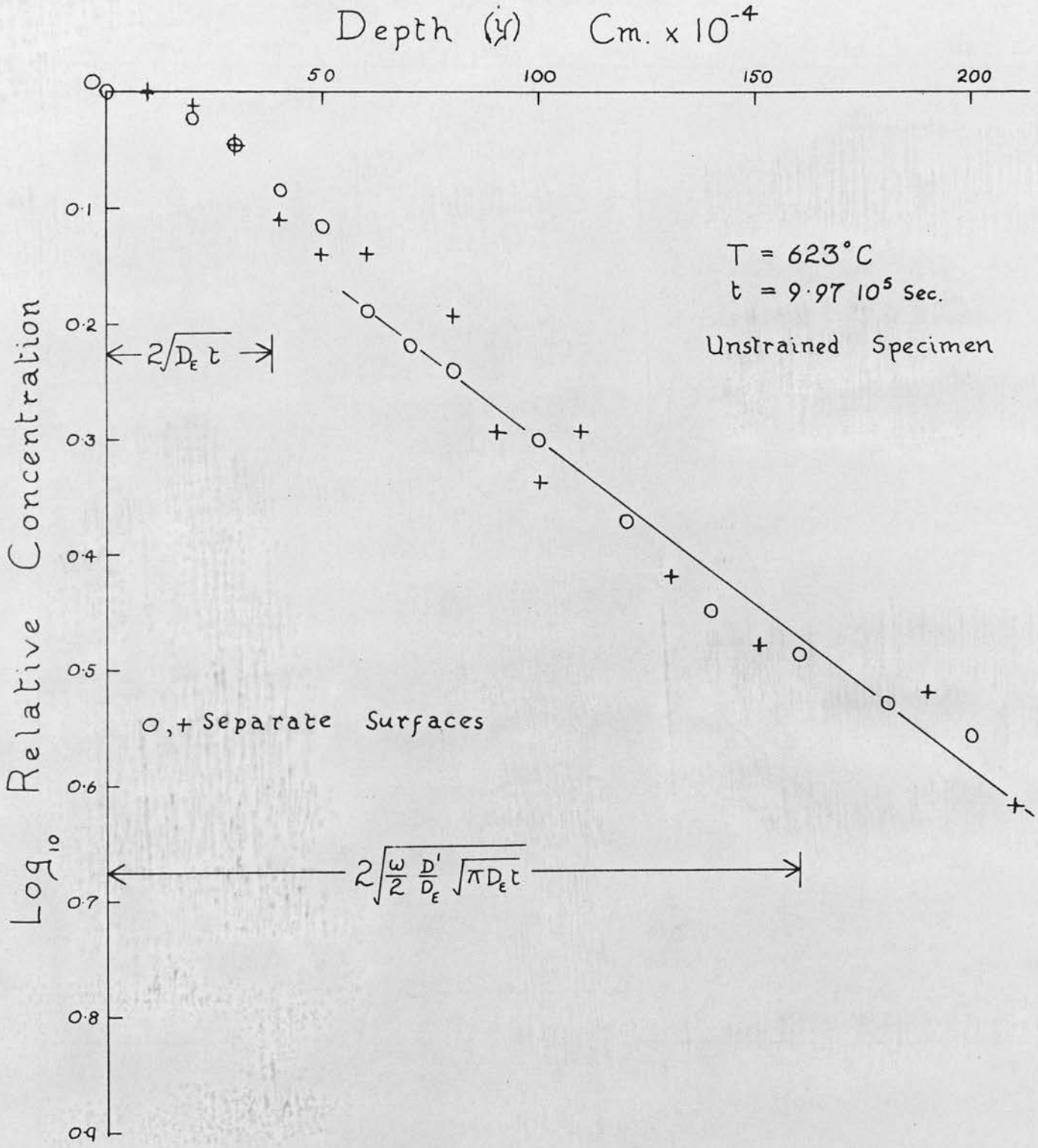
Depth (y) Cm. x 10⁻⁴
50
100
150
200
0·1
0·2
0·3
0·4
0·5
0·6
0·7
0·8
0·9
Log₁₀ Relative Concentration
T = 623°C
t = 9·97 10⁵ Sec.
Unstrained Specimen
2√(Dε t)
O, + Separate Surfaces
2√((ω/2)(D'/Dε)√(π Dε t))

Graph 16.

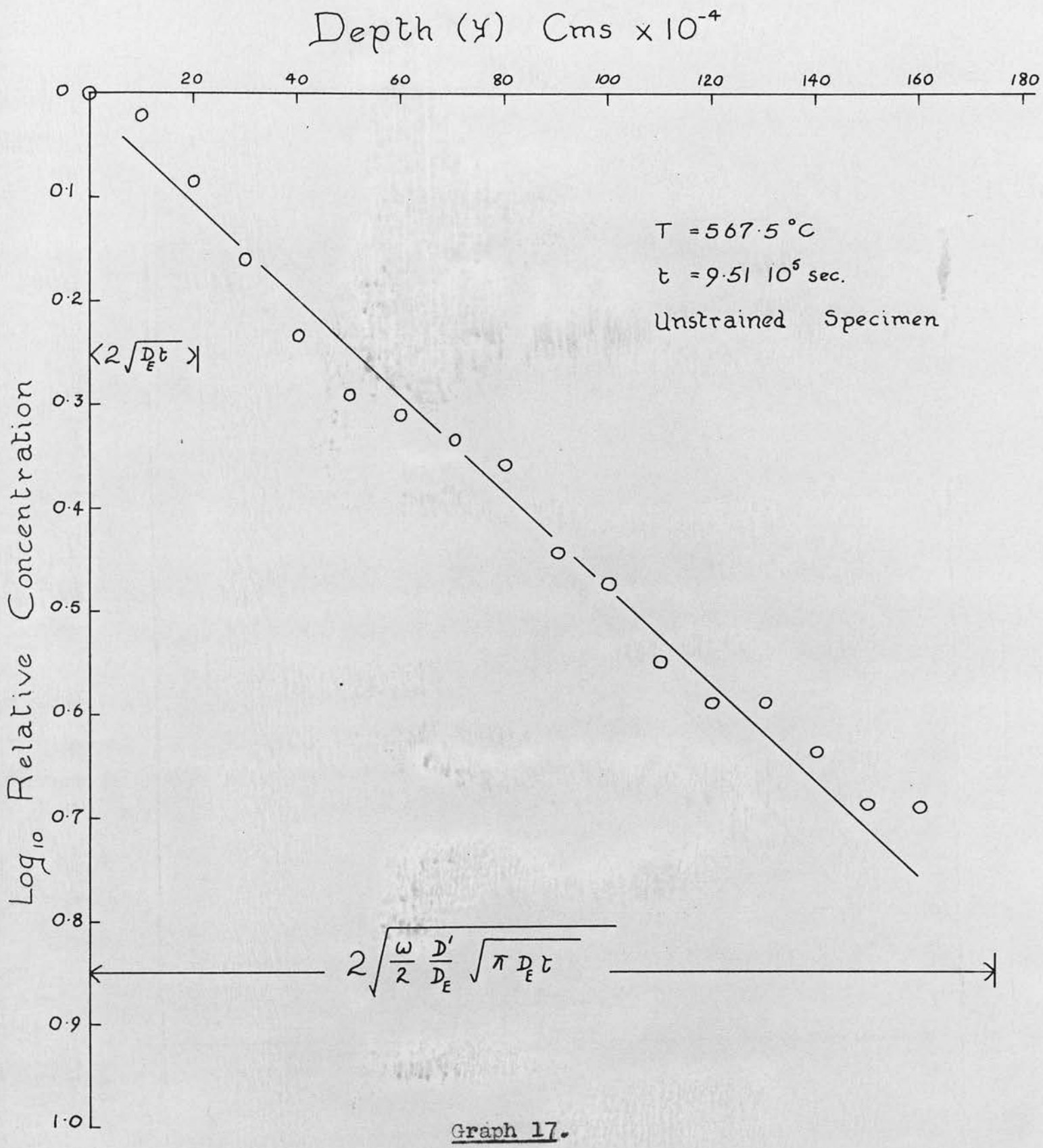
Depth (Y) Cms x 10^{-4}
0
20
40
60
80
100
120
140
160
180
0·1
0·2
0·3
0·4
0·5
0·6
0·7
0·8
0·9
1·0
$\log_{10}$ Relative Concentration
$T = 567{\cdot}5\,^{\circ}C$
$t = 9{\cdot}51\ 10^{5}$ sec.
Unstrained Specimen
$2\sqrt{D_E t}$
$2\sqrt{\frac{\omega}{2}\,\frac{D'}{D_E}\,\sqrt{\pi D_E t}}$

Graph 17.

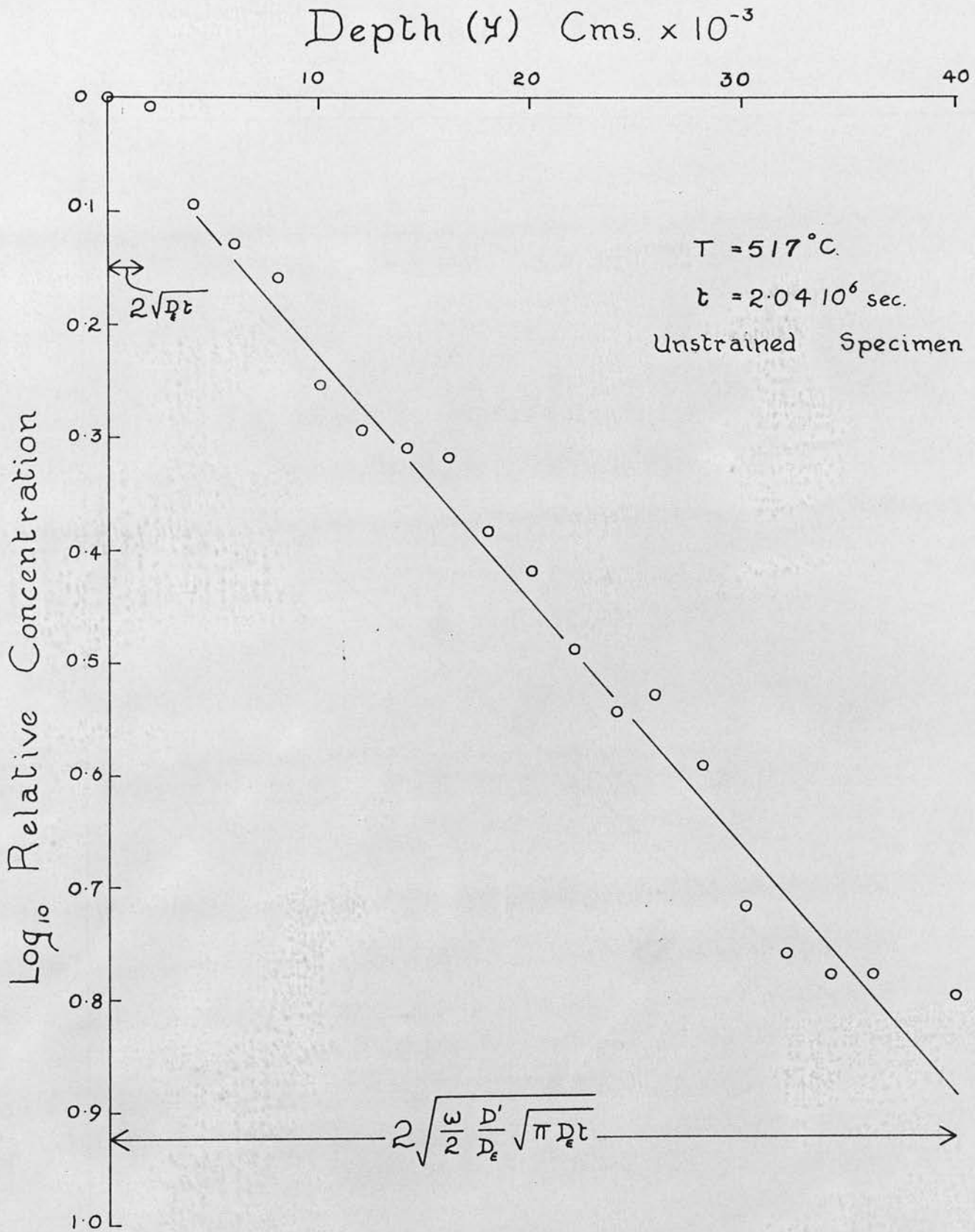
Depth (Y) Cms. x 10^{-3}
10
20
30
40
0
0·1
0·2
0·3
0·4
0·5
0·6
0·7
0·8
0·9
1·0
Log_{10} Relative Concentration
T = 517 °C.
t = 2·04 10^6 sec.
Unstrained Specimen
$2\sqrt{D_\epsilon t}$
$2\sqrt{\frac{\omega}{2}\frac{D'}{D_\epsilon}\sqrt{\pi D_\epsilon t}}$

Graph 18.

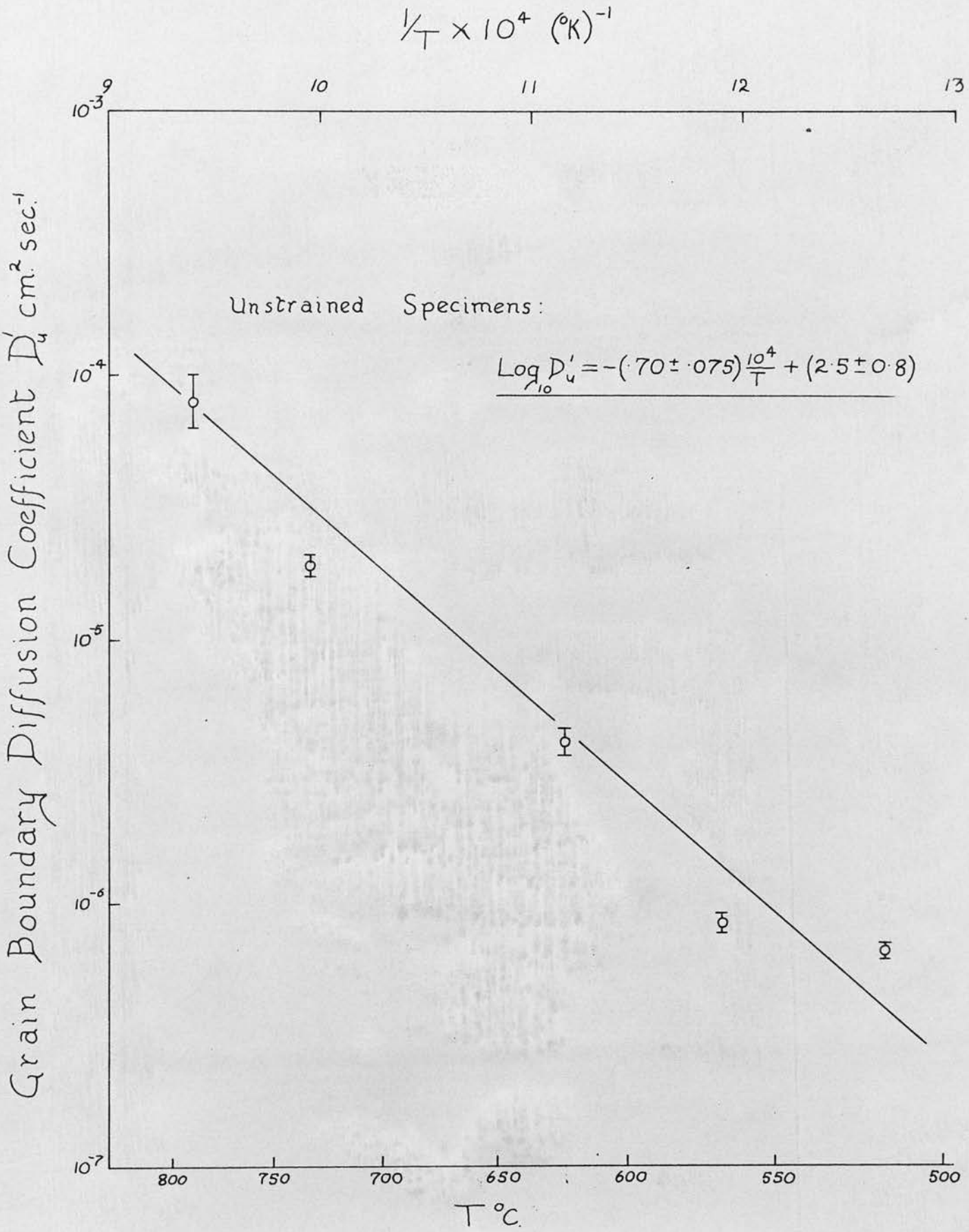
1/T × 10⁴ (°K)⁻¹
9
10
11
12
13
10⁻³
10⁻⁴
10⁻⁵
10⁻⁶
10⁻⁷
Grain Boundary Diffusion Coefficient D'u cm.² sec.⁻¹
Unstrained Specimens:
Log10 D'u = -(·70 ± ·075) 10⁴/T + (2·5 ± 0·8)
800
750
700
650
600
550
500
T °C.

Graph 19.

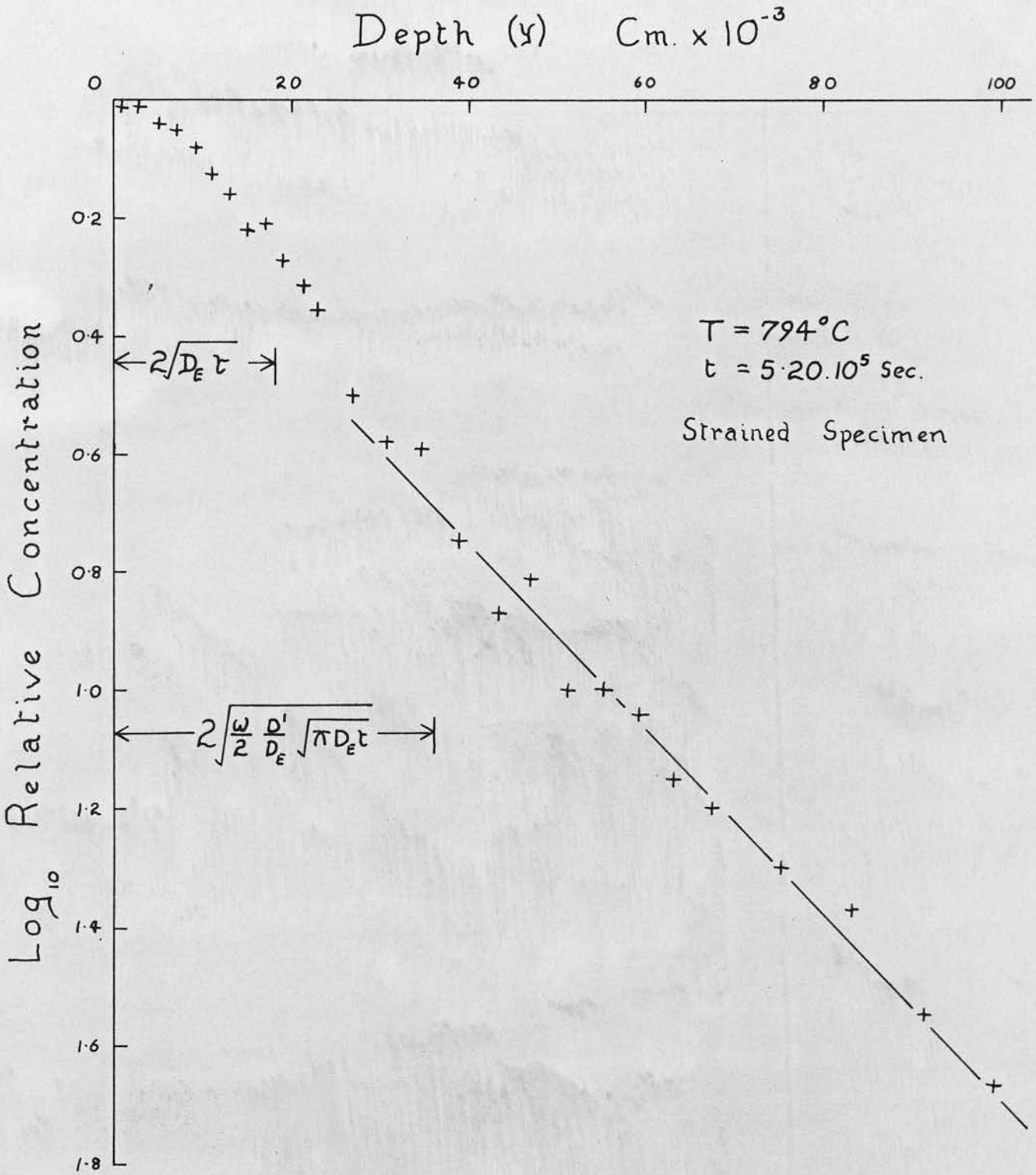
Depth (y) Cm. x 10^{-3}
0
20
40
60
80
100
0·2
0·4
0·6
0·8
1·0
1·2
1·4
1·6
1·8
$\log_{10}$ Relative Concentration
$2\sqrt{D_\varepsilon t}$
$2\sqrt{\frac{\omega}{2}\frac{D'}{D_\varepsilon}\sqrt{\pi D_\varepsilon t}}$
T = 794°C
t = 5·20.10^5 Sec.
Strained Specimen

Graph 20.

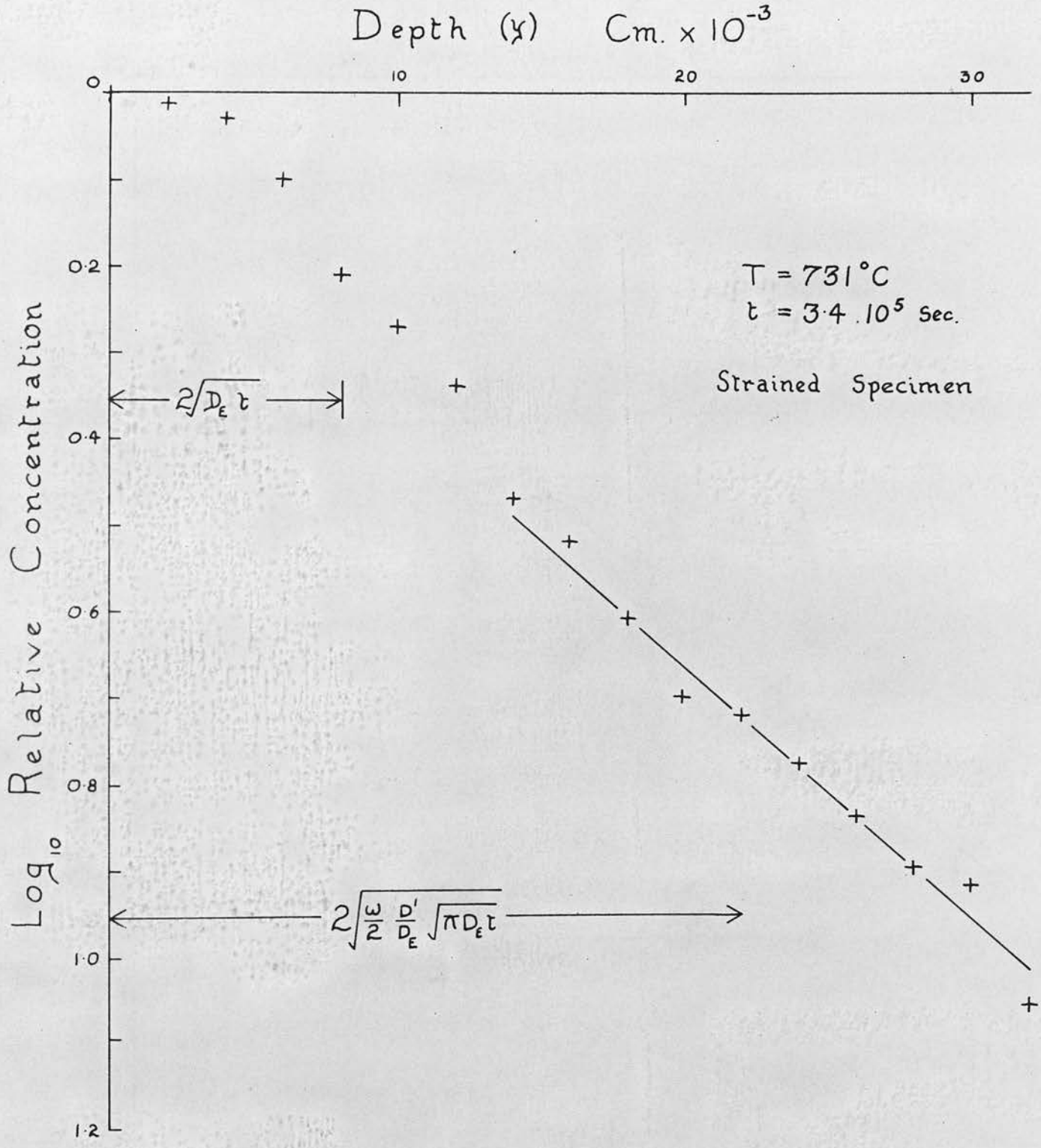
Depth (y) Cm. x 10^-3
0
10
20
30
Log10 Relative Concentration
0·2
0·4
0·6
0·8
1·0
1·2
T = 731 °C
t = 3·4 . 10^5 Sec.
Strained Specimen
2√(Dε t)
2√((ω/2)(D'/Dε)√(π Dε t))

Graph 21.

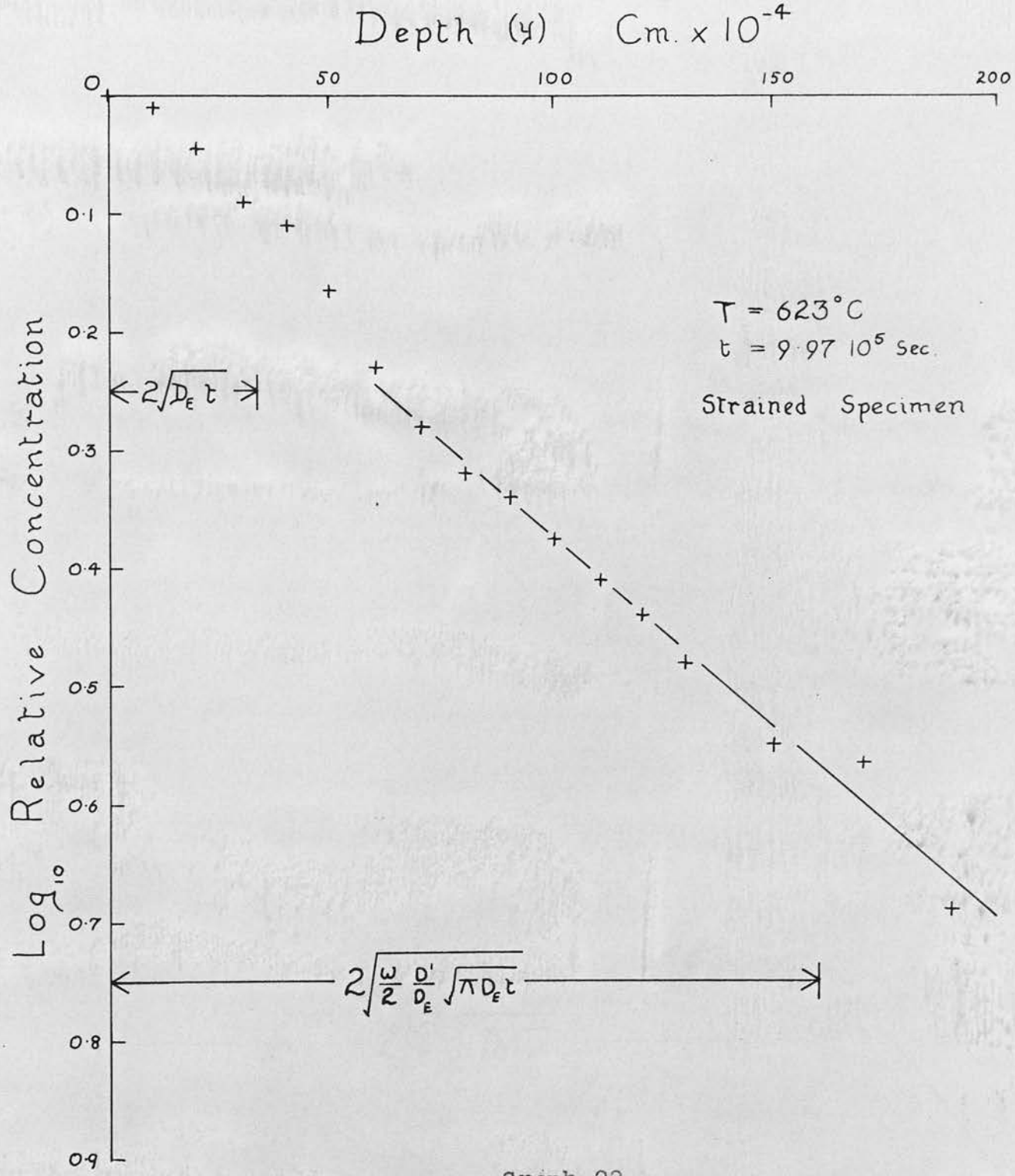
Depth (y) Cm. x 10^-4
0
50
100
150
200
0·1
0·2
0·3
0·4
0·5
0·6
0·7
0·8
0·9
Log10 Relative Concentration
T = 623°C
t = 9·97 10^5 Sec.
Strained Specimen
2√(Dε t)
2√((ω/2)(D'/Dε)√(π Dε t))

Graph 22.

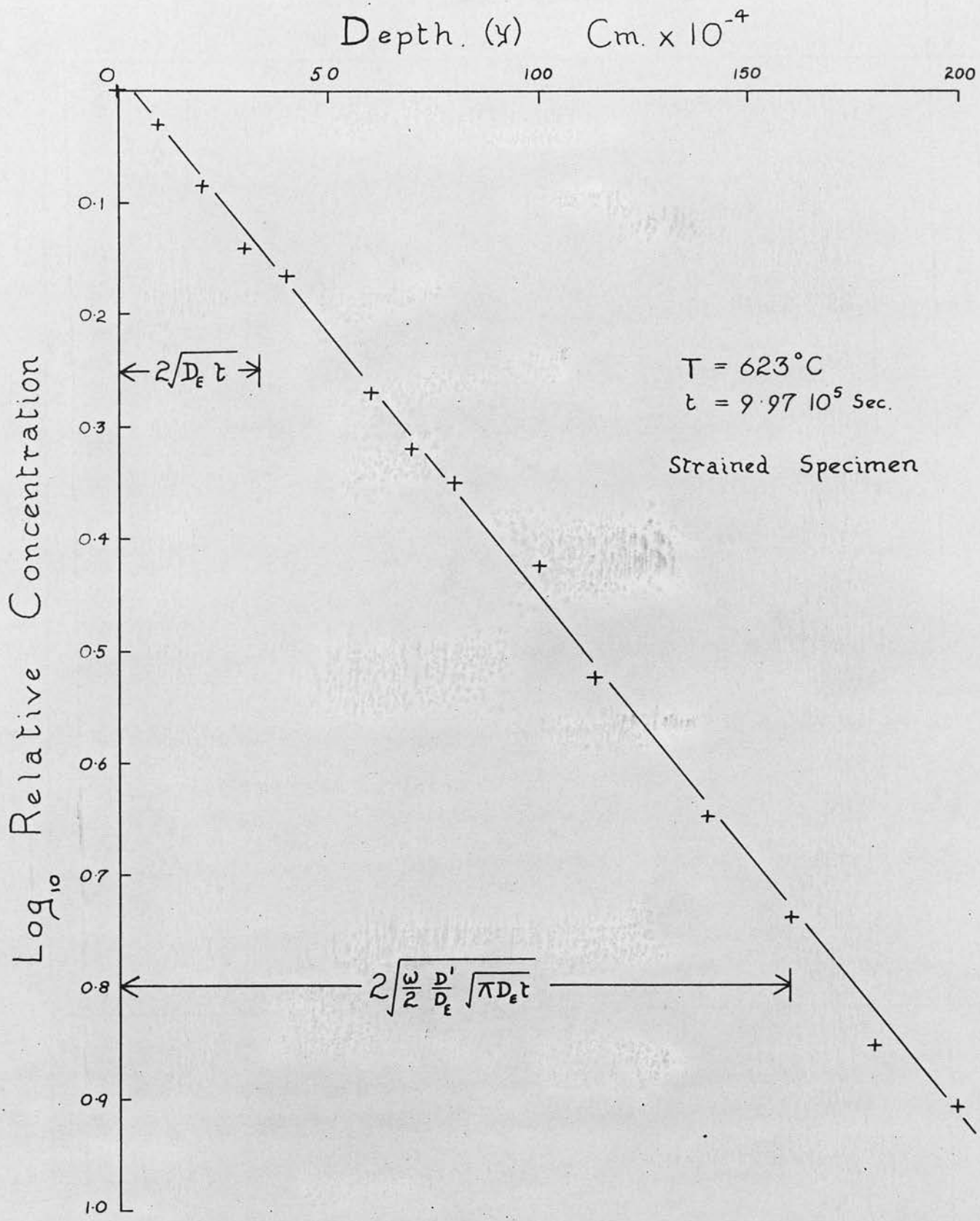
Depth. (y) Cm. x 10^{-4}
0
50
100
150
200
0·1
0·2
0·3
0·4
0·5
0·6
0·7
0·8
0·9
1·0
$\log_{10}$ Relative Concentration
$2\sqrt{D_\epsilon t}$
$2\sqrt{\frac{\omega}{2}\frac{D'}{D_\epsilon}\sqrt{\pi D_\epsilon t}}$
T = 623°C
t = 9·97 10^5 Sec.
Strained Specimen

Graph 23.

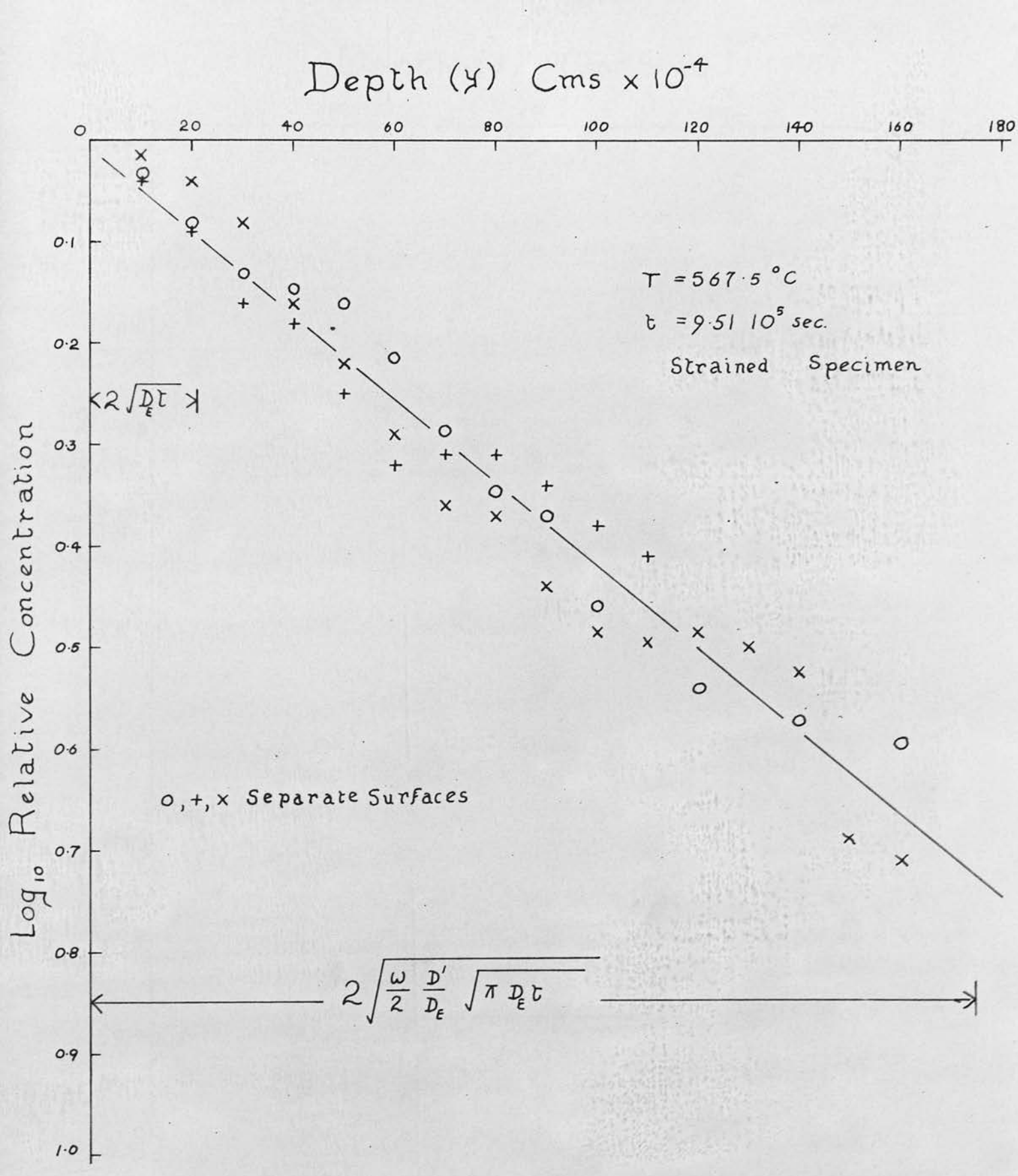
Depth (Y) Cms x 10^{-4}
0
20
40
60
80
100
120
140
160
180
0·1
0·2
0·3
0·4
0·5
0·6
0·7
0·8
0·9
1·0
$\log_{10}$ Relative Concentration
T = 567·5 °C
t = 9·51 10^5 sec.
Strained Specimen
$2\sqrt{D_\epsilon t}$
0, +, x Separate Surfaces
$2\sqrt{\frac{\omega}{2}\frac{D'}{D_\epsilon}\sqrt{\pi D_\epsilon t}}$

Graph 24.

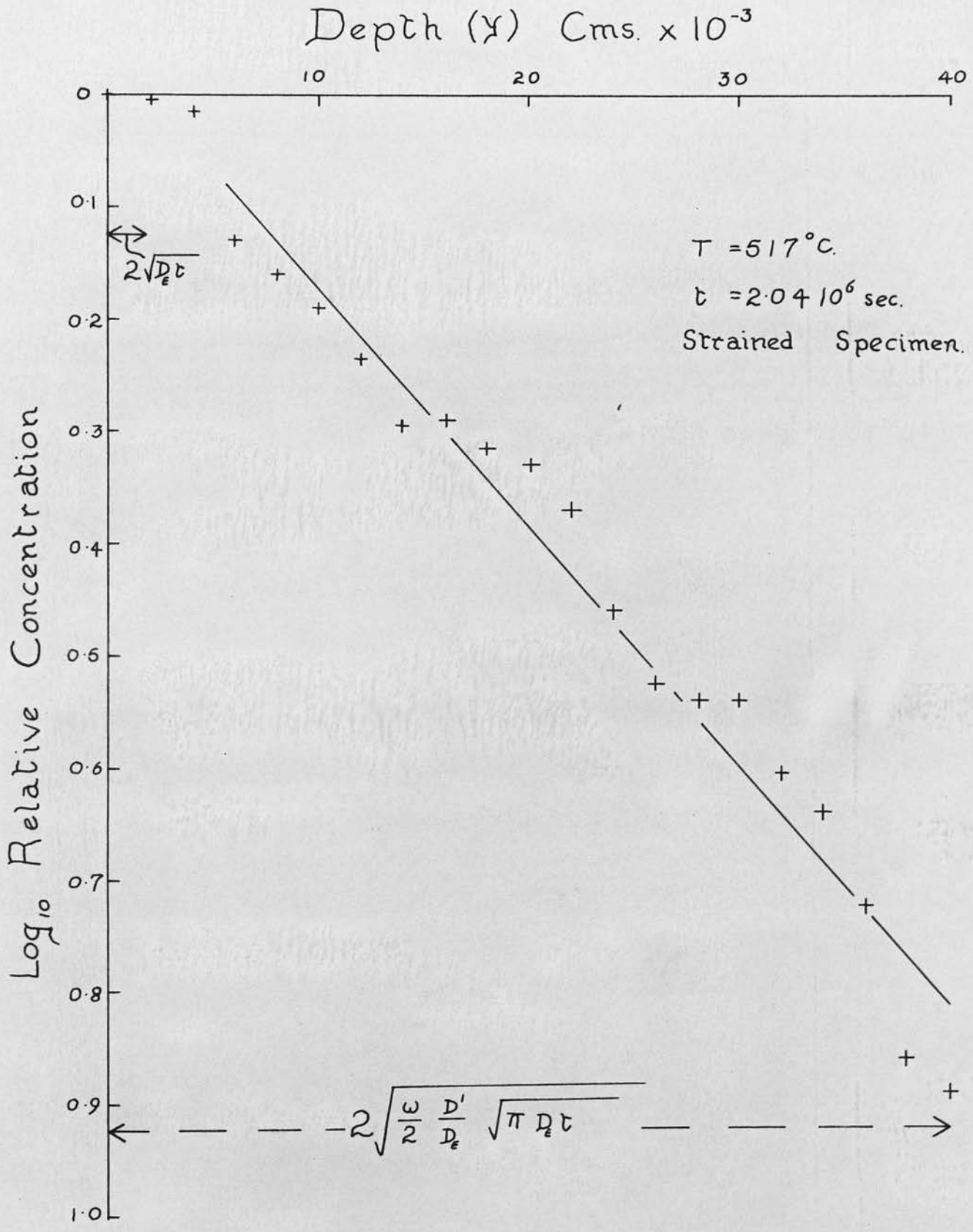
Depth (Y) Cms. x 10^{-3}
10
20
30
40
0
0·1
0·2
0·3
0·4
0·5
0·6
0·7
0·8
0·9
1·0
$2\sqrt{D_\epsilon t}$
T = 517 °C.
t = 2·04 10^6 sec.
Strained Specimen.
$\log_{10}$ Relative Concentration
$-2\sqrt{\frac{\omega}{2}\frac{D'}{D_\epsilon}\sqrt{\pi D_\epsilon t}}$

Graph 25.

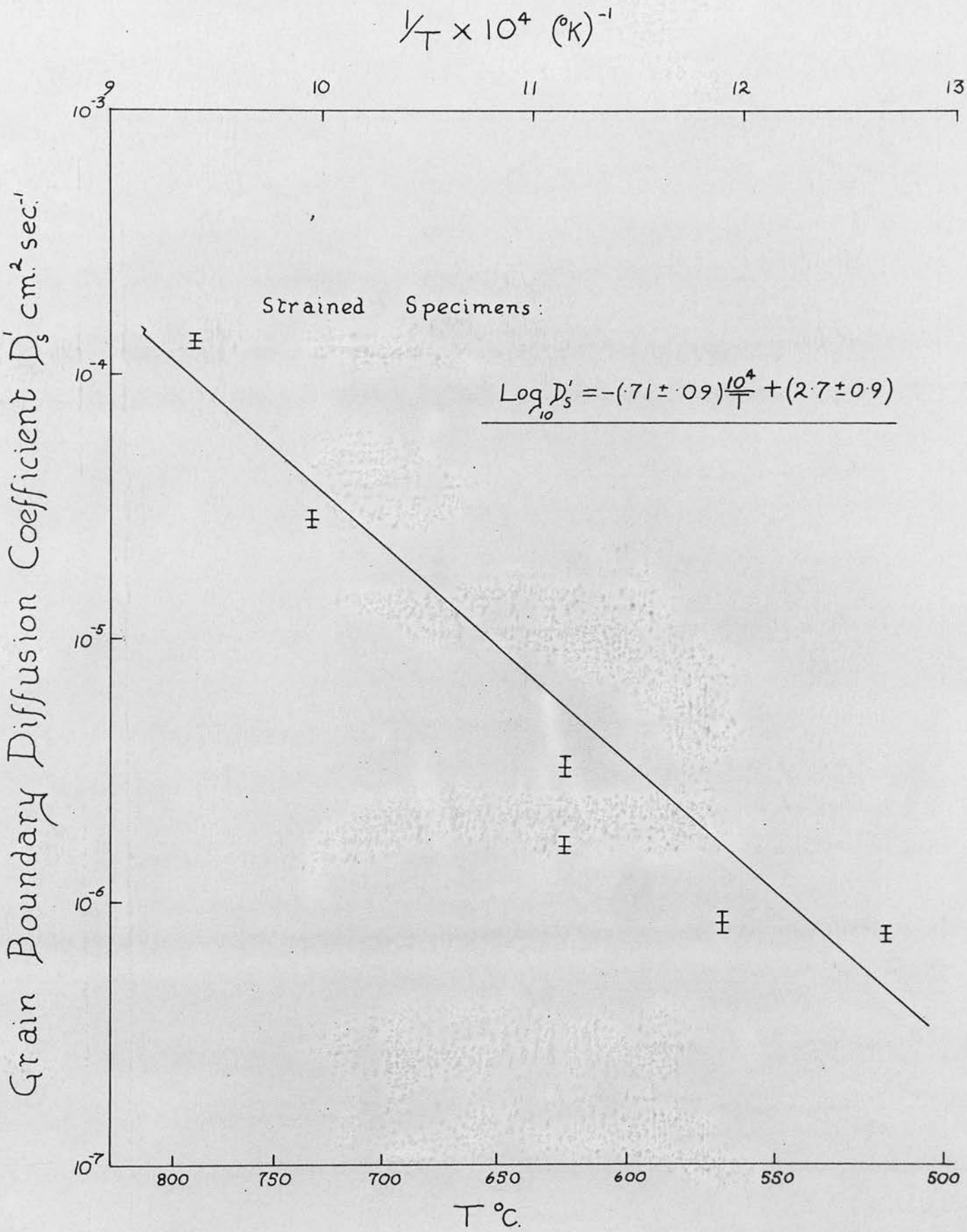
1/T × 10⁴ (°K)⁻¹
9
10
11
12
13
10⁻³
10⁻⁴
10⁻⁵
10⁻⁶
10⁻⁷
Grain Boundary Diffusion Coefficient D'ₛ cm.² sec.⁻¹
Strained Specimens:
Log₁₀ D'ₛ = −(·71 ± ·09) 10⁴/T + (2·7 ± 0·9)
800
750
700
650
600
550
500
T °C.

Graph 26.

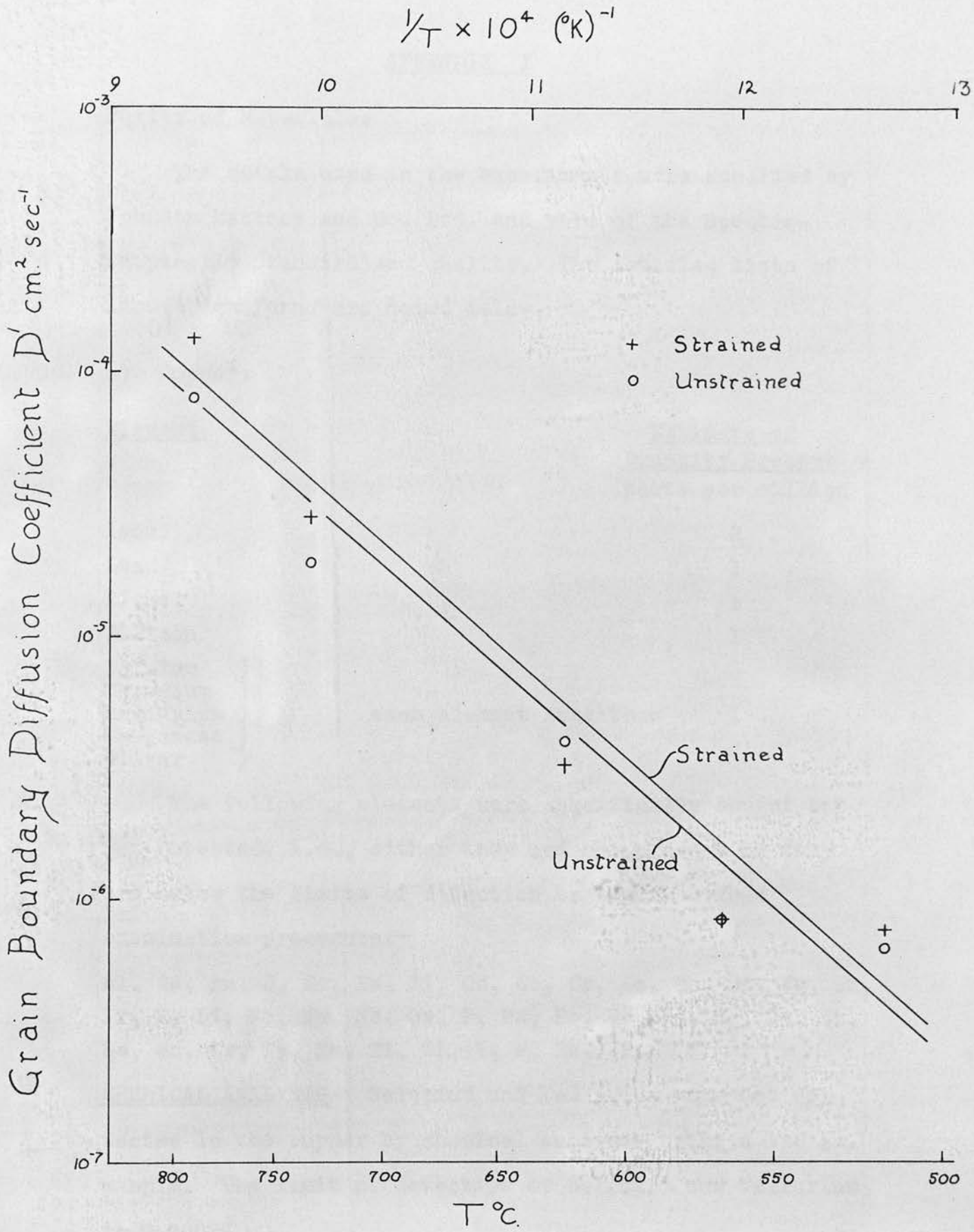
1/T × 10⁴ (°K)⁻¹
9
10
11
12
13
10⁻³
10⁻⁴
10⁻⁵
10⁻⁶
10⁻⁷
Grain Boundary Diffusion Coefficient D' cm.² sec⁻¹
+ Strained
o Unstrained
Strained
Unstrained
800
750
700
650
600
550
500
T °C.

Graph 27.

APPENDIX I

Purity of Materials:

The metals used in the experiments were supplied by Johnson Matthey and Co. Ltd. and were of the Spectroscopically Standardised quality. The detailed lists of impurities found are noted below.

a) Copper:

Element	Estimate of Quantity Present parts per million
Iron	2
Lead	1
Nickel	1
Silicon	1
Calcium, Chromium, Magnesium, Manganese, Silver	each element less than 1

The following elements were specifically sought but not detected, i.e., either they are not present or they are below the limits of detection by the described examination procedure.

Al, As, Au, B, Ba, Be, Bi, Cd, Co, Cs, Ga, Ge, Hf, Hg, In, Ir, K, Li, Mo, Na, Nb, Os, P, Pd, Pt, Rb, Re, Rh, Ru, Sb, Se, Sn, Sr, Ta, Te, Ti, Tl, V, W, Zn, Zr.

CHEMICAL ANALYSIS Selenium and Tellurium were not detected in the copper by chemical analysis using a 150 gm. sample. The limit of detection of selenium and tellurium is 0.0002%.

Appendix 1 (Contd.)

OXYGEN After heating for half an hour at 800°C in hydrogen a metallographic examination failed to show any signs of the presence of oxygen in the sample.

b) Silver:

Element	Lines detected			
Iron	all sensitive lines			
Tin	all sensitive lines faintly visible			
Copper	3247.540			faintly visible
Gallium	2943.637	2874.244		faintly visible
Manganese	2801.064	2798.271	2794.817	faintly visible
Nickel	(3414.765	3057.638		faintly visible
	(3054.316	3050.819		faintly visible
Calcium	4226.728	3968.468	3933.666	faintly visible
Magnesium	2852.129	2802.695	2795.53	faintly visible
Lead	2833.069			very faintly visible
Cadmium	2288.018			very faintly visible
Silicon	Evidence doubtful; 2881.578 and 2516.123 faintly visible but slightly fainter than in the graphite blank.			

No lines of the following elements were observed:-

Al, As, Au, Ba, Be, Bi, Co, Cr, Ge, Hg, In, K, Li, Mo, Na, Rb, Sb, Sr, Ti, Tl, V, W, Zn, Zr.

ACKNOWLEDGEMENTS

I wish to thank Professor N. Feather, F.R.S. for extending to me the facilities of his laboratory, and Dr. A.F. Brown for his advice and encouragement during the course of the work.

I acknowledge gratefully a maintenance grant, during part of the work, from the United Kingdom Atomic Energy Authority.
